2015-01-08

Measuring Brain Connectivity and Hemodynamic Alterations Following Pediatric Mild Traumatic Brain Injury in the Primary Motor Cortex

Urban, Karolina

UNIVERSITY OF CALGARY

Measuring Brain Connectivity and Hemodynamic Alterations Following Pediatric Mild Traumatic Brain Injury in the Primary Motor Cortex

by

Karolina Urban

A THESIS

SUBMITTED TO THE FACULTY OF GRADUATE STUDIES

IN PARTIAL FULFILMENT OF THE REQUIREMENTS FOR THE

DEGREE OF MASTERS OF SCIENCE

GRADUATE PROGRAM IN NEUROSCIENCE

CALGARY, ALBERTA

DECEMBER, 2014

Abstract

Concussion, or mild traumatic brain injury, is a growing concern especially among the pediatric population. Symptoms may persist beyond one month after injury and result in long term disability called Post-Concussion Syndrome (PCS). There is a lack of measures to quantitatively monitor and explore pathophysiological mechanisms of PCS. We hypothesized that since fiber tracts are often impacted in concussion, functional activation and inter-hemispheric brain communication may be impaired. We used functional near-infrared spectroscopy (fNIRS) to quantify the magnitude of activation and inter-hemispheric communication between motor cortices using a coherence analysis. Subjects completed a resting state and tapping paradigm. We detected differences between patients and controls in coherence, suggesting alterations in inter-hemispheric communication. Given the critical need for a quantitative biomarker for recovery following a concussion, we present this data to highlight the potential of fNIRS, coupled with coherence analysis, as a sensitive measure to detect functional changes.

Acknowledgements

First of all I would like to thank my amazing supervisors Dr. Jeff Dunn and Dr. Karen Barlow for giving me the opportunity to be your graduate student. Both of you have been great role models for me and I am very lucky to have had this opportunity to grow academically and personally as part of your research teams. Jeff, I have been challenged to learn all about the medical imaging world and have discovered a new fascination for physics, one that my grandpa would have been extremely happy of. Karen, I hope that one day I can have an impact on people's lives like you do every day. I would also like to thank my supervisor committee, Dr. Signe Bray and Dr. Adam Kirton, for all the help and contributions towards my academic endeavor. Ms. Brenda Turley you always made my day and have always been so willing to help us students with whatever we need.

Trevor, Angela, Liz, Runze, Ying, Tom, and Nabeela I would like to thank you for an amazing last year and half. Your support has been great, and I wouldn't have gotten this far without it. Thank you for always being a fun time when I needed most, but also for all the fascinating science talks. Nabeela, since day one you have shown how important working hard and being passionate about your studies is, setting a great example for all of us.

Most of all I would like to thank my friends and family for all the support and encouragement during my studies. Mom, you have been an inspiration and role model for me since day one. You're always pushing me to be the best I can be. Dad, you have always made sure I can pursue whatever dream I have. I am extremely lucky to have a family who supports and loves science just as much as I do.

Dedication

I would like to dedicate my thesis in loving memory of my dziadek (grandpa), Eugeniuz Wareda. An intelligent, caring and inspirational man who was always looking for the answers to the world's mysteries.

I finally understand the importance of physics that you shared with me from the day I was born. I think about you every day and wish you could be here to teach me more.

Table of Contents

List of Tables

List of Figures and Illustrations

List of Symbols, Abbreviations and Nomenclature

Symbol	Definition
AGC	Automatic Gain Control
ASL	Arterial spin labeling
ATP	Adenosine triphosphate
BOLD	Blood oxygen level dependent
Cho	Choline
$CMRO^2$	Cerebral metabolic rate
Cr	Creatine
CSF	Cerebrospinal fluid
CT	Computed Tomography
CW	Continuous wave
dOD	Delta optical density
DMN	Default mode network
DLPFC	Dorsal lateral prefrontal cortex
DSM-IV	Diagnostics and Statistics Manual-IV
DTI	Diffuse tensor imaging
EEG	Electroencephalogram
FA	Fractional anisotropy
fMRI	Functional magnetic resonance imaging
fNIRS	Functional Near infrared spectroscopy
Glu	Glutamate

Glx	Glutamine
Hb	Hemoglobin
ICD-10	International Classification of Diseases-10
Ins	Myo-insitol
M1	Primary motor cortex
MRI	Magnetic resonance imaging
MRS	Magnetic resonance spectroscopy
mTBI	Mild traumatic brain injury
NAA	n-acetyl-aspartate
OD	Optical density
PCr	Phosphocreatine
PCS	Post-concussion syndrome
SPECT	Single photon emission computed tomography
TBI	Traumatic brain injury
TMS	Transmagnetic stimulation

Chapter One: **Introduction**

1.1 Thesis Overview

Traumatic brain injuries (TBI) are a major cause of mortality and morbidity among children and adults [1]. Mild TBI (mTBI) is caused by a direct or indirect biomechanical force that causes an acceleration or deceleration of the brain within the skull causing altered brain function [2]. Nearly 90% of all TBI's are in the mild spectrum known as a mTBI or concussion [3]. By age ten, 20% of children will suffer an mTBI, and by age 25 the incidence may be as high as 30% [1,4]. Although most people with mTBI have complete recovery of symptoms by 7 to10 days after initial injury, many children continue to suffer as a result of the injury.

In a study conducted at the Alberta Children's Hospital, nearly 60% of children continued to have symptoms at 1 month, and 13% at 3 months [5]. If persistent post-concussion symptoms continue past three months they become known as post-concussion syndrome (PCS) [5]. PCS is associated with significant disability in the child and is a burden on his/her family. The recovery period may be greater in youth when compared to adults [6–8]. The biological explanations for prolonged PCS symptoms are unclear but need investigation due to their high incidence, and occur at a critical period of brain maturation and potential for long-term consequences [9,10]. Although this is a significant public health issue, there is still a lack of understanding for the neurobiological causes of PCS [10–12].

Our understanding of the pathophysiology of acute mTBI is increasingly clear; however the development of persistent symptoms still needs to be evaluated further. The brain is complex and contains many neurobiological processes with multiple interactions. This allows us to function smoothly, coherently and makes each and every one of us who we are. Each action, and

thought process is complex and brain activity increases and decreases to achieve these processes. Our neurons and glial cells increase in their metabolic demand and in turn require more nutrients[13,14]. In order to fulfill this need, there is an increase in regional cerebral blood flow (CBF) and perfusion bringing in oxygen and taking away end products. This process is known as neurovascular coupling [15]. Without tight coupling of blood flow and energy requirements our neurons may not be as efficient, affecting communication between the brain areas required to achieve the task. In order to gain a better understanding of the pathophysiology behind PCS, it is important to explore this relationship in children with persistent symptoms. The aim of this thesis is to explore whether adolescents with persistent PCS have altered hemodynamic responses and functional connectivity of the motor cortex, as measured with functional near-infrared spectroscopy (fNIRS).

1.2 Rationale

mTBI can lead to persistent symptoms that can affect the quality of life. The understanding of the neurobiological underpinnings of PCS is still unclear. Furthermore, current return to 'play' or 'life' protocols involve the subjective rating of symptoms, which do not necessarily reflect healthy brain function. Therefore it is important to keep exploring objective methods to detect brain dysfunction. The current literature has shown acute and chronic changes in brain metabolism, brain function, and altered white matter tracts. The primary motor cortex (M1) offers a relatively accessible target to measure brain function. There have been a few studies focusing on M1, which showed alterations in metabolism, white matter tracts and the functional connectivity of the motor network. Most of these studies have focused on adults, however as

children are in a rapid state of neurological development, it is important to evaluate the long-term impact of mTBI, especially in symptomatic PCS patients (for a discussion see section 2.4).

This thesis explores the utility of fNIRS in evaluating pediatric brain activation and communication, and compares healthy children to those that continue to have persistent symptoms after a mTBI. fNIRS is a non-invasive, quick and relatively easy to use method to study brain function. This method can measure changes in brain microvascular hemoglobin (Hb) saturation (oxy-Hb and deoxy-Hb) in the underlying cerebral cortex with high temporal resolution. Similar to functional magnetic resonance imaging (fMRI), fNIRS can evaluate functional connectivity, or the synchrony of oscillations in brain regions, which are reflective of brain regions in close communication with each other.

1.3 Objectives of Thesis

The first aim of this thesis is to establish whether fNIRS is capable of detecting functional alterations in the response to task activation in children with PCS. The hypothesis is that PCS children have altered hemodynamic responses with task activation in the motor cortex.

The second aim of this thesis is to assess brain communication with fNIRS, using a coherence analysis between controls and PCS patients at resting state and during task activation. The hypothesis is that there is reduced inter-hemispheric communication in the motor cortex in patients with PCS as compared to controls.

1.4 Thesis Outline

This thesis begins by reviewing the current literature on mTBI and PCS in adult and pediatric populations. The review includes the biomechanics of mTBI, incidence rates, and the

pathophysiological changes that occur following injury. The next chapter includes an explanation of current fNIRS technology and how to derive relative hemoglobin saturation and functional communication within brain networks. Chapter four is a description of the methodology and protocol used. The results are present in chapter five. Chapter 6 includes a discussion on the utility and feasibility of fNIRS technology in measuring brain function. The final chapter is a discussion of the results, comparison to current the literature, limitations and possible future directions.

Chapter Two: **Background**

2.1 Chapter Overview

This chapter will provide an overview of the current state of literature on mTBI and PCS beginning describing their incidence rates, and signs and symptoms. The next section describes the evidence of pathophysiological alterations as a result of mTBI in metabolic, functional and structural domains. There will be an overview of healthy neurovascular coupling and how it can be measured.

2.2 Mild Traumatic Brain Injury

mTBI has become a major health issue in the past decade [16]. TBI is the leading cause of injury under the age of 25, with 90% of injuries being classified as a mTBI or a concussion [1,17]. There is a wide spectrum of TBI including severe, moderate, and mild [18]. mTBI is defined with subtle neurocognitive and neuro-affective deficits which may recover with time [2]. Furthermore, a clear indication is the lack of structural damage evident on CT or MRI imaging. For mTBI, determining incidence is difficult, as 80% of individuals do not seek medical attention, therefore the incidence may be higher than estimated [19]. The pediatric population is at greater risk of having a TBI: by age ten, one in five children will suffer an mTBI, and by age 25, the incidence may be as high as 30% [1,20].

The leading cause of TBI between the age of 15 to 25 is a motor vehicle accident [21]. The next highest cause of TBIs and the majority of mTBIs are due to sport related injuries [22–24]. Although sports remain one of the largest causes, it has been suggested that mTBIs caused by motor vehicle accidents represent a more serious injury with longer recovery duration [25].

Head injuries are responsible for 3-15% of all pediatric injuries presenting to the emergency department [26,27]. Nearly, 24% of pediatric serious head injuries that are admitted to the emergency department are a result of a sports related injury [27]. In the emergency department, for example, one study found that 33% of mTBI in children between 12 and 16 years of age were caused sports or bicycling [28]. In high school sports, 8.9% of sports-related injuries are mTBIs [29]. In a study of high school athletes, the highest rate of mTBIs occurred in football (41%), girls' soccer (21%), and boys' soccer (15%) [29].

2.2.1 Biomechanical Causes of Injury

There is a considerable heterogeneity in the mechanism of mTBI. They can occur with direct contact to the head (e.g. when the head strikes an object or is stuck by an object), or indirectly where the head is set in motion without contact [8]. An example of an indirect impact is a hit to the body that causes it to stop while the head continues to move. This mechanism results in rotational acceleration-deceleration forces with the head pivoting on the neck. Acceleration-deceleration forces can occur in one of more of the sagittal (anterior-posterior), coronal (medial-lateral) and axial (rotational) planes depending on the initial point of contact [30–32].

There are variations in the mechanism of injury that may be the result of a combination of direct, indirect, linear and/or rotational acceleration-deceleration forces. The primary brain injury occurs at the initial point of contact of the brain with the skull when deformations of brain tissue occur, and throughout the brain at the axons from the sheering, tensile or stretching forces [31,32]. The biomechanics of injury are dependent on the properties and type of contact made to the head as well as the brain tissue (e.g. immature brain tissue has a greater water content than the adult

brain). There are many inter-individual differences, including increased vulnerability following repeat injury, relative musculoskeletal strengths or weaknesses, may play a role in mTBI [33].

2.2.2 Signs and Symptoms

Every mTBI is different and can lead to a variety of symptoms. Acutely, the most common are headaches, vomiting, cognitive disturbance, sleep disturbance, fatigue and behavioural changes [34]. Other symptoms may include fogginess, irritability, sensitivity to light and difficulty concentrating [34]. Symptoms are often categorized into four specific domains: somatic or physical (e.g. headaches), cognitive (e.g. concentration difficulties), behavioural (e.g. irritability) and sleep disturbance (e.g. difficulty falling asleep) (Table 2-1) [35]. In adults, nearly 80% of mTBIs symptoms recover within the first 2 weeks of injury [36]. Symptoms may resolve spontaneously in a short period of time, however our data and others suggest that 60% of children continue to have symptoms at one month after injury and nearly 13% will continue to have persistent symptoms at 3 months [5].

2.3 Post-Concussion Syndrome (PCS)

There are two main definitions of PCS including the Diagnostics and Statistics Manual (DSM-IV) and International Classification of Diseases (ICD-10) [37]. The DSM-IV states that the patient must have history of TBI, symptoms must be present following injury and may get worse, evident deficits in memory and attention (based on performance from neuropsychological tests), at least 3 symptoms persisting for 3 months with a lasting neurological impairment, and cause a disruption in regular activities as school or work. The symptoms include apathy or affective disturbance, dizziness, fatigue, headaches, irritability, sleep disruption and/or personality

changes. The ICD-10 identifies 8 possible symptoms: dizziness, difficulty concentrating, fatigue, headache, insomnia, irritability, memory disruption, and/or intolerance to alcohol, emotion or stress. The criteria states that 3 or more symptoms need to be present, and develop any time within one month of the injury [38,39]. The ICD-10 and DSM-IV were developed for adults and had not been validated for the pediatric population. Recently, a new definition for PCS has been proposed in the pediatric population [37]. The criteria includes: mTBI with onset of symptoms within 72 hours, 3 or more symptoms including dizziness, insomnia, irritability, headaches, emotional labiality, memory problems and difficulty concentrating, and must be symptom present for at least 4 weeks. The symptoms may not be explained by any other disorder.

2.3.1 Risk Factors and Quality of Life

A follow-up study of pediatric mTBI reported that 11% of children suffered from PCS, with symptom presence more than three months after injury [5]. Other studies have shown lingering symptoms occurred in 20-30% of children [34,40]. One year after injury it has been shown that 2.3% of children continue to experience symptoms related to the initial injury [5].

There are a variety of risk factors associated with developing PCS including age, pre-morbid factors, presence of headache and hospital admission [37,41]. Children between the age of 13to 18 years are the more likely to develop persistent symptoms than other cohorts [5,41]. Premorbid factors such as difficulty learning at school, attention deficit disorder, coping strategies, parental pre-injury anxiety, adverse life events and stress have an effect on injury outcome and persistence [42–44] Poorer outcome has also been associated with headache at acute presentation in the emergency room in children 11 to18 years old [41].

There are long term consequences of PCS which cause significant disability to the child. Symptom presence can vary and include cognitive difficulties, behavioural changes, physical (e.g. headaches and dizziness) and sleep disturbances. These may have an impact on the developing brain affecting quality of life in the child, and increasing school absenteeism [5,16]. The effects are evident a year after with suffering from PCS patients have a lower health-related quality of life [16]. The biological explanations for prolonged PCS symptoms are unclear despite the high incidence and occurrence at a critical period of brain maturation [9,10].

2.3.2 Common Symptoms in PCS

In the pediatric population, the most common symptoms reported one month after injury were fatigue (79%), emotional (60%), headache (58%) and irritability (58%) [5]. Sleep disturbances including difficulty falling asleep and staying asleep were also common in children following their mTBI [5,45,46]. Signs of persistent instability, particularly when removing the ability to use vision for vestibular information, is often present in PCS [47–49]. The most common behavioural symptoms one month after injury have included irritability (30%), feeling more emotional (25%), nervousness (22%) and sadness (19%). One year after injury, 1.3% of children continued to experience post-traumatic headaches [5].

There is a progression in the development of PCS over time. Initially, there is a larger presence of symptoms in the physical category. As PCS progresses there is an increase in the presence and development of cognitive category symptoms [50]. Consistently, physical symptoms decreased within one month of injury with a corresponding increase in cognitive symptoms at 3 months in children with persistent PCS [51]. Sleep disturbances are commonly reported during

PCS, initially there is hypersomnia followed by increased difficulty to fall asleep and continuing arousal [37].

2.4 Pathophysiology

2.4.1 Overview of Brain Pathology

A characteristic of mTBI is the lack of macroscopic damage using standard imaging techniques such as MRI or computed tomography (CT) imaging [10]. In order to understand the neurobiology and physiological underpinnings of the injury, animal models of mTBI have been utilized [52]. The uses of newer neuro-imaging techniques as Magnetic Resonance Spectroscopy (MRS), fMRI, and diffuse tensor imaging (DTI) have supported these findings in human and have been linked to clinical symptoms of mTBI [12].

2.4.2 Neurometabolic Alterations

2.4.2.1 The Neurometabolic Cascade

Animal studies have shown the direct impact of mTBI on brain metabolism. A neurometabolic cascade has been used to characterize the microscopic damage following mTBI [12,53]. Immediate neurobiological perturbations following mTBI can serve as a potential biological mechanism which may help explain persistent symptoms [12,53–55]. The acute pathophysiology of mTBI involves neurochemical alterations, an energy crisis, cytoskeleton and mitochondrial damage, axonal dysfunction and cell death [12,52]. Following mTBI, there is a large release of glutamate from presynaptic vesicles. This causes a disruption in cellular equilibrium and a corresponding increase in potassium (K^+) efflux, and sodium (Na^+) and calcium (Ca^{2+}) influx. These perturbations cause disruptions in normal neuron function [52]. Key distinguishing factor

here is cell death versus transient dysfunction and recovery - the latter being the norm for mTBI and persistence presumably underlying PCS.

To re-establish homeostasis, cells utilize adenosine tri-phosphate (ATP) by processing glucose. The increase in ATP demand may lead to a "mismatch" between cerebral glucose requirement, energy demand, and regional CBF leading to a relative cerebral "energy crisis" [56]. Initially there is an increase in glucose uptake, however this leads to a metabolic depression that may last for days varying on injury severity [52]. The consequences of the cellular disruptions are referred to a secondary injury to the mTBI, as they develop over time. The cell membrane perturbations can lead to a mitochondrial dysfunction, oxidative stress, free radical generation and alterations in CBF [57,58].

The effect of these events causes cytoskeleton damage as microtubule disruption that disrupts neurotransmission and axonal function [12]. Axons are particularly vulnerable to the effect of biomechanical forces including stretching and sheering forces [30,32]. There is evidence of shrinkage and atrophy of neurons caused by these biomechanical forces, without cellular death occurring.

It is suspected that the disruption in cell membrane and CBF leads to a secondary injury that occurs over time. This may lead to a hypoxic environment [59,60], ischemia [61] and CBF alterations [62–65]. Furthermore, mitochondrial dysfunction impairs cellular repair mechanisms leading to the activation of both apoptotic and necrotic pathways.

2.4.2.2 Acute Metabolic Alterations

There is established evidence for acute metabolic dysfunction, particularly in the adult population. MRS has been used to evaluate several metabolites including glutamate (Glu),

creatine (Cr), phosphocreatine (PCr), N-acetylaspartate (NAA), myoinsitol (Ins) and choline (Cho). A decrease in NAA may be reflective of neuro-axonal cell damage, and raised Cho and Ins may be reflective of glial proliferation [66]. Three days following mTBI, significant alterations in NAA:Cr and NAA:Cho were decreased, whereas Cho/Cr and Ins/Cr ratios were significantly increased as compared to controls in M1 and prefrontal cortex. These ratios recovered slower than symptom resolution [66–69]. Glu was significantly lower in the M1, while NAA and NAA: Cr ratio were lower in prefrontal and M1 cortices [54,55]. The Glu levels in M1 were correlated to self-reported symptom severity [55].

Weeks after initial injury, the decrease of NAA and NAA/Cr, and increases in Cho and Cho/NAA were also found in the splenium and frontal lobes [70,71]. Another study found a decrease in NAA/Cho and NAA/Cr ratios in the genu of the corpus callosum, and no difference in the splenium [72]. While exploring white matter, there was an increase in PCr and Cr concentrations, while in the grey matter there was a decrease in glutamate-glutamine (Glx) levels which were predictive of executive function and emotional distress [73,74].

Although there are contradicting results, it is important to consider the heterogeneity of the injuries and how different regions of the brain could be affected. Regardless, there are lasting metabolic changes in symptomatic patients.

2.4.2.3 Metabolic Alterations in PCS

There are fewer studies exploring the metabolic deficits in PCS patients, however there is some evidence of disruption. NAA/Cr continued to be reduced in the chronic stage of mTBI nearly 6 months after injury [66,75]. Decreased levels of Ins were found in hippocampus and M1 [76]. Similarly, Cr/Cho ratio were reduced in the dorsal lateral prefrontal cortex (DLPFC) of PCS

patients as compared to controls [66,77]. It may be that the reduction in Cr was due to residual energy impairment in chronic mTBI, as it is involved in energy level maintenance [77]. A study of the pediatric population was conducted to explore disruption in metabolism in PCS patients. NAA/Cr and NAA/Cho ratios were reduced in the corpus callosum and parietal white matter of PCS patients [78]. This disruption in cellular metabolism that could be causing continued brain dysfunction, and could affect CBF mechanisms during neuronal activation.

2.4.3 Cerebral Blood Flow

As there is a strong coupling between brain function, perfusion and metabolism, assessment of functional activation through measurements of the hemodynamic response may provide insight into the ongoing pathology. An increase in brain activity is associated with an increase in microvascular Hb saturation, as well as an increase in oxy-Hb concentration and a decrease in deoxy-Hb concentration [79,80]. Following mTBI there is evidence for abnormal metabolism, CBF, brain oxygenation and perfusion [81]. The coupling between brain activation and blood flow delivery known as neurovascular coupling, is critical to normal brain function [78]. Increases in cellular metabolic demands are matched by increases in regional blood flow in healthy tissue. This coupling is critical in providing oxygen as a substrate in energy metabolism. Regions of the brain are structured around perforating blood vessels, which are in direct contact with astrocytes. These astrocytes are integral in monitoring the neuron's environment. With increases in activity there is a decrease in fuel availability, causing the astrocytes to signal to the perforating blood vessels to dilate, increasing perfusion to that specific area. Disruption to any of these mechanisms may lead to altered brain function.

Transcranial Doppler and Single Photon Emission Computed Tomography have been used to evaluate more global and regional CBF, respectively, in several stages of concussion. Immediately following mTBI, there is an increase in CBF, particularly in temporal and frontal lobe areas [82]. Within a day of injury, there was an increase in middle cerebral artery blood flow velocity (responsible for changes in CBF), followed by a decrease in the following days relative to controls [83]. Examination of the middle carotid artery also revealed a low mean blood flow velocity [84]. In sub-acute and PCS stages of mTBI, there was hypo-perfusion of frontal and temporal lobes [57,64].

Other methods have also shown alterations in neuronal activation and regional CBF. In the thalamus, there was a decrease in CBF shown by an MRI technique, arterial spin labelling (ASL) [58]. This finding was correlated with processing speed, response speed, learning, verbal fluency and executive function in PCS patients. Similarly, in the pediatric population using perfusion-weighted imaging, a significant decrease in CBF in the thalami between 3 to 12 months post mTBI was found [78]. It has been suggested that regional decreases in CBF may be reflective of decreased neuronal activity, altered metabolism, and/or disruption of network functioning [85].

2.4.4 Alterations in Brain Function

2.4.4.1 Altered Hemodynamic Response

With neuronal activation there is an increase in metabolism, to accommodate for this the brain increases regional CBF. A way to assess brain function is to investigate whether following mTBI there are changes in the response to neuronal activation. fMRI has the ability to evaluate brain function by measuring deoxy-Hb concentration with a method called Blood Oxygen Level

Dependent (BOLD) imaging [86]. Alteration of the hemodynamic properties is reflective of neurovascular coupling or the relationship between an increase in metabolism due to neuronal activation and the corresponding increase in CBF [79]. Evidence in acute and chronic mTBI, of adult and pediatric populations have shown differences in activation patterns with control populations.

Alteration in brain function following mTBI can be seen within a week of injury. In a study of adults, comparison between pre- and post-BOLD revealed that mTBI subjects had an increased amplitude of activation during a finger sequencing task in the parietal, lateral frontal and cerebellar regions [87]. This alteration in brain response to task activation was evident without any effect on performance, suggesting that performance does not necessarily correlate with brain health. Interestingly, subjects (age 13-24) who demonstrated hyperactivation in medial, frontal and right temporo-parietal gyri during initial testing one week after injury were more likely to have a prolonged recovery [88]. Furthermore, this study found that lowered activation in the posterior parietal cortex was correlated with neuropsychological parameters on Immediate Post-Concussion Assessment and Cognitive Testing (IMPACT) testing, and cognitive and somatic symptom severity [89]. Similarly, hyperactivation in DLPFC, ventrolateral prefrontal cortex (VLPFC), and/or parietal areas, involved in working memory, have been correlated to subjective symptoms severity scores [90,91].

Symptom presence in the semi-acute stage continues to show evidence of altered response to brain activation. Brain activation in adult mTBI subjects in response to attention tasks demonstrated hypoactivation in several brain regions including right posterior parietal cortex, right VLPFC, thalamus and cerebellum [92]. In the pediatric population, the hypoactivation was also evident in the cerebellum and thalamus during task of spatial reorienting and inhibition

of return task [93]. During working memory tasks, mTBI subjects have shown disproportionate activation patterns in DLPFC and parietal cortex, depending on processing loads [94,95]. In working memory tasks all of these studies demonstrated increases in BOLD response outside of this network, suggesting that the brain is using compensatory mechanisms to achieve similar performance [90,91,94–97]. This allocation of resources has been evident in the pediatric mTBI patients during tasks of working memory and inhibitory control [98]. Although the activation patterns did not differ during working memory task, there was an increase in activation in the posterior cerebellum during the inhibitory task in mTBI subjects. This study however had a small sample size and large variation in days post- injury.

There is evidence of disruption in the hemodynamic response in patients with persistent post-concussion symptoms greater than one month after injury. Several studies using working memory tasks in adults and one in pediatrics have consistently identified hypoactivation in the DLPFC [99–103]. Decreased DLPFC activation was accompanied by increased activation outside typical regions involved in working memory [100]. Similar to acute mTBI, symptom severity was associated with lower BOLD signal activation in DLPFC [102]. Interestingly, asymptomatic subjects that previously showed decreased DLPFC activation, showed recovery in brain activation similar to that of control patients [99,101,104]. This has also been shown in subjects with no persistent symptoms within 6 months of the injury [105].

To summarize, there are alterations in patients who have suffered an mTBI and continue to have persistent symptoms. Some evidence suggests that Pperformance on working memory or neuropsychological tasks do not necessarily relate to brain recovery, as the brain uses other resources outside of typical networks to achieve the task at hand. Another method to explore brain function is by evaluating the functional connectivity of brain networks.

2.4.4.2 Functional Brain Connectivity

Fluctuations in the BOLD signal have been suggested to reflect neuronal activity of the brain. Functional connectivity in brain can be monitored by quantifying these regional fluctuations or oscillations in activity. These fluctuations have been shown to be synchronous between brain regions that make up functional networks in the brain [106]. fMRI data collected during subject rest (so-called resting-state fMRI) has identified a number of these brain networks. Resting-state analysis typically identify these networks through a variant of temporal cross-correlation, where the significance of the correlation implies the strength of the functional connectivity [107,108].

Most of the studies involving mTBI have evaluated functional connectivity in the default mode network (DMN), a network of brain regions that are active when the individual is laying at rest without paying attention to the outside world [106,109]. In adults, during resting state, the DMN have been shown to be altered following mTBI including changes in the strength and length of connectivity between normally synchronous brain regions [108,110–112]. Symptomatic patients demonstrated decreased functional connectivity in the DMN, however upon symptom resolution and follow up, the functional connectivity in DMN had recovered [113,114].

Studies of functional connectivity have not been limited to the DMN, but have also explored other brain networks. There has been evidence of disruption in inter-hemispheric connectivity in several networks including primary visual cortex, hippocampal, DLPFC, and parietal regions [115,116]. In another study, whole brain resting state network analysis found that there was decreased motor-striatal network connectivity that aligned with deficits in psychomotor and speed of information processing [117]. This study suggested that the

accompanying increase in functional connectivity in right fronto-parietal network could be related to increased post-concussion symptoms such as headache, fatigue or sensitivity to light and noise. Thalamic resting state networks were found to be disrupted in mTBI, with decreased functional connectivity to other brain regions in resting state and during task activation [118–120]. Interestingly, not all studies found that symptom recovery lead to resolution of functional connectivity in brain networks [120]. In this study, comparison at 6 months after mTBI of patients with PCS and those with symptom resolution found that there were alterations in patterns of long-range functional networks. However those with PCS have the greatest alterations in temporal and thalamic regions. Our understanding of long term alterations in brain activation and the importance of functional connectivity help to describe some of the underlying causes of brain dysfunction following mTBI.

2.4.5 White Matter Tract Alterations

Functional disruptions can be due to the underlying changes in brain communication pathways, the white matter tracts. There is evidence of structural damage using DTI which provides data on the integrity of communicating fiber tracks [121]. White matter tracts are important in transmitting information between left and right hemispheres, and studies have evaluated the internal capsule, corona radiata, inferior longitudinal fasciculus, forceps minor, cortico-spinal tracts, and genu and splenium of corpus callosum [76,122–135].

One particular measure used in DTI is Fractional Anisotropy (FA), which is the degree of water diffusion along a fiber that reflects fiber density and myelination in white matter. Higher FA values are reflective of larger diffusion of water in a particular direction, while lower FA values implicate less directionality. Twelve of fourteen studies found differences in FA values in

the corpus callosum in mTBI patients at various time points from 3 days to 1 year post injury, suggesting a possible imaging biomarker of PCS pathophysiology. The corpus callosum is a particularly susceptible to damage as the impact on the brain leads to translational effects on the hemispheres with an increased shearing at the corpus callosum [32]. Thus alterations are suspected to be evident at white matter tracts in the corpus callosum. Six studies concluded that FA values were increased in the corpus callosum [76,126,128,129,133,135]. Contrary to this, four studies reported decreases in FA values following mTBI [76,124,125,129]. However, two studies found that there were no significant differences between the control and mTBI group's overall, but when individuals were compared to controls they found changes that included either increased or decreased FA [136,137]. Furthermore, two studies found no differences in FA values in the corpus callosum in group and individual analysis [112,132].

Structural changes in white matter tracts from mTBI can affect brain connectivity in resting state and task specific brain network activation. The results indicate a wide variety of alterations, which may due to the heterogeneity of injury. Each injury could produce damage in different brain regions. Another explanation for the variability may be time after injury, type of injury, age, gender, region of the brain and methodology of the study [138].

There is some evidence of alterations in DTI measures in relation to symptom presence [125,139]. Increased FA and decrease apparent diffusion coefficient (ADC), a measure of diffusion within a tissue, in the corpus callosum was correlated with severity of post-concussion symptoms [125]. Whereas, decreased FA values in the uncinate fasciculus, corpus callosum, partial and frontal white matter were correlated with the severity of post-concussive symptoms [90]. Interestingly, lower FA values were also associated with worse memory scores [133].

2.5 Neurovascular Coupling

Regional blood flow and oxidative metabolism are linked through a regulatory process termed neurovascular coupling [79,140]. This relationship between metabolism and CBF was first described by Roy and Sherrington in 1890 [141]. When there is neuronal activation in brain through increased cognitive function, there is an increase in regional CBF corresponding on the increased need for oxygen requirements [140,142]. The response of the brain to activation by increasing CBF is known as the hemodynamic response. Increases in cerebral metabolic rate for oxygen ($CMRO^2$) are dependent on neuronal activation [143]. This increase in CBF is fractionally larger than the increase in $CMRO^2$, resulting in a decrease in deoxy-Hb and an increase in the oxygen saturation within the microvasculature. Figure 2-1 illustrates the relationship between metabolism, CBF and neuronal activation.

Factors that change network functionality, metabolic rate, or neurovascular coupling will change the relationship between brain activation and microvascular oxy-Hb saturation. This prediction forms the foundation of our hypothesis that measuring brain oxygenation will provide a novel biomarker of brain injury.

2.5.1 Main Methods to Explore Neurovascular Coupling

Neurovascular coupling is based on metabolism, CBF and microvascular oxygenation therefore we can explore neuronal activation in many ways. Figure 2-2 illustrates the relationship between metabolism, and CBF on deoxy-Hb and oxy-Hb concentration in the cortex following neuronal activation. This linkage forms the underlying mechanism for the fMRI BOLD response imaging [86]. Currently, fMRI has been the most widely used method to measure the hemodynamic response in the brain [86,144]. fMRI uses BOLD imaging to evaluate deoxy-Hb saturation in

response to neuronal activation. Based on neurovascular coupling, fMRI measurement of deoxy-Hb allows one to evaluate activation during cognitive and/or physical tasks. Another way to explore brain function has been looking at the temporal correlations of brain hemodynamic oscillations in brain regions that are related, termed functional connectivity [107].

Recently, another method called functional near-infrared spectroscopy (fNIRS) has become utilized in studying functional activation and connectivity in the brain. In comparison to fMRI, fNIRS has greater temporal resolution, but less spatial resolution and is limited to the outer cerebral cortex [80,145]. fNIRS calculates oxy-Hb and deoxy-Hb microvascular saturation by measuring light intensity through near-infrared light wavelengths that are specifically absorbed and scattered by Hb molecules [80,146]. A particular advantage of fNIRS is the possibility of evaluating brain function at the bedside, or even courtside. This relatively inexpensive method also allows testing to be completed quickly, without entering a loud MRI machine.

2.6 Overall Summary

It is important to study children who struggle with persistent symptoms which may have long term behavioural and development effects. The understanding of the acute pathophysiology of mTBI has been described through animal studies and further explored with newer neuro-imaging techniques that are sensitive enough to detect microstructural damage. There is evidence of long term changes in brain function in PCS as studied by fMRI BOLD and functional connectivity. In order to better understand PCS, we will apply fNIRS, a non-invasive imaging technique to study brain activation and functional communication.

Physical	*Cognitive*	*Sleep*
Headache	Feeling Mentally Foggy	Drowsiness
Nausea	Slowed Down	Sleep Less than Usual
Vomiting	Difficulty Concentrating	Sleep More than Usual
Balance Problems	Difficulty Remembering	Trouble Falling Asleep
Dizziness		
Visual Problems	*Behavioural*	
Fatigue	Irritable	
Sensitivity to Light	Sadness	
Sensitivity to Noise	More Emotional	
Numbness/Tingling	Nervousness	

Table 2-1. Symptom checklist for acute mild traumatic brain injury (mTBI)

Symptoms are grouped into physical, cognitive, emotional and sleep categories. These are typical and commonly acknowledged symptoms that occur acutely after mTBI that may suggest brain injury. The patient is asked whether they have any of these symptoms present immediately after injury. This chart is derived from the Center of Disease Control (CDC) [147].

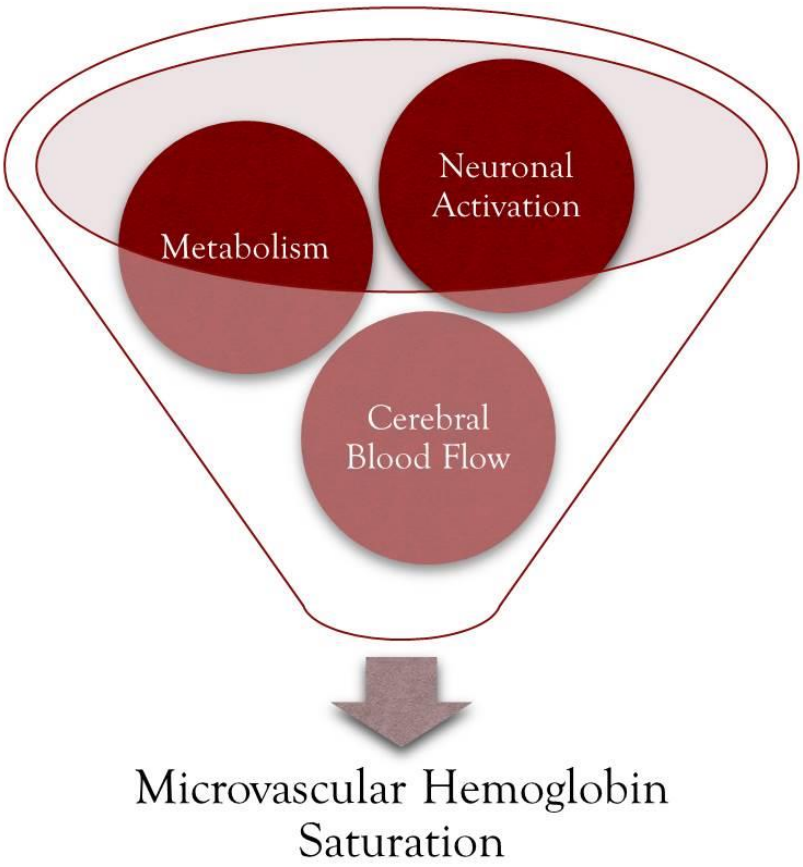

Figure 2-1. Components contributing to neurovascular coupling

This figure illustrates the complex interaction between neuronal activation, cellular metabolism and CBF. All of these factors affect and contribute to the microvascular hemoglobin saturation. Disruption to any of these factors will alter microvascular hemoglobin saturation, which can be measured by fMRI BOLD or fNIRS.

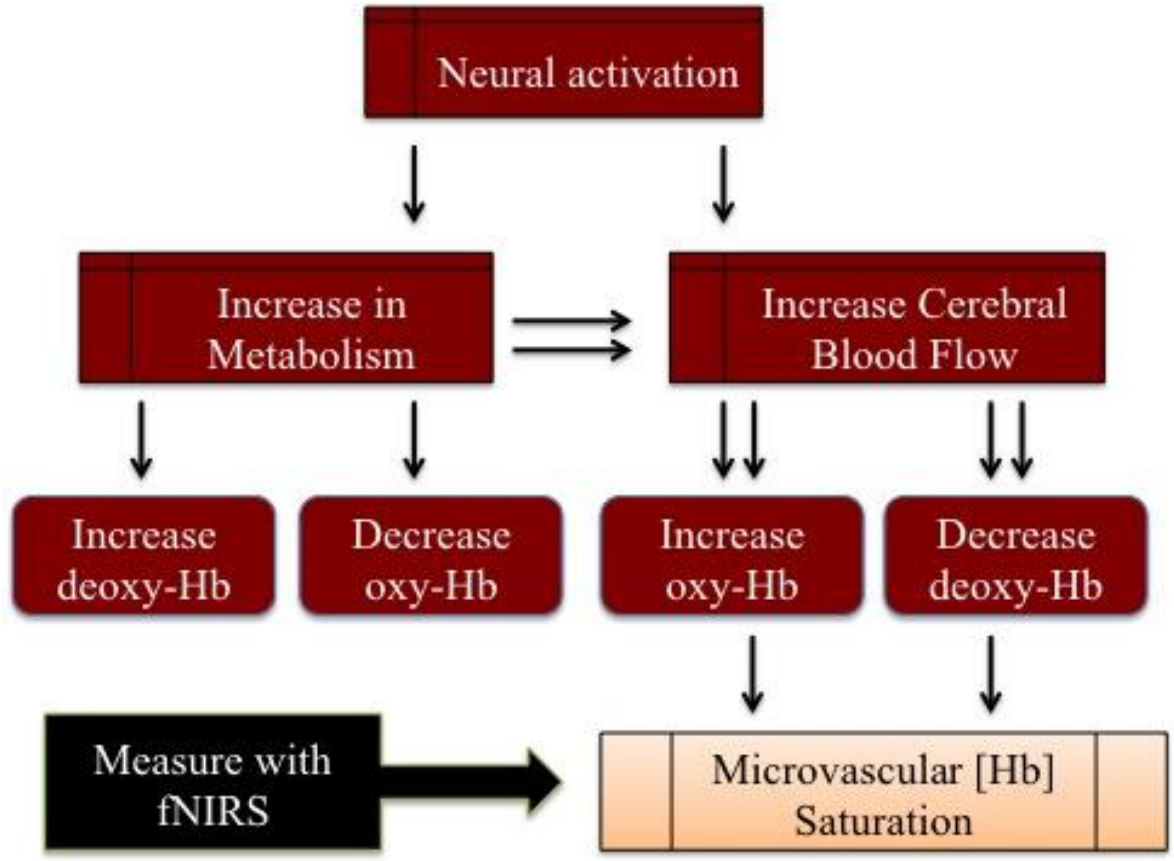

Figure 2-2. Microvascular hemoglobin saturation is changed by neuronal activation
An increase in neuronal activation leads to changes in microvascular Hb saturation which can be measured using fNIRS. Neuronal activation causes an increase in metabolism that utilizes oxygen to provide energy for the cell. There is an immediate decrease in oxy-Hb and increase in deoxy-Hb concentration that triggers an increase in regional CBF. The increase in CBF is proportionally greater than metabolic increase therefore there is an increase in oxy-Hb and decrease in deoxy-Hb that is much greater than utilized by the cell. With neuronal activation there is a greater increase in oxy-Hb that can be measured by fNIRS and fMRI BOLD.

Chapter Three: **Technical Aspects of Near Infrared Spectroscopy**

3.1 Chapter Overview

One method to investigate alterations in brain function following mTBI is by NIRS. Alterations in brain function can be detected using various imaging techniques as discussed in the previous chapter. NIRS can allow the monitoring of hemodynamic changes and also functional communication. As discussed in the previous chapter, there are disruptions in brain function following mTBI. These functional alterations may result in a wide variety of symptom presence and recovery of the brain may not coincide with standard neuro-psychological tests. There is evidence of hemodynamic alterations in task activation, along with reduced functional communication in brain networks. One possible way to monitor microvascular brain oxygenation and functional communication is by fNIRS.

In this chapter, I will start by discussing how NIRS systems use near infrared light to measures absorption and scattering, describe how continuous wave systems operate, explain the modified beer-lambert law, introduce coherence analysis to measure functional communication, and expand on the advantages and disadvantages of the fNIRS system.

The next part of the chapter will aim to describe the methods used to monitor and detect microvascular brain oxygenation including use of near infrared to detect concentration changes in chromophores, methods for data collection using the Continuous Wave (CW5) (built by Dr. David Boas and TechEn, Inc.), data analysis using a MatLab based analysis system called HomER (developed by Dr. Ted Huppert at Havard University), and coherence analysis (MatLab program developed by Dr. Brad Goodyear and PhD student Ali Golestani at the Seaman Family MR research center).

3.2 Near Infrared Spectroscopy

3.2.1 Using Near Infrared Light

Light has particular absorption and scattering properties that are dependent on the wavelength within the visible and non-visible spectrum. Absorption of light into body tissues is particularly high in the visible spectrum, however when approaching near-infrared wavelengths the absorption of light drops significantly [148]. The near infrared spectral range is between 650 and 950 nm, which can propagate a few centimeters into the cerebral cortex [149]. This phenomenon occurs as proteins, collagen, and water are weakly absorbed by near infrared light. Within the near infrared range or optical window, particular wavelengths are more sensitive to absorption by deoxy-Hb and oxy-Hb [150,151].

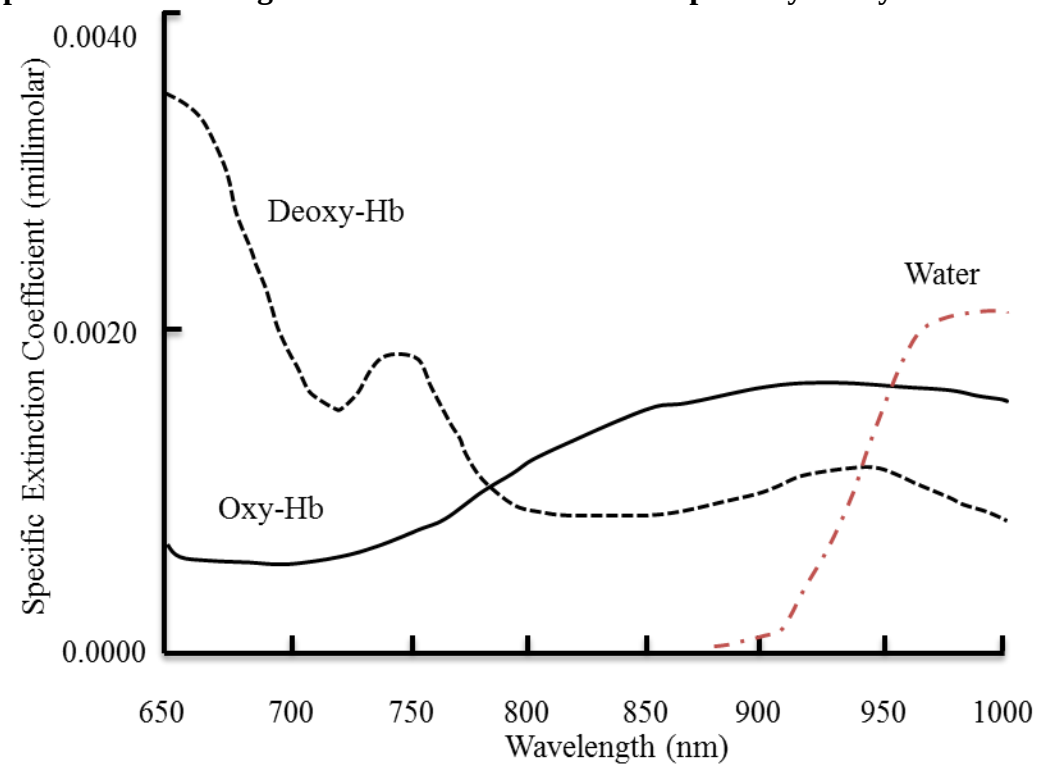

Figure 3-1 illustrates the absorption spectra of oxy-Hb and deoxy-Hb of near infrared light. Other substances within the optical window are at too low of concentrations to affect the measurement of oxy-Hb and deoxy-Hb [149].

The particular sensitivity of near-infrared absorption lies within the selection of wavelength. Water, which has a high concentration within the brain, which is greatly absorbed above 900 nm. At wavelengths above the 950 nm water is strongly absorbed and affects the

receiving measurements. Whereas, oxy-Hb and deoxy-Hb are better absorbed at wavelengths between 400-900 nm. Oxy-Hb absorption is stronger at higher wavelength, whereas deoxy-Hb at concentrations closer to 600-700 nm. By shining near-infrared light at a specific wavelength and known intensity, allows us to measure reflection of light. Applying this to the modified Beer-Lambert Law then gives us the relative concentration of chromophores over time (Gu et al., 2005; Sevick et al., 1991).

In fNIRS systems, multiple wavelengths can be chosen for measuring oxy-Hb and deoxy-Hb, where the signal to noise ratio is affected by the crosstalk between these wavelengths [146,152]. Wavelengths such as 830nm for oxy-Hb and 780 for deoxy-Hb have shown a low SNR due to high cross talk. In our fNIRS system, the wavelengths 830nm and 690nm for oxy-Hb and deoxy-Hb, respectively, are chosen. This pair of wavelengths have a high signal to noise ratio, with minimal crosstalk [153].

3.2.2 Types of NIRS systems

There are several types of NIR systems used including the Continuous Wave (CW), time-domain and frequency domain. The CW system obtains measurements of light intensity by applying light at a constant frequency and amplitude (Figure 3-2a). This particular type of NIRS system measures changes in optical density at a range of source detector pairs, allowing for mapping of cortical surface activity over time. The measurements are relative to the amount of optical density detected in the sources. In order to measure the absolute value of optical properties time domain or frequency domain NIRS systems would have to be used. The time domain system has this capability as it measures the time it takes for a photon to arrive after a short pulsation of light (Figure 3-2b). The frequency domain system measures light intensity

detection and phase shift by modulating light intensity being produced (Figure 3-2c). For the rest of my thesis the focus will be on the CW NIRS system that we utilized in our research.

3.2.3 Advantages

A key advantage of the CW system used in this study is the ability to detect data from all source detector pairs simultaneously, instead of turning on the source light to individual fibres in series. This is possible by having the amplitude of light modulated at each source fibre. Light in the detector fibres is differentiated into the respective source by undertaking a Fourier Transform of the incident data to increase the spatial resolution [154]. This allows one to differentiate light from each source fibre and gives the ability for mapping cortical activity with spatial resolution [155]. Another advantage of this CW system is the high temporal resolution involved with continual measurement. The system can detect fast changes in brain activation within seconds of brain activity. Some CW systems have the capability to be MRI compatible, offering multi-modal imaging options.

3.2.4 Disadvantages

One of the major disadvantages of using a CW system is that measurements can only be relative because the light scattering and absorption values are unknown. Due to this all values are relative and no absolute values of oxy-Hb and deoxy-Hb can be gathered. This issue will be further discussed in the section deriving oxy-Hb and deoxy-Hb concentrations.

3.2.5 Modified Beer Lambert Law

In order to extract oxy-Hb and deoxy-Hb relative measurements the modified beer lambert law is used. The Modified Beer Lambert Law was adapted from the original beer-lambert law to measure the relationships of near-infrared light [150,156,157]. The beer-lambert law did not take into account that light propagation through biological tissues is diffuse and does not follow a linear relationship [156]. Therefore the modified beer lambert law takes into account the additional distance caused by light scattering and the effect of different tissue mediums on light scatter. Thus the modified beer lambert law includes pathlength and partial volume correction in the differential pathlength factor. This law is used to explain light attenuation (including absorption and scattering) and the concentration of the chromophores through a medium:

$$\text{OD} = -\log \frac{I_f}{I_o} = \varepsilon \text{ CLB} + \text{G},$$

where OD is optical density (light attenuation), I_o is the incident (initial) light intensity, I_f is the detected (final) intensity, ε is the extinction coefficient of the chromophore, C is the concentration of the chromophore, L is the distance between of where the light enters the tissue and where the light exits the tissue, B is the pathlength factor that accounts for scattering also known as differential pathlength factor, and G is a factor that accounts for the measurement geometry. L is the distance between the source-detectors, while B or differential pathlength factor is determined by calculating pulse time length by a time domain instrument. Differential pathlength factors have been calculated for each specific tissue and at each light wavelength [150].

In this equation, extinction coefficient ε, B pathlength factor, G factor of measurement geometry and the distance L are based on head-cap arrangement, however OD and chromophore concentration changes over time. The change in optical density or attenuation is defined as:

$$\Delta \text{ OD} = - \log \frac{I_f}{I_o} = \varepsilon \Delta \text{ CLB}$$

There are particular wavelengths that are more sensitive to measuring particular chromophores such as 690nm and 830nm for deoxy-Hb and oxy-Hb, respectively. This is considered in the modified beer lambert law in order to calculate particular absorption of the specific chromophores. Thus light attenuation and wavelength are included in the final equation:

$$\Delta \text{ OD}^{\lambda} = (\varepsilon^{\lambda}_{HbO} \Delta [\text{HbO}] + \varepsilon^{\lambda}_{HbR} \Delta [\text{HbR}]) B^{\lambda} L$$

where λ refers to the wavelength measured and included concentration changes for oxy-Hb (HbO) and deoxy-Hb (HbR) individually. In this equation the molar extinction co-efficient are used, therefore the resulting concentrations are delivered in milliMolar (mM).

A limitation of the fNIRS system is not being able to absolutely Hb concentrations. NIRS experiments cannot measure the propagation of light through the tissues. Thus, modified Beer Lambert law adjustment for partial volume correction results in an underestimation of the oxy-Hb and deoxy-Hb changes in the cortex [156]. In order to account for the effects of scattering and partial volume there would be a need for knowledge of the individual's tissue volumes, and cortical layers. A way to minimize the effect is by properly selecting wavelengths to limit the amount of cross talk (discussed below).

3.3 Coherence Analysis

3.3.1 Understanding Functional Communication

There are brain regions that undergo spontaneous fluctuations of brain activity and those in synchrony comprise a functional network [106,107]. The strength of the inter-regional communication among these brain regions within a network is termed functional connectivity

[158,159]. Changes in functional connectivity are associated with changes in communication between regional networks, for instance several neurodegenerative diseases demonstrate a decrease in functional connectivity between brain regions in a network [160].

These changes can be reflective of a variety of alterations in the brain as metabolic, neuronal, CBF/perfusion, or structural damage to white matter tracts [15,161]. Intra-hemispheric connectivity is used to measure communication within the same hemisphere. This can include brain regions in close proximity (short length connectivity) or further away (long length connectivity). Inter-hemispheric connectivity is used to measure communication between corresponding brain regions in left and right hemispheres. Corresponding brain regions in left and right hemisphere are connected by white matter tracts through the corpus callosum. Disruption of inter-hemispheric connectivity may reflect white matter tract damage [162].

3.3.2 Coherence analysis explanation

Functional connectivity can be measured using a variant of cross-temporal correlation analysis or a coherence analysis. Correlation analysis is more commonly used however this method is limited by temporal components including delay of message transmission. In correlation analysis the frequencies are similar however there are phase shifts and changes in amplitude resulting in a low correlation.

In this thesis we applied a coherence of temporal frequency signal components. Coherence analysis is similar to the correlation analysis used in fMRI functional connectivity studies. Coherence uses a specific algorithm to compare the synchrony of coupling signals [163]. This algorithm can be used to study connectivity, as functional connectivity is known as temporal correlation between neuropsychologically related brain regions. The advantage of

coherence analysis is the comparison of two signals of the stability of temporal relationship without the effect of phase shift and amplitude changes. Phase shift and amplitude effect correlation analysis measurements, which is eliminated in coherence analysis. High coherence can occur in situations where there are differences in phase shift and amplitude but have similar frequencies. In coherence analysis, the signals are measured over time, thus coherence will change in responses to alterations in amplitude, frequency and phase over time.

Correlation analysis in fMRI was used to find brain regions in communication known as functional connectivity [159,164]. These particular regions are similar in frequencies and can be connected between different brain regions and between similar regions in the left and right hemispheres. Correlation is effected by vasculature in the brain which results in a temporal delay and phase shift as mentioned above. These factors reduce correlation and can be better analyzed by coherence analysis. Vasculature responses are critical in task activation and the use of coherence can eliminate temporal in-phase differences.

During coherence analysis, connectivity is measured by the oscillations in related networks that are phase locked [165]. Phase locked maintains that a neural signal (excitatory or inhibitory) arrives from one network at the peak activation (signal) to the functionally related signal. Coherence has an advantage in that the signals may be phase locked but are not necessarily in-phase, allowing for the time delay to occur. Coherence has been applied to fMRI, and electro-encephalogram (EEG) studies evaluating functional connectivity [163,166,167].

The frequencies of 0.04 to 0.1 hertz (Hz) range are the frequencies most typically used in fMRI and fNIRS motor cortex functional connectivity analysis [159,163,168]. fMRI relies on hemodynamic concentration measurements of deoxy-Hb therefore this analysis can be applied to optical imaging.

3.3.3 Coherence formula

Coherence analysis is calculated using a formula [163]:

$$Coh_{xy}(\lambda) = \frac{\left| f_{xy}(\lambda) \right|^2}{f_{xx}(\lambda)\, f_{yy}(\lambda)},$$

where (Coh_{xy}) is the coherence between the event-related time series of two given signals (x and y); $f_{xy}(\lambda)$ is the cross-spectrum of x and y; and $f_{xx}(\lambda)$ and $f_{yy}(\lambda)$ represent the power spectrum of x and y, respectively, at frequency λ.

3.4 Cortical Mapping

3.4.1 Continuous Wave Systems

The CW5, a laser specific system designed by TechEn.Inc in the United States was used for data collection (Milford, MA)[156]. The CW5 has a time resolution of 10-50 Hz, or the range for sample rate. There are 4 to 48 possible laser sources, where one source includes the wavelengths of 830 nm for oxy-Hb and 690 nm for deoxy-Hb which are emitted together onto the head (Figure 3-3). The system uses the Frequency multiplexing method to distinguish signals from different sources and wavelengths. This means that the diodes are continually turned on and the diodes are modulated in a different frequency.

In the CW5, there are 32 avalanche photodiodes used as light detectors, and the data collected is based on cap design. The near infrared light is guided by the fiber optic bundles to probes located placed on the head in a particular formation. Near infrared source is modulated at 200 Hz between frequencies of 6.4 and 12.6 kHz. The cap design typically allows for detection of 3 to 4 detectors to 1 source dependent on the head cap set-up. The distances between the

source-detector pairs is variable and can be adjusted however, the smaller the distance the greater depth penetration into the brain thus most head caps takes this into consideration in order to increase the amount of cortex being measured [169]. Figure 3-4 illustrates the possible photon path-length that can be taken during NIR sampling. Data sampling from detectors is sampled at 41.7 kHz onto data acquisition cards (National Instruments NI6062E).

3.4.2 Current Uses of fNIRS CW Technology

There has been a wide application of fNIRS to the study healthy brain function and several brain disorders [170,171]. The development of fNIRS technology has been matched with increased use in clinical settings, particularly due to its easy applicability and portability. fNIRS is not limited to investigating the hemodynamic response, it also has the capability to calculate functional connectivity [171,172]. Validation of fNIRS measurements has been completed through comparisons to BOLD fMRI [173,174]. It was found that oxy-Hb concentrations were highly correlated to BOLD measurements administered simultaneously.

Currently the largest application of fNIRS includes studying behavior and cognition in children and infants, stroke, brain injury, epilepsy, depression and schizophrenia [171,175]. Important advances in our knowledge of brain development will come from fNIRS studies. It is difficult to understand brain activation due to motion artifacts in fMRI studies, whereas fNIRS studies allow the participant to move with the headcap tightly secured. Several brain regions have been investigated as the frontal (DLPFC and VLPFC), parietal, temporal and occipital lobes [171]. Similar to EEG and fMRI, functional connectivity has been used to study lateralization of activation from infants to adults [176]. There have been developmental studies conducted in intensive care unit finding that children with Down's syndrome have lower connectivity [177]. A

fNIRS study of multiple sclerosis found decrease in functional connectivity between hemispheres during resting state and task activation [178]. The method has even adapted to study brain function while participants were biking outside [179]. These technological advances could provide us of information on the most complex processes in natural settings that our brain encounters. The ability of fNIRS to be used in multiple settings also gives us the opportunity to study brain function while individuals undergo rehabilitation.

3.5 Localization

3.5.1 Probe Localization

The head cap was designed for placement over the motor cortex in the left and right hemispheres. A study by Varshney et al (2010) in adults, established that placement based on measurement of a distance 40% between the eye brow and occipital bone anteriorly was accurate 100% of the time in correctly placing over the motor cortex as shown in Figure 3-5 a. These measurements were verified in the study as accurate due to prior studies completed by EEG system of Electrode Placement [142,180].

In total, the use of 16 detectors and 16 sources may be combined for 28 pairs allowing creating a cortical map of the underlying cerebral cortex. The cap was designed for each hemisphere separately including 4 sources and 8 detectors (Figure 3-5b,c). The source detectors are placed 2.5 cm apart in order to gain light penetration of 2.5 cm into the underlying skull and brain. The cap has spacing to allow removal of underlying hair to maximum contact between the skull and probes. To verify, a heart rate frequency can be measured at above 1.0 Hz. The cap was secured into place by Velcro straps attached to the plastic (bendable) cap with probes.

3.6 System Safety

fNIRS safety is dependent on selection of power being emitted through the sources. One way is to set the optical power to an appropriate level at which there will be no tissue heating. Tissue heating can cause discomfort to the subject however the CW5 has pre-set optical power levels to prevent any possible discomfort to the individual [181]. In our study, the optical power per source has been adjusted to between 2-3.5 mW for each wavelength. However we have the option to adjust the power up to 9 mW without any discomfort.

3.7 Data Collection

3.7.1 Raw Data Collection

Raw data collection is initiated by the researcher upon selection of record data option. This is completed after source-detector and head cap configuration is finalized. Each source contains a fiber with a laser wavelength of 690 λ and 830 λ. The CW5 program applies a bandpass filter to decrease the noise of system. The data is then converted from analog to digital and output is illustrated on computer for user (illustrated in Figure 3-6). Based on the data collection we can then adjust data collection to increase signal to noise.

3.7.2 Source-Detector Set up

Head cap set up is critical in data collection as placement determines the final cortical areas being analyzed. Once the head cap is strapped into place on the participant's head then the calibration process takes place. The CW5 data collection program (TechEn. Inc.) has a calibration process where a file specific to the set up of the sources and detectors is selected to ensure that the desired sources/ detectors are turned on. The program demonstrates the fourier

plot for each detector. The autonomic gain control (AGC) is selected to adjust the power elicited by each source, this may account for some of the lost signal due to hair type (example darker hair). By selecting AGC increases the amplitude of the peaks in correspondence to the source frequencies. Next, each detector is analyzed individually to ensure the detector is receiving the signal. If the signal does not provide an adequate fourier plot (with specific pattern) then the experimenter has the ability to adjust the source and detector. Some ways the experimenter can do this is by moving any hair between the sensor and skin out of the way, and/or tightening the headcap to ensure contact. Once each detector is calibrated and sensor signals are satisfactory, the test can begin.

3.8 Data analysis

3.8.1 Raw Data Analysis

Data collection is saved to the computer every 30 seconds as it is collected at 41.7 kHz by each detector. Once data collection is completed the raw data filtering on 'DOS' can begin. The files are saved as extensions: '_0A00000.bin' for left and '0B00000.bin' for right hemisphere extensions. The file name is pre-selected prior to data collection. In DOS, the raw data is demodulated to remove laser carrier frequencies, next a Butterworth low-pass filter removes the high frequencies and then down-samples the data from 41.7 kHz to 100.15 Hz. This process results in the ability to detect frequencies up to 50 Hz.

The next step required prior to data processing is to arrange the data into specific matrices and simultaneously aligns source-detector geometry for the data set. This is completed in a MatLab program written by Ted Huppert (Harvard University, part of Dr. Boas' laboratory).

Here the data can be further down-sampled to 10 Hz, or maintained at 100 Hz. This is the last preparation needed prior to importing data into HomER, a data processing system.

3.8.2 HomER – Data Analysis

HomER, is a MATLAB based data analysis program designed at Massachusetts General Hospital, that is available open source for download. In order to complete the analysis, source-detector pair geometry is formatted to imitate the measurements and coordinates that were used in the cap. The program does a Fourier Transform to the data in order to locate source-detector location. Here we can look at tomographic maps for delta optical density, oxy-Hb, deoxy-Hb and total-Hb based on individual measurements, average of all source detector pairs, each individual source-detector pair, averages of resting state and task activation and compare among each parameter. The program is capable of signal processing and contains tools to apply filters for time course, band pass filters, motion artifact correction, and systematic fluctuation removal (options show in Figure 3-7). The hemodynamic response is imported in optical density (OD), and the delta-OD (dOD) can describe the intensity changes associated with absorption and scattering (Figure 3-8a). For relative values of total-Hb, oxy-Hb, and deoxy-Hb the program applies the modified beer lambert law (Figure 3-8b). Oxy-Hb and deoxy-Hb values are measured directly through the relative absorption and scattering of the wavelengths. HomER calculates total-Hb through the addition of oxy-Hb and deoxy-Hb signals.

Another feature of HomER includes image reconstruction (tomographs) based on event or block designs can be calculated with temporal selection to generate cortical activation maps. Figure 3-9 demonstrates the magnitude of activation at each source detector pair (mapped to

form over cortical area), therefore it is possible to locate the motor cortex area responsible for tapping.

3.8.3 Coherence Analysis

In order to complete coherence analysis we use HomER to save each source data separately. Each source is saved with its detector pair information for resting state, task activation and for either hemisphere as a MatLab file. Coherence analysis is completed by comparing each source detector pair to a chosen region of interest In this case it is selected based on the source-detector pair with greatest magnitude of activation during tapping. Each source-detector pair can then be compared to the reference seed. Another parameter selected in the coherence analysis is the frequency ranges. Heart rate is detected in the frequency of 0.8-1.7 Hz, therefore similar to fMRI analysis we chose the frequency band of 0.04-0.1 Hz for coherence analysis (Sun et al 2004). Higher frequencies between 8-10 Hz, 10-50 Hz have been used to study fast optical signal or event related optical signal.

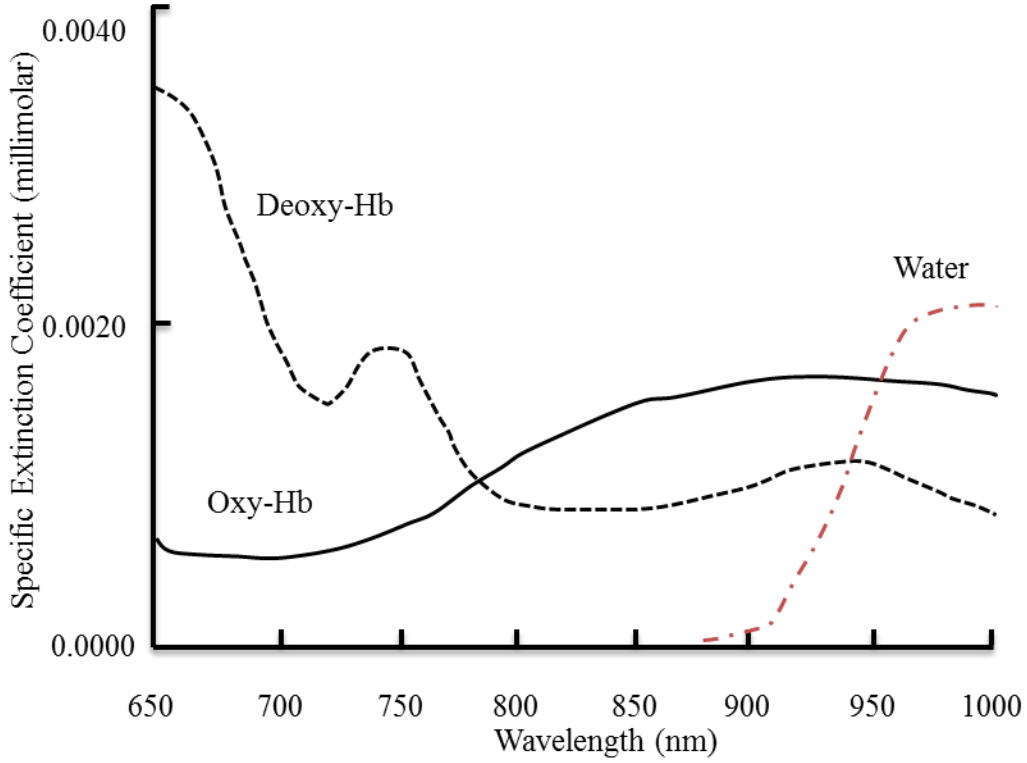

Figure 3-1. Absorption spectra of chromophores

The absorption of oxy-Hb, deoxy-Hb, and water are illustrated for wavelengths between 650 and 1000 nm. The NIR optical window lies between 650 and 900 nm. Deoxy-Hb (dotted line) is more sensitive to wavelengths closer to 700 nm. Oxy-Hb (solid line) is more sensitive in the 800-850 nm range. Also represented is absorption spectra of water (red dashed line) which rises around 870 nm. (adapted from [151,182])

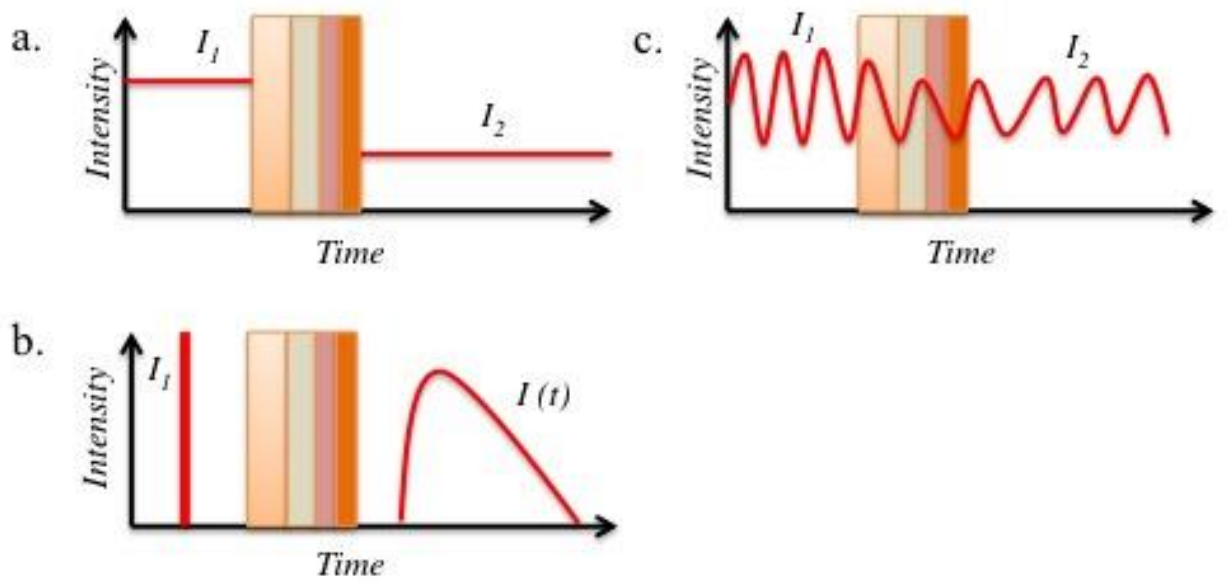

Figure 3-2. Types of fNIRS systems

Illustration of fNIRS system types and signal delivery methodology. The light intensity is on y-axis and time on x-axis. As light is emitted it propagates through tissues: skin, skull, cerebro-spinal fluid, and into the cerebral cortex. The pathlength is dependent on the tissues which is highly variable amongst individuals and affects the light intensity measured. (a.) Is an example of a continuous wave (CW) system where transmission light intensity is constant and detectors measure relative absorption of light intensity. (b.) A time domain system emits a light impulse and measures time for photons to arrive at detector. (c.) A Frequency Domain system modulates light intensity, allowing for phase shift measurements which can be used to calculate pathlength. *I_1: Light intensity administered from NIRS system; I_2: Light intensity after passing through tissues; $I_{(t)}$: Temporal point spread function for frequency domain function.*

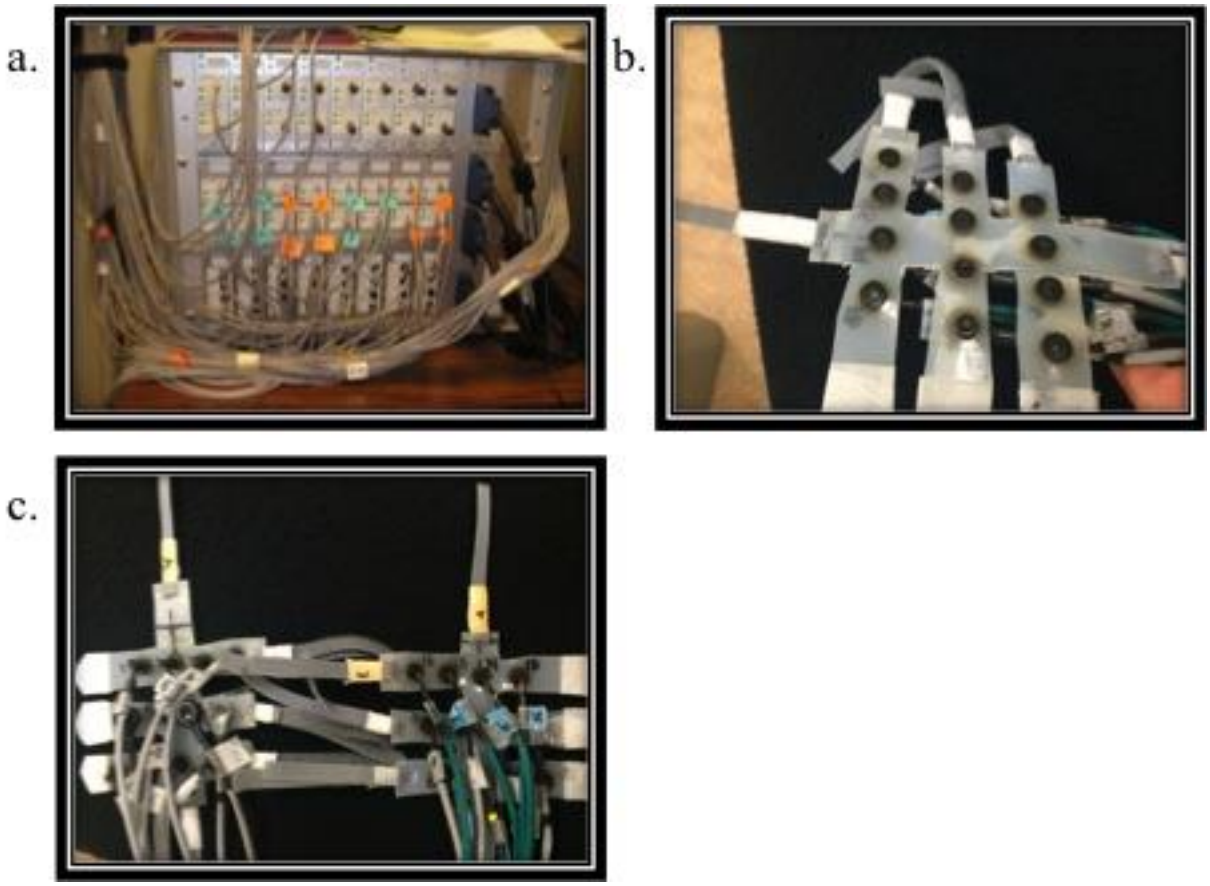

Figure 3-3. The CW5 fNIRS system

a. In this picture is the CW5 system used at the Alberta Children's Hospital. Detectors and sources can be seen extending from the machine. Top row of optodes are detectors, bottom row is the sources with 690 and 830 nm wavelength specification.

b. The image is of the optodes ending to which connects to the head. The bottoms of the optodes protrude beyond the head cap to bypass hair, which is moved aside during head cap placement.

c. Image of source-detector optodes inserting into semi-rigid headcap to keep distance between optodes consistent. Optodes are flexible and can be easily moved and bent allowing for a comfortable wear.

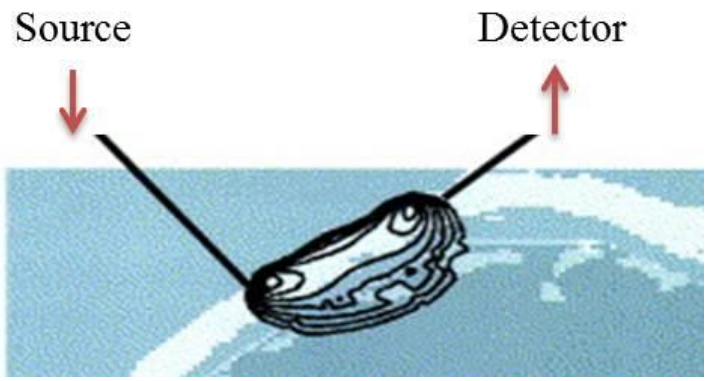

Figure 3-4. Example of the path near-infrared light takes form source to detector in CW5 system

The colors, red and yellow indicate a high number of photons detected at a given point; blue and purple indicate low sensitivity or low amount of photons reaching the medium. b. Light propagation through the skull, cerebrospinal fluid and into the gray matter of the cerebral cortex. The lines are indicative of the banana shaped voxels that are measured using fNIRS. (adapted from [182])

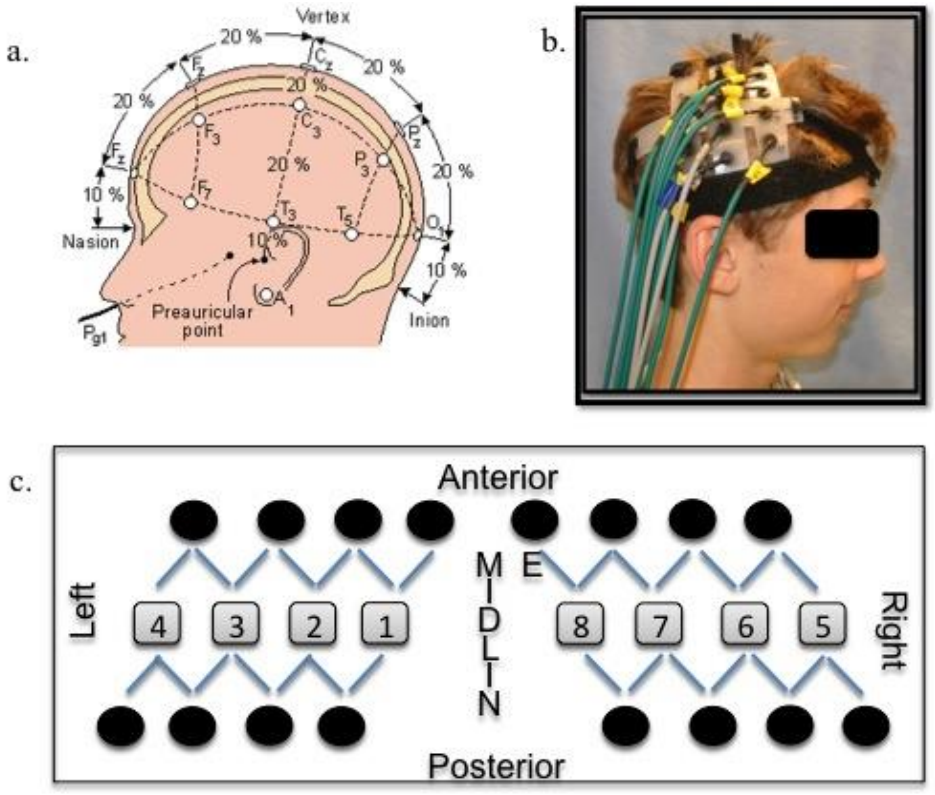

Figure 3-5. fNIRS head cap positioning and preparation

a. An EEG map (Retrieved from http://www.edfplus.info/), where placement of our head-cap was based from; Varshney et al, 2012, completed the initial experimentation. F- frontal pole, A- auricular, O-occipital, P-parietal, T-temporal, Fp- fronto-polar and C- central. The anterior placement of head cap is 40 from the naison.

b. Example of head-cap placed on patient. The cap is secured into place with a Velcro band. Patient is comfortable, as the head-cap and attached optodes are light and can bent to accommodate any position.

c. Illustration of our head-cap design for left and right hemisphere. The source-detector pairs are 2 cm apart. Here you can see the source-detector pairs; there 3-4 detectors per source.

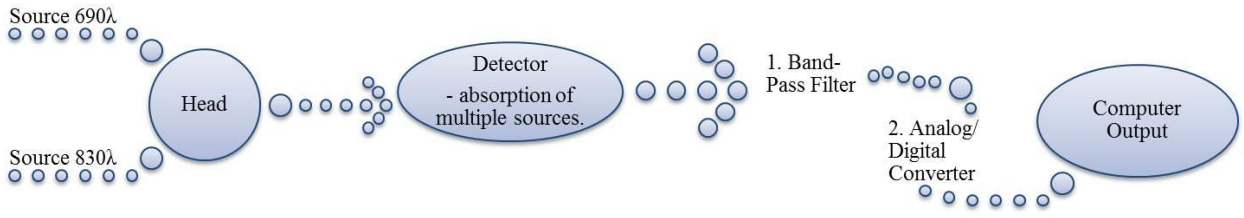

Figure 3-6. Data collection paradigm

Source probe provides a dual wavelength near-infrared light into head, through which the light is scattered and then measured by the detector. Multiple sources are collected by the detector. A band-pass filter is applied to remove noise. In order to be used by a computer the data is converted to digital from analog signal. The data is now ready for interpretation.

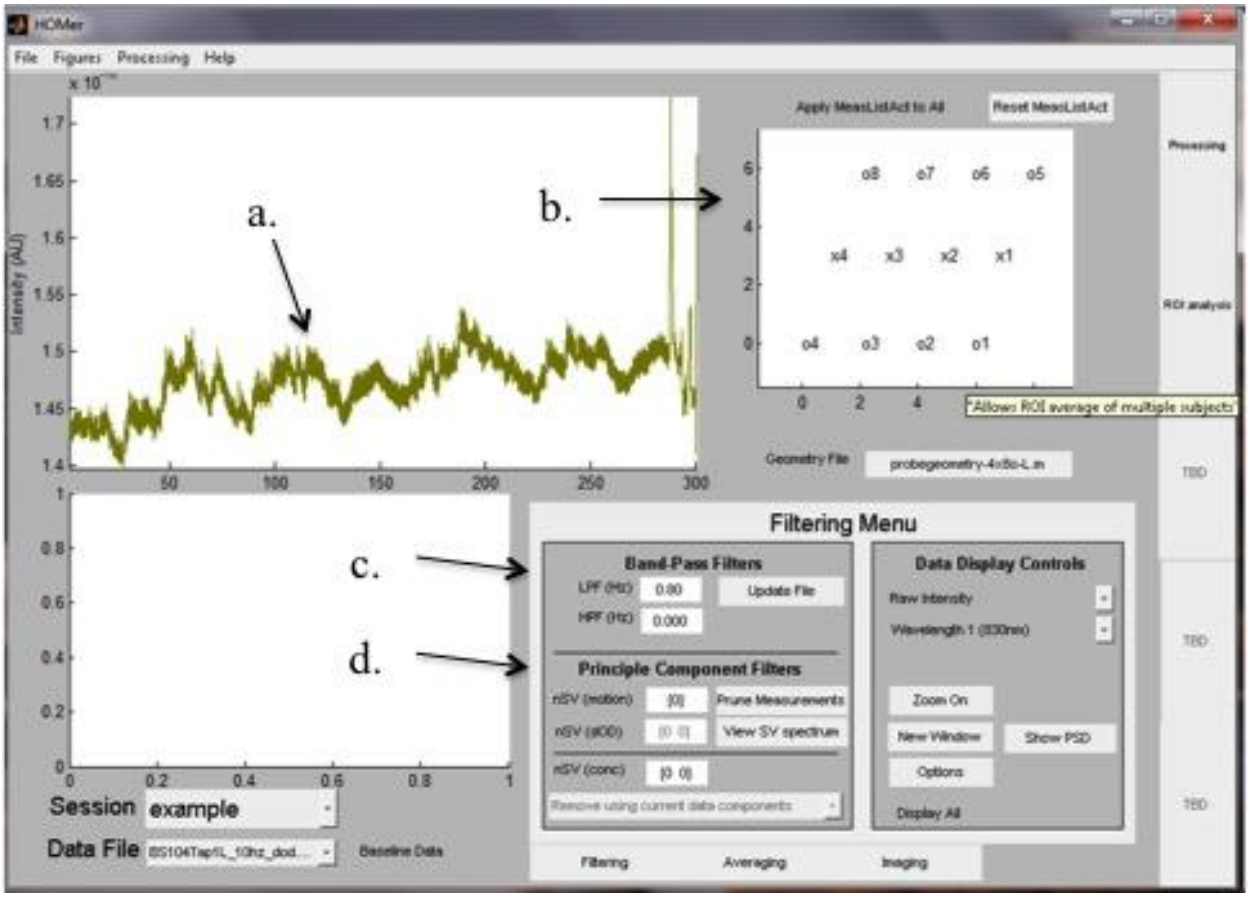

Figure 3-7. Screenshot of the HomER processing system

A screen shot of HomER as initial data is imported.

a. Average intensity of signal of all source-detector pairs over time (seconds).

b. The source-detector map of the left-hemisphere head cap is illustrated. The head cap is pre-set prior to being imported into HomER using MatLab.

c. Bandpass filters including low and high pass filters. Our data using a 0.8 Hz low pass filter to eliminate any physiological data that may affect the signal to noise ratio.

d. Principle Component filters can be set to eliminate any irrelevant signal such as shown in a. at 290 seconds. This signal could be due to head excessive head movement of patient.

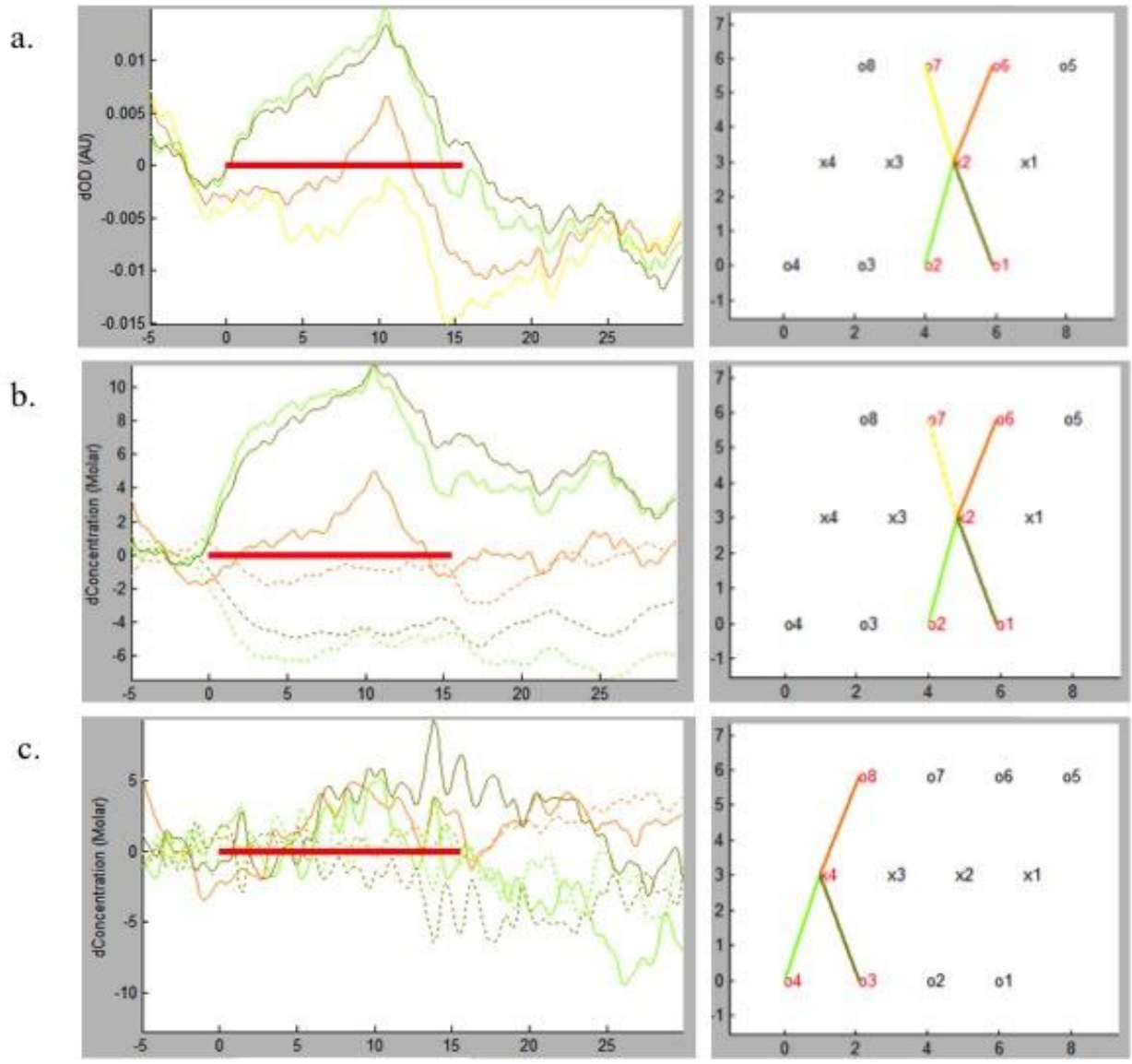

Figure 3-8. Average hemodynamic response and corresponding source-detector pairs

a. Example of dOD from one subject during on – off tapping task. The right chart depicts the chosen source detector pairs used for averaging of data. In this sample source 2, detector 1 and source 2- detector 2 show greatest activation during the tapping paradigm. The red line depicts time of tapping.

b. Example of concentration total-Hb (line) and deoxy-Hb (dotted line). Colors still correspond to the source-detectors pairs chosen.

c. Example of data lacking task activation. In this example different source-detector pairs were chosen to illustrate cortical area not involved in the finger tapping. This data would not be used for region of interest or hemodynamic response calculations.

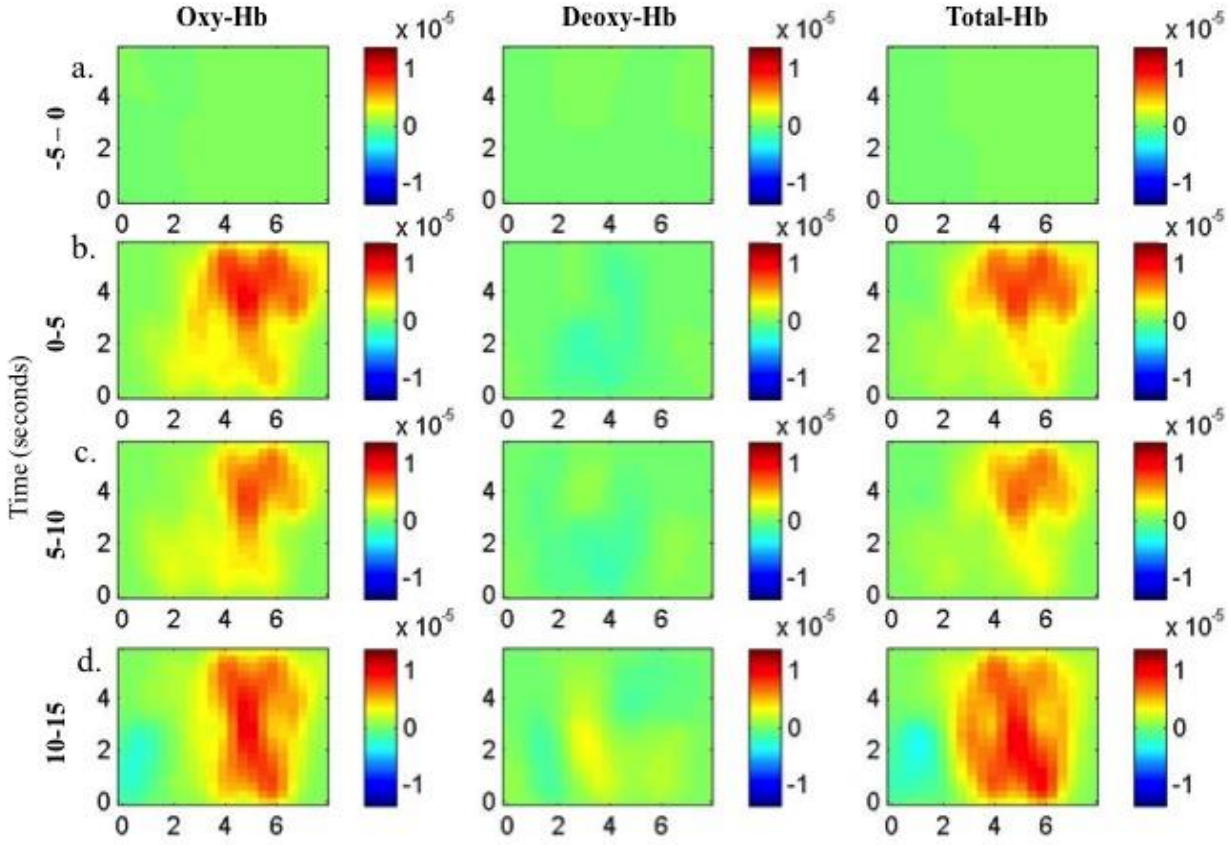

Figure 3-9. Single control subject example tomographic maps

Each tomograph is depicted for an average activation based on time during the data collection for all source detector pairs. The first column corresponds to the magnitude in activation of oxy-Hb, second is for deoxy-Hb and last column is for total-Hb. Each tomograph is based from measurements during selected times as: a. -5 to 0s is prior tapping, b. 0-5s during tapping, c. 5-10s and d. 10-15s. Red colors signify activation or greater concentration, which is evident during tapping in oxy- and total-Hb. The colors are measured in magnitude based on molar units ($x10^{-5}$). The tomographic maps are arranged on source-detector pairs, therefore you can localize the activation of the motor cortex during tapping. The x-axis is the distance (cm) from anterior to posterior, and the y-axis is the distance (cm) from medial to lateral on the head.

Chapter Four: **Methodology**

4.1 Research Question and Rationale

The first objective of this study was to establish whether fNIRS is capable of detecting functional alterations in response to task activation in children with PCS. To evaluate this we compared the magnitude of activation during a tapping task in M1 between control and mTBI subjects. We hypothesized that PCS children will have decreased hemodynamic responses with task activation in the motor cortex.

The second objective of this study was to assess alterations in brain communication between controls and PCS patients using a coherence analysis. Intra-hemispheric and inter-hemispheric connectivity was compared during resting state and task activation in M1 between controls and mTBI participants. We hypothesized that there is reduced inter-hemispheric coherence in patients with PCS as compared to controls.

4.2 Study Design – A cross-sectional observational controlled study

4.3 Participant Recruitment

4.3.1 Target Population

Children between 12-18 years of age were recruited to take part in the studies. Patients with diagnosis of persistent PCS symptoms were recruited from the Alberta Children's Hospital. Controls were recruited through friends, email, flyers and the healthy control program (HICCUP) at the Alberta Children's Hospital. The protocol was approved by Conjoint Health Research Ethics Board at the University of Calgary (E-20287).

4.3.2 Inclusion criteria for mTBI patients

1. Neurologist confirmed diagnosis of mTBI defined as any direct or indirect biomechanical force resulting in a change in neurological state without the following: loss of consciousness for more than 30 minutes, focal neurological deficits, and/or post traumatic amnesia for more than 24 hours [2].
2. Right handed as assessed by self and parent report.
3. Persistent symptoms present one month after mTBI in PCS patients.
4. Between the age of 12-18
5. Informed consent and assent.

4.3.3 Exclusion Criteria for mTBI patients

1. Previous significant medical history (e.g. hormonal disorders, diabetes, liver or kidney disease, cerebral palsy, seizure disorders, hypertension) or as advised by specialist
2. Present or past alcohol or drug abuse
3. Previous diagnosed concussion within the last 6 months
4. Use of neuro-active drugs

4.3.4 Recruitment

Participants were recruited from Brain Injury Clinics, or the PLAYGAME study at Alberta Children's Hospital [183]. Brain Injury clinic patients and parents were approached following their appointment by student researcher to explain the research study and given time to consider participation. The patient and parent than were given time to read over consent, discuss among each other and ask any questions pertaining to the study. Secondary recruitment was through Dr.

Karen Barlow's PLAYGAME research study, which includes patients with persistent PCS. The study is a double-blinded melatonin treatment study in children with PCS. Following participation in the study patients were approached and asked to consider if they would like to participate. In order to part-take in the study informed consent and assent needed to be completed.

4.4 Study Design

4.4.1 Participant Questionnaire

Patient demographics, injury details, and past medication were collected using a standard questionnaire. The participants were asked if they experience any of the following symptoms within the last few days (yes or no) within physical, cognitive, behavioural and sleep categories. Physical symptoms included headache, nausea, vomiting, balance problems, dizziness, visual problems, fatigue, sensitivity to noise, sensitivity to light, and numbness or tingling. Cognitive symptoms included feeling mentally foggy, slowed down, difficulty concentrating and difficulty remembering. Behavioural symptoms included irritability, sadness, more emotional and nervousness. The last category was sleep including drowsiness, sleep less than usual, sleep more than usual and trouble falling asleep.

The Rivermead Post Concussion Symptoms Questionnaire (Rivermead) was used to document the number and degree of symptoms present in relation to their pre-injury symptom status (see appendix 1) [184]. The Rivermead is based on a likert-scale questionnaire including symptoms categories of physical, cognitive, sleep and behavioural categories. The likert-scale was from 0 to 4, 0 with no symptoms present and 4 significantly worse. The participants were asked to compare the symptoms to how they were compared before the accident. Although the

scale is not considered up to psychometric standards, the scores were similar to Post Concussion Symptom-Inventory (PCS-I) in a pediatric population [5].

4.4.2 Study Procedure

To begin, the headcap was positioned, calibrated and participants were comfortably seated. The patient then underwent a 5 minute (300 seconds) resting state measurement of which they are asked to sit in silence in a chair with eyes open, and asked to refrain from any movement. Next the participants completed a 5 minute on and off interval tapping task, of which they are sitting still for 30 seconds and then cued to being tapping with the right hand (left hemisphere activation) for 15 seconds. The subject is then cued again to seize tapping and return to resting state for 30 seconds. The tapping is completed by tapping index and middle finger to thumb at a frequency of 1 Hz to the beat of a metronome.

4.4.3 Sample Size

As this is a pilot study, this was a convenience sample achieving at least 10 participants in each group. In order to complete our objectives, our goal was to test ten PCS and control patients each group. For protocol one we tested: 19 PCS patients and 10 controls.

4.4.4 Outcome Measures

1. Time since injury (days), mechanism of injury, previous mTBI, sports participation, and types of symptoms present
2. PCSI to evaluate degree of current symptoms

3. Measure the magnitude of activation through Hemodynamic response by change in total-Hb, and oxy-Hb
4. Coherence values within and between hemispheres during resting state and task activation for total-Hb, oxy-Hb, and deoxy-Hb.

4.5 fNIRS Protocol

4.5.1 Headcap Placement

The head cap was designed for placement over the motor cortex in the left and right hemispheres. A study by Varshney et al (2010) in our lab established that placement based on measurement of a 40% distance between the eye brow and occipital bone anteriorly. These measurements were verified in the study as quite accurate due to prior studies completed by EEG system of Electrode Placement [142,180]. Tapping task was used to verify that the head-cap was covering the motor cortex.

The cap was designed for each hemisphere separately including 4 sources and 8 detectors. The source detectors are placed 2.5 cm apart in order to gain light penetration of 2 cm into the underlying skull and brain. In total the use of 16 detectors and 16 sources to combine for 28 pairs was used to create a cortical map of the underlying cerebral cortex. The cap has spacing to move the underlying hair to increase maximum contact between the skull and probes. To verify this a heart rate frequency can be measured at above a frequency of 1.0 Hz. The cap was secured into place by Velcro straps attached to the plastic (bendable) cap with probes. Verification of probe contact to head was completed in the CW5 data collection program.

Each detector is isolated to evaluate the frequency patterns through a log-fourier view. Poor contact between the source/detectors and the skin could be identified as a lack of signal for

a fibre pair. Successful probe contact was evident with several peaks appearing on the Log-Fourier display window corresponding to the amount of sources the detector is collecting data from. The gain can be adjusted in order to be able to identify the peaks from the noise by selecting the automatic gain control (AGC).

4.5.2 Magnitude of Hemoglobin Concentrations

Table 4-1 includes data collection process and analysis. After down-sampling of data into delta optical density measurements it is then applied to the modified beer-lambert law within the HomER MATLAB program (Huppert 2009). A low pass bandpass filter is applied at 0.8 Hz to remove physiological oscillations from our data (shown in Figure 4-1).

Figure 4-2 is an individual example of calculated concentrations for complete data collection and averages of the 6 tapping sessions. The oxy-Hb, and total-Hb is used to choose the seed-detector pair with highest activation during motor task (tapping) on the ipsilateral side. To analyze the magnitude of the hemodynamic response the chosen source-detector pair plus three anatomical adjacent pairs are used to calculate relative concentrations. The resting state concentrations are then averaged for the source-detector pairs using 5 second prior to beginning motor task. Each individual will have variability resting state levels therefore here we need to measure each magnitude of changes based on subtracted the task activation relative oxy-Hb, and total-Hb levels in the last 10 seconds of the tapping task. The last ten second of the tapping task are used as there is a time to activation that is roughly 2-3 seconds following initial of the task. Furthermore, there is a period of overshoot following cessation of the task, therefore we will analyze the data points prior to task activation to give us a better measurement of resting state level.

4.5.3 Tomographic Maps

Tomographic maps were synthesized for participants during task activation in the right and left hemisphere. Time points collected including 5 seconds prior to beginning tapping during resting state, 0-5 seconds, 5-10 seconds, 10-15 second, 0-15 seconds during tapping and 15-25 seconds after tapping ceased. These maps are visual presentations of the hemodynamic response. The maps include all source detector pairs averaged over the 6 tapping sessions of the hemodynamic response. Maps can be represented by wavelength (830 λ for oxy-Hb; 690 λ for deoxy-Hb) in delta-optical density (dOD) or by oxy-Hb, deoxy-Hb and total-Hb concentration measurements following calculation by modified beer lambert law. The maps give an idea of the source-detector specific activation during task activation. Figure 4-3 provides an example of dOD tomographic maps during tapping that are used to investigate possible source-detector pair with the largest magnitude of activation. Figure 4-4 is an example of source-detector selection based on oxy-Hb and deoxy-Hb activation during tapping. We chose to use oxy-Hb concentration to choose our source-detector pair with greatest magnitude of activation.

4.5.4 Coherence Analysis

To obtain values of coherence, the source detector pair with largest activation of total-Hb and oxy-Hb during the tapping task (motor cortex activation) will be chosen as analysis seed. This seed was compared to all other source-detector pairs. The analysis is performed in MATLAB and provided coherence maps of left and right hemisphere activation [185]. In this case we used a band range frequency of 0.04 to 0.1 Hz which has been used previously for studies of brain region functional coherence with fNIRS [178,185].

Coherence values are compiled by averaging data from surrounding 3 source-detectors pairs of the chosen seed on the ipsilateral side. Data in the right hemisphere (contralateral side) are calculated from the four source detector pairs that are anatomically similar. Values of 0.0 are indicative of no linear relationship between two signals, whereas values of 1.0 correspond to a complete linear relationship. The chosen seed pair is not used in the coherence analysis because it has a value of 1.0.

Completion of coherence analysis will be completed in a pre-written Matlab program (Dr. Goodyear Lab). The Matlab program is written specifically for the data retrieved from the CW5 machine used in our studies. In order to use this formula there must be a selection of the source-detector pair. The seed or region of interest is chosen by identifying the source-detector pair with highest magnitude of activation during finger tapping. Coherence is then completed by comparing each source detector pair to the pre-chosen seed.

4.6 Statistics

Mean, standard deviations and ranges were used to describe the samples. The Kolmogorov- Smirnov test was used to test for normal distribution of the ages between groups. This test is a non-parametric test which considers whether the groups were similar in distribution. The null hypothesis is considered to have continuous distribution between groups. The Chi squared test was used to determine whether gender was equally distributed.

For hypothesis 1, between-group chromophore magnitude of change (Δ-total-Hb, Δ-oxy-Hb) during motor task performance were compared using Student's t-test, with a P-value set to 0.05. To determine inter-hemispheric connectivity, differences in mean coherence between hemispheres and participant groups were compared using two-way Analysis of Variance

(ANOVA). This test is used to look at the effect of two independent variables on a dependent variable. The two-way ANOVA determines the contribution of the independent variables on the main effect and also examines the interaction between the variables. In this case the independent variables are groups control and mTBI. The dependent variable is the coherence values for each group and hemisphere. In order to complete this test our population sample needs to be normally distributed with equal variances, and within and between group observations need to be independent. Our comparison includes total-Hb, oxy-Hb and deoxy-Hb coherence calculations. Next, in order to allow for multiple comparisons, Tukey-B post-hoc analysis was used to compare means through pairwise comparisons and to determine which variables were significantly different from each other. The Tukey compares every mean with every other mean, and takes into account the amount of scatter of all groups (mean of square residuals). The p-values are adjusted, and depend on the entire family of comparisons called the multiplicity adjust P-value. This value is based using the smallest threshold (alpha) of statistical significance at which the result is statistically significant [186]. These tests were then used to compare the effect of task activation on coherence intra-hemispheric (within the same hemisphere). This comparison was completed for left and right hemispheres between control and mTBI subjects.

Pearson r correlation analysis was used to analyze whether coherence values were correlated with outcome measures including days after injury, and Rivermead scores.

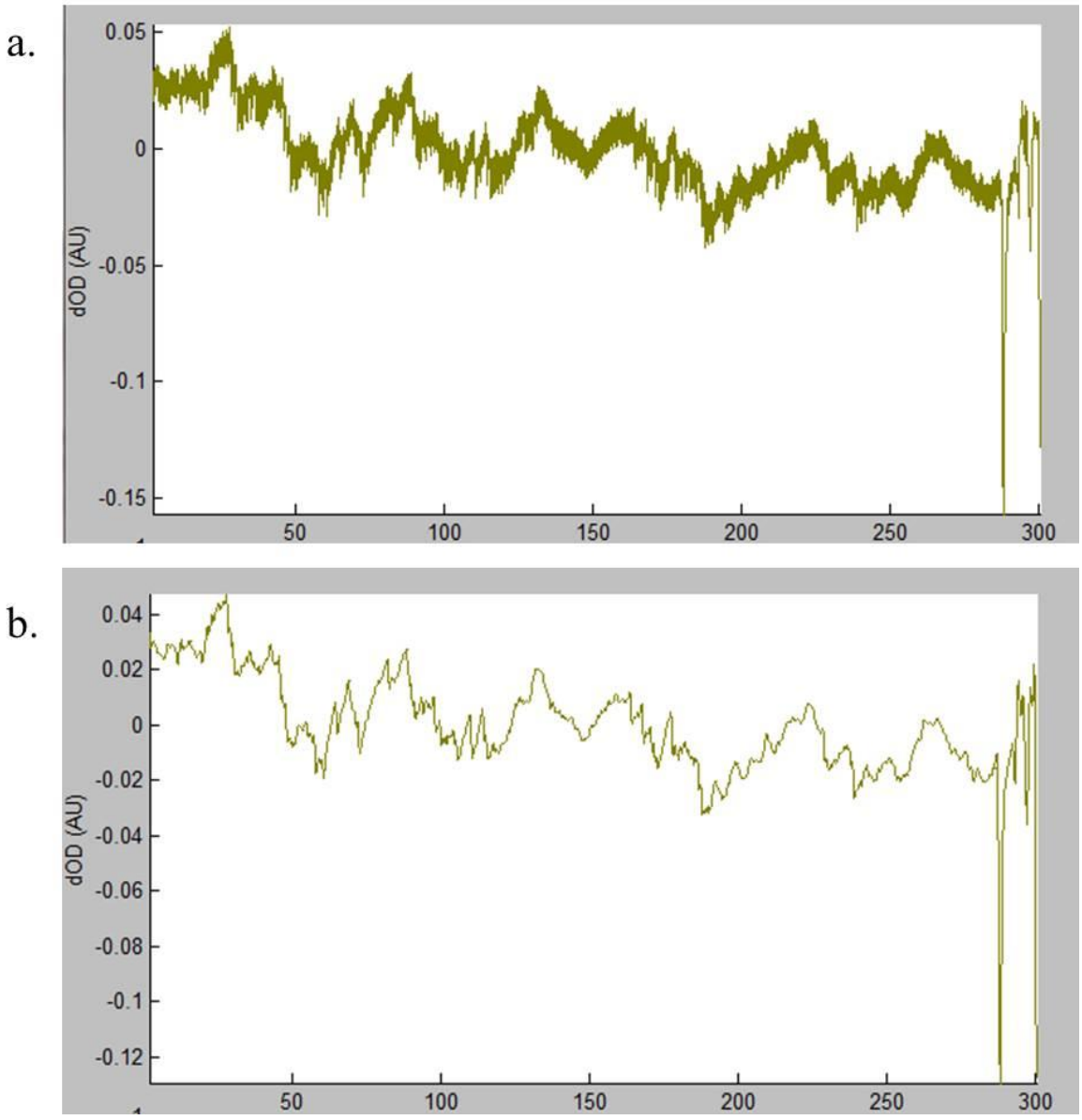

Figure 4-1. Example of raw and filtered data in HomER processing system

Raw data (a) is imported into HomER prior to data analysis. Here it is evident to see the high frequency noise present in pre-processed data. A low pass bandpass filter at 0.8 Hz is applied to raw data in order to remove physiological noise. There is evidence of a high frequency oscillation that could be due to subject movement; this can be removed by isolating the noise and using a single component filter.

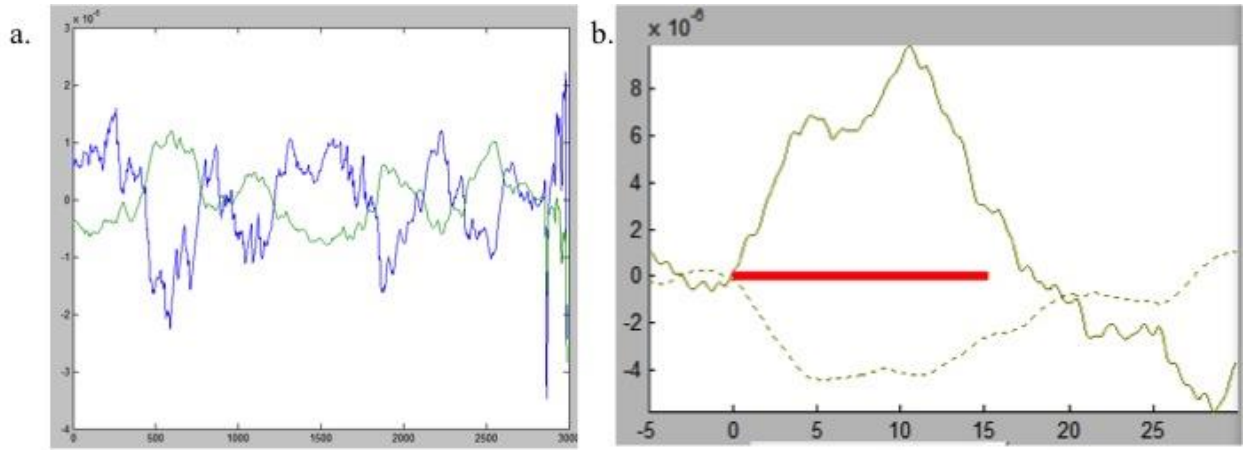

Figure 4-2. Example of Deoxy-Hb and Oxy-Hb concentration during task activation

Example of participant hemodynamic response during tapping task. a. graph of average signal from all source-detector pairs during all five minutes of data collection; the blue line represents deoxy-Hb concentration and green line represents oxy-Hb concentration. b. is average response to task activation over 6 tapping sessions, the red line illustrates 15 seconds of tapping task. This graph includes chosen source-detector pair that is used for evaluating response to tapping task.

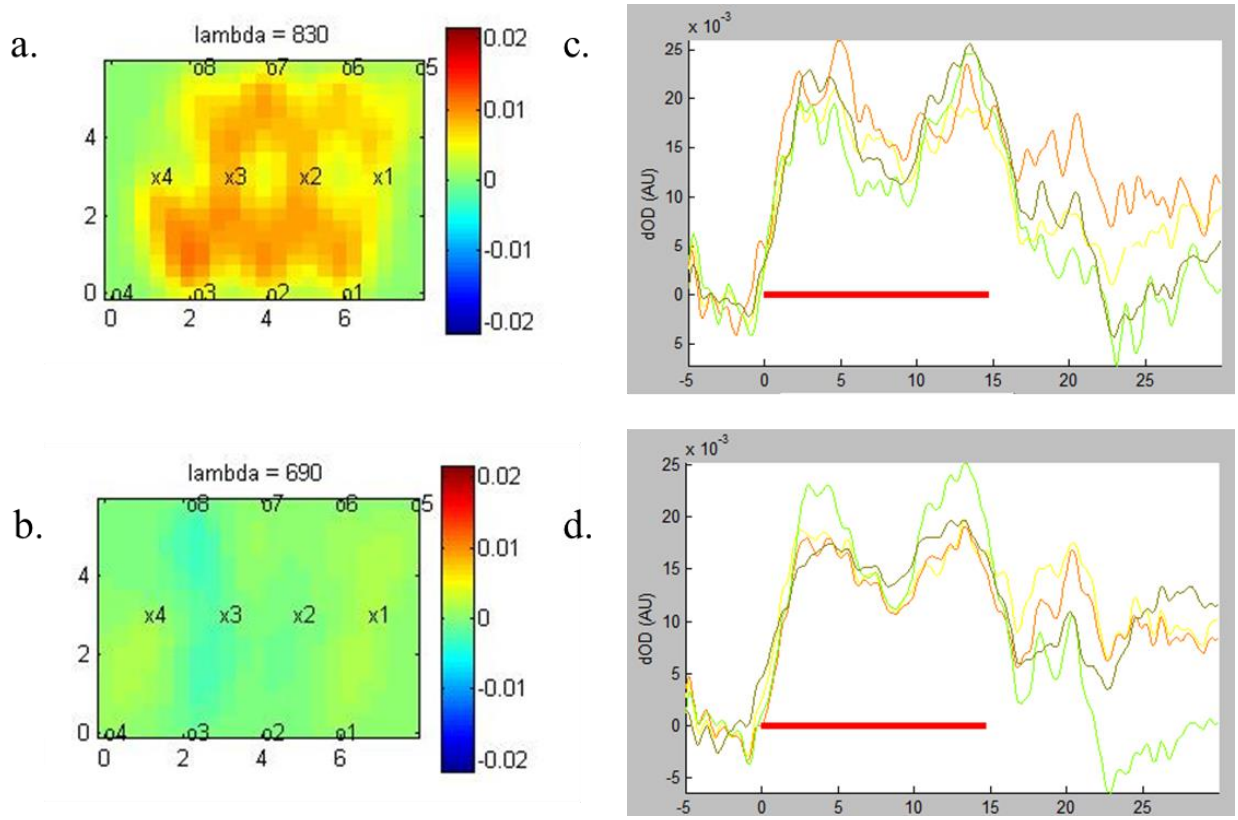

Figure 4-3. Tomographic maps and hemodynamic response at selected sources during task activation for dOD

Tomographs are depicted at a. 690λ for deoxy-Hb and b. 830 λ for oxy-Hb during tapping task. These tomographs include sources (marked by x) and detector (o) locations. There is an increase in dOD with tapping that is averaged over 6 sessions of 15s tapping. From this we select our source-detector pairs to inspect further. Visually, the majority of activation is seen at source 2 – detector 2 and source 3 –detector 3. The graphs represent sources c. 2 and d. 3. Each color line represents a separate detector. The greatest magnitude of activation was in source 2-detector 1 as magnitude is based on subtraction from resting state.

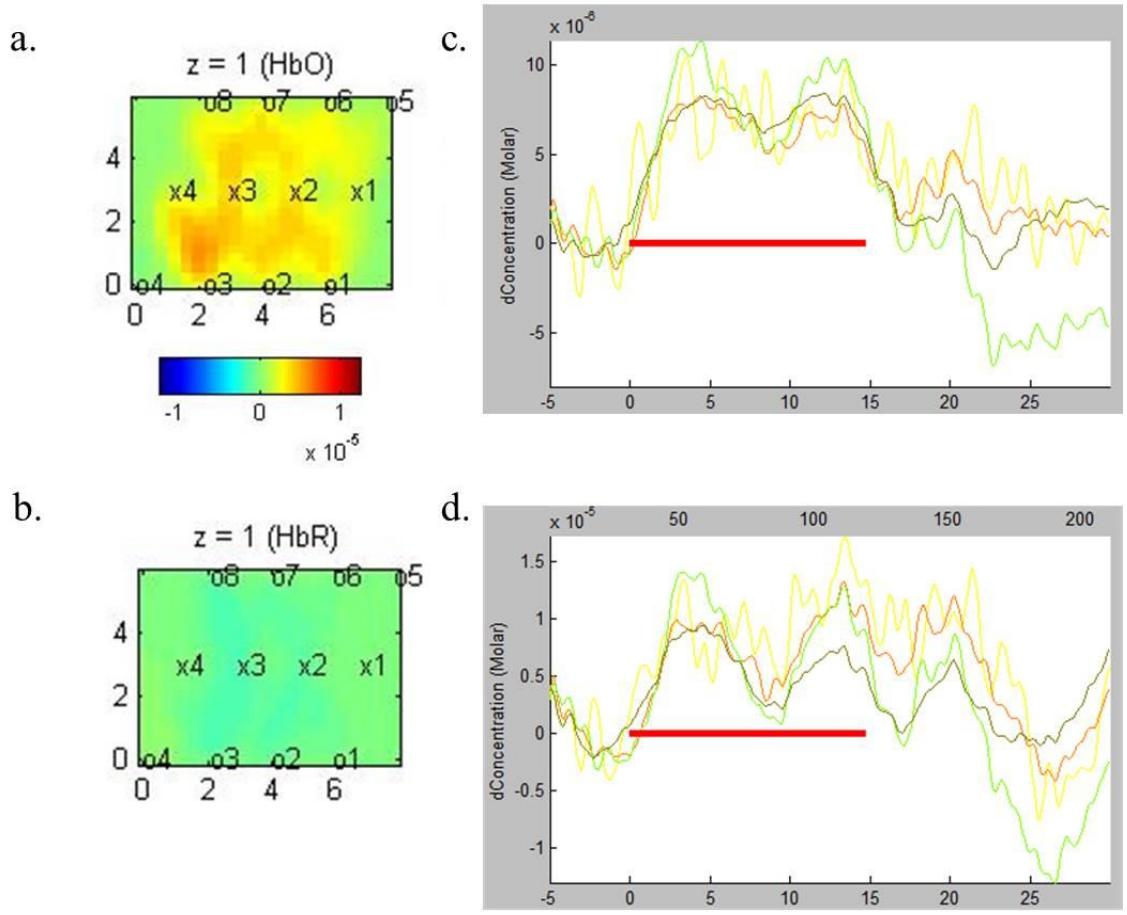

Figure 4-4. Example of tomographic maps based on measurements of oxy-hb and deoxy-hb concentrations

Tomographs are depicted at a. oxy-Hb and b. deoxy-Hb during tapping task. These tomographs include sources (marked by x) and detector (o) locations. There is an increase in oxy-Hb with tapping that is averaged over 6 sessions of 15s tapping. From this we select our source-detector pairs to inspect further. Visually, the majority of activation is seen at source 2 – detector 2 and source 3 –detector 3. The graphs represent sources c. 2 and d. 3. Each color line represents a separate detector. The greatest magnitude of activation was in source 2-detector 1 as magnitude is based on subtraction from resting state.

Step	Process	File Type	Time (min)	Time (max)
1	Data Acquisition: CW5 System	sample100test_0A00000.bin (2 files per test, Left and Right)	15	20
2	Data extraction: CW5 system	sample100test_0A00000.bin	3	5
3	Data file conversion using DOS + CW5filter.exe + btr50.flt	sample100test_LOA.cw5	32	40
4	Data file conversion and completion in MATLAB: ssdcna8s.mat	sample100L_10Hz.dod.mat	2	3
5	Import to HomER MATLAB based program + probegeometry_4x8oL.mat	need to complete per hemisphere plus rest and task	5	10
6	Haemoglobin concentration data extraction	Dependent on S-D or average combination	5	10
7	Coherence analysis file saving, each source (4) * state (2) * hemisphere (2)	specific to hemisphere and baseline vs task = MATLAB	6	10
8	Coherence analysis, seed selection + processing	MATLAB program including DoD, HbT, HbO, HbR	20	30
		Total time (estimate min)	**88**	**128**

Table 4-1. Estimated time to derive final analysis values

The processing steps for concentration extraction and coherence analysis including estimated processing times. *dOD, delta optical density; HbT, total-hemoglobin; HbO, oxy-hemoglobin; HbR, deoxy-hemoglobin.

Chapter Five: **Results**

5.1 Demographic Information

5.1.1 Subject Population

Nineteen mTBI participants (9 male, average age 15.1 ± 1.6 years, mean ± S.D.) and 10 controls (6 male, average age 14.0 ± 2.0) were enrolled in our study. Groups were similar in age (t -1.52, p=0.15) and sex (χ^2 1, .42; p=0.52). Details of mTBI participants are shown in Table 5-1. The average time post injury was 134.9±107.1 days with a range from 31 to 473 days.

5.1.2 Injury Characteristics

Symptoms were organized into physical, cognitive, sleep and emotional categories. All reported symptoms are evident in Table 5-2. The most common symptoms in the physical category were headaches (63%), fatigue (63%), dizziness (58%), sensitivity to light (47%), and balance problems (47%). In the cognitive category, difficulty concentrating was the highest reported symptom at 68%, whereas sadness (42%) was the most present emotional symptom. Trouble falling asleep and drowsiness (47%) were most reported in the sleep category.

Fourteen of nineteen mTBI subjects completed the Rivermeed. The scores ranged from 0 to 56 (25.1±15.1; mean±S.D.), out of a possible 80. Five mTBI participants did not complete the questionnaire. mTBI participants reported an average of 10.4 ±4.6 scores. When analyzing categories there was an average of 4.6±2.4 physical, 2.4±1.5 cognitive, 1.6±1.5 emotional and 1.7±1.2 sleep symptoms.

Sports were the cause of 74% of mTBI's in participants, 16% were due to motor vehicle accidents and 10% due to falls. Sports-related injuries included hockey, soccer, football, horseback riding, and wrestling.

5.2 Technical Results

5.2.1 Source-Detector Pair Detection

For coherence analysis, the region of interest was selected by choosing the source-detector pair with greatest activation. From 31 participants, 29 successfully showed a hemodynamic response with task activation. The two participants whose data was not used in this study was due to poor source-detector pair contact to scalp. For all successful participants, 41% (12 out of 29) of seeds selected were from source 3. Source 1 and 2 were selected 21% of the time and source 4 was selected 17% of the time. Data collection was successful 94% of the time.

5.3 Functional Activation

5.3.1 Magnitude of Activation

Figure 5-1 shows example tomographic maps of the increase in oxy-Hb concentration during task performance. The magnitude of the increase in total-Hb and oxy-Hb concentration is similar between the patient and control subjects (Figure 5-2). Group statistical analysis confirmed that the change in total-Hb concentration during the motor task was not significantly different ($p = 0.81$) between mTBI (10.9 ± 3.5 μM; mean ± S.E.M.) and controls (12.2 ± 2.8 μM). There was also no difference in the change in oxy-Hb concentration in mTBI (11.0 ± 2.8 μM) and control (14.7 ± 3.6 μM) ($p = 0.44$).

5.4 Coherence Analysis

5.4.1 Total-Hb Inter-hemispheric Coherence

Table 5-3a. contains calculated coherence values for control and mTBI subjects during resting state and task activation in both hemispheres. Figure 5-3 provides coherence maps examples for controls and mTBI subjects. During the resting state, coherence differed significantly between right-left hemispheres for total-Hb [$F(1,54) = 15.68$; $p < 0.001$], but not between groups [$F(1,54) = 0.42$; $p = 0.517$]. During task activation, there was a significant difference between right-left hemispheres [$F(1,54) = 13.47$; $p < 0.001$] and between groups for total-Hb [$F(1,54) = 18.18$; $p < 0.001$]. Post-hoc analysis for multiple comparisons (Figure 5-4) revealed that coherence was significantly different between hemispheres for mTBI patients only during resting state. Total-Hb was significantly lower in the right hemisphere (inter-hemispherical) as compared to the left hemisphere in mTBI participants ($p < 0.001$; 95% confidence interval: 0.09 to 0.44).

During task activation, there was a significant difference between control and mTBI coherence in the left ($p = 0.034$; 95% confidence interval = 0.01 to 0.37) and right hemisphere ($p = 0.012$; 95% confidence interval: 0.04 to 0.40). There was also a significant reduction in coherence between left and right hemispheres in the mTBI participants ($p < 0.001$; 95% confidence interval: 0.04 to 0.34).

5.4.2 Oxy-Hb Inter-hemispheric Coherence

Table 5-3b contains coherence values for control and mTBI subjects during resting state and task activation for oxy-Hb. During the resting state, coherence differed between left-right hemispheres for oxy-Hb [$F(1,54) = 15.65$; $p < 0.001$], but not between subject groups [$F(1,54) =$

2.29; $p = 0.15$]. During task activation, there was a significant difference between left-right hemispheres [$F(1,54) = 24.08$; $p < 0.001$] and between groups for oxy-Hb [$F(1,54) = 16.36$; $p < 0.001$].

Post-hoc analysis for multiple comparisons (Figure 5-5) revealed that coherence was significantly different between hemispheres for mTBI patients only during resting state. Oxy-Hb was significantly lower in the right hemisphere (inter-hemispherical) as compared to the left hemisphere in mTBI participants ($p < 0.001$; 95% confidence interval: 0.07 to 0.37).

During task activation, there was a significant difference between control and mTBI coherence in the right hemisphere ($p < 0.001$; 95% confidence interval: 0.10 to 0.39). There was also a significant reduction in coherence between left and right hemispheres in the control ($p = 0.031$; 95% confidence interval = 0.01 to 0.42) and mTBI participants ($p < 0.001$; 95% confidence interval: 0.10 to 0.39).

5.4.3 Effect of Task activation on Coherence: Total-Hb

Intra-hemispheric coherence was significantly different between groups [$F(1,54) = 4.84$; $p <= 0.03$], but not between tasks [$F(1,54) = 0.14$; $p = 0.71$] (resting state and task activation, or tapping). There was also a significant interaction between groups and task [$F(1,54) = 5.76$; $p = 0.02$]. For inter-hemispheric coherence there was only a significant difference between groups [$F(1,54) = 6.1$; $p = 0.017$], but not in task [$F(1,54) = 0.95$; $p = 0.331$] and for interaction [$F(1,54) = 1.3$; $p = 0.258$].

Tukey's post-hoc multiple comparisons (results shown in Figure 5-6) revealed that coherence was only significantly different between control and mTBI subjects in intra-hemisphere values. Intra-hemispheric total-Hb coherence was significantly lower during task

activation for mTBI as compared to the controls ($p = 0.014$; 95% confidence interval: 0.04 to 0.35).

5.4.4 Effect of Task activation on Coherence: Oxy-Hb

Intra-hemispheric coherence was a significant difference between groups [$F(1,54) = 6.5$; $p < 0.017$], but not between tasks [$F(1,54) = 0.06$; $p = 0.813$] (resting state and task activation, or tapping) and for interaction [$F(1,54) = 1.5$; $p = 0.217$]. For inter-hemispheric coherence there was only a significant difference between groups [$F(1,54) = 7.59$; $p < 0.001$], but not in task [$F(1,54) = 0.01$; $p = 0.923$] and for interaction [$F(1,54) = 0.77$; $p = 0.392$].

Tukey's post-hoc multiple comparisons (results shown in Figure 5-7) revealed there were no significant differences in coherence between control and mTBI subjects in intra-hemisphere and inter-hemisphere values. There were also no significant differences between resting state and task activation within control and mTBI subjects.

5.5 Correlation Analysis

5.5.1 Inter-hemispheric Coherence versus Time from Injury

Figure 5-8 illustrates the relationship between time after injury to inter-hemispheric coherence values during rest and task activation. There was no significant relationship between time after injury and the total-Hb during resting state ($r^2 > 0.001$; $p = 0.951$) and task activation ($r^2 = 0.083$; $p = 0.228$). Similarly, there was no significant relationship in time after injury for resting state ($r^2 = 0.02$; $p = 0.573$) and task activation ($r^2 = 0.0012$; $p = 0.892$) for oxy-Hb coherence values.

5.5.2 Inter-hemispheric Coherence versus Rivermead Symptom Scores

Figure 5-9 shows individual intra-hemispheric coherence values in comparison to symptom scores. Total-Hb intra-hemispheric coherence values showed a trend towards an increase in scores and decrease in coherence values during resting state. There however was no significant correlation in total-Hb for resting state (r^2: 0.12; p; 0.228) and during task activation (r^2 =0.056; p= 0.391). There was no correlation for Oxy-Hb coherence during resting state (r^2 =0.009; p= 0.74) and task activation (r^2 =0.069; p= 0.337).

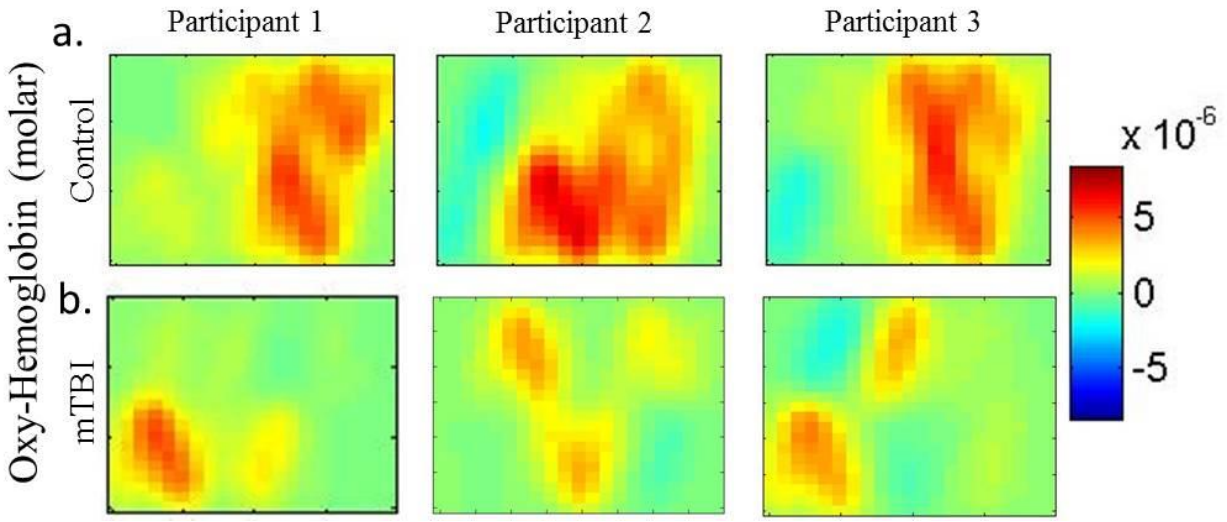

Figure 5-1. Examples of motor cortex activation during task activation

Each tomograph represents motor cortex activation averaged over 5 seconds during task activation. Three participants are illustrated for a. control and b. mTBI groups. Tomgraphs are taken at 10 seconds into tapping task for 5 seconds. These tomographs are from the left-hemisphere. Here we can get an idea of a region of interest that is representative of motor cortex, which then is further verified by looking at the qualitative measurements.

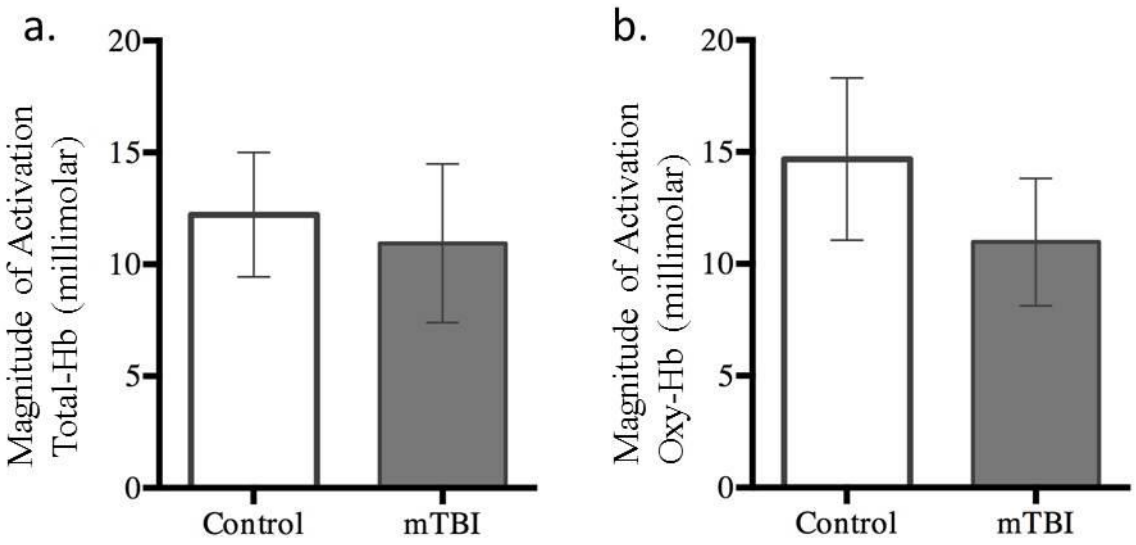

Figure 5-2. The magnitude of activation during tapping task

The magnitude of activation is illustrated for control and mTBI participants in concentration of a. total-Hb and b. oxy-Hb (as calculated by the modified beer-lambert law). The means and standard error of mean (S.E.M.) are illustrated in this image. There was no significant difference between control and mTBI participants in the magnitude of activation following the tapping task in either a. or b.

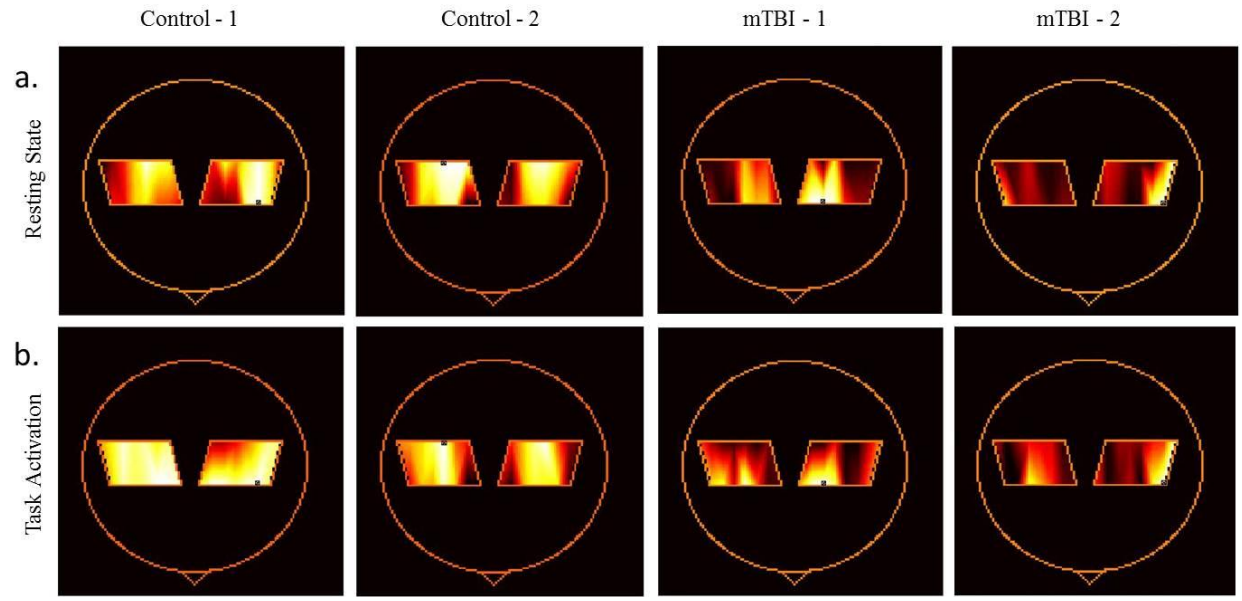

Figure 5-3. Examples of coherence maps during resting state and task activation

Coherence maps are represented during a. resting-state and b. task activation for sample control and mTBI subjects. Brighter pixels have high coherence closer to 1, whereas darker pixels (black) have lower coherence with region of interest or seed chosen. In the control subjects it is evident that coherence increases with task activation in comparison to resting state. There are lower coherence values in the mTBI subjects during a. resting state and b. task activation.

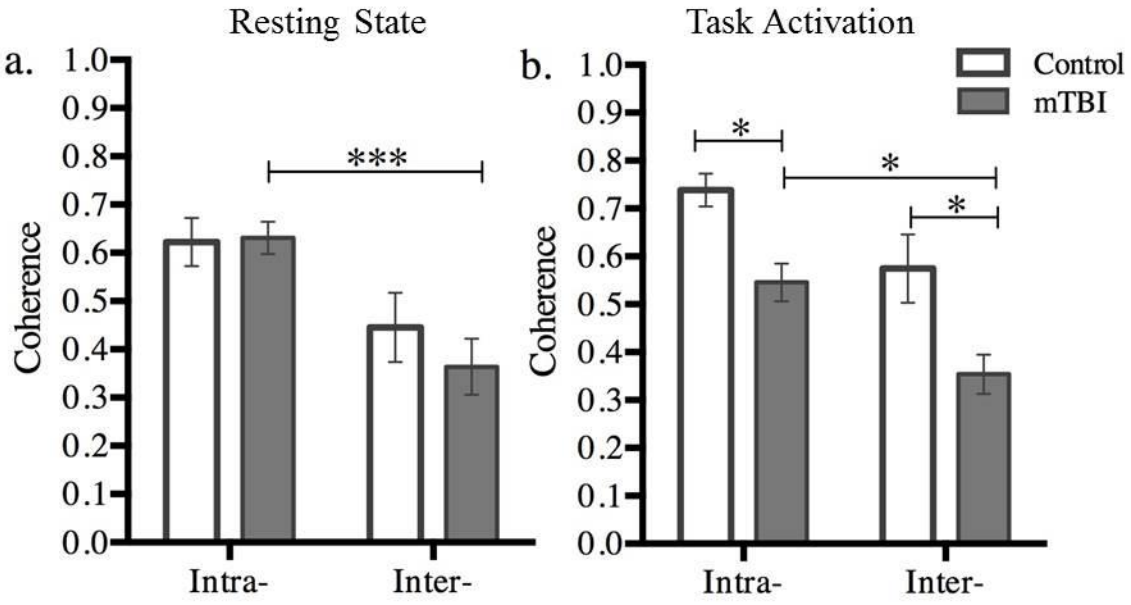

Figure 5-4. Coherence in the motor cortex in controls and mTBI patients for total-Hb

Intra- refers connectivity within hemisphere of region of interest or seed that was selected for comparison; in this case the task is right hand tapping, therefore region of interest in the left hemisphere. Inter- refers to connectivity in the contralateral hemisphere to reference seed chosen. a. shows data from the resting state, and b. shows data from the motor task (task activation). The bars indicate standard deviation of the mean (*$p<0.05$, **$p<0.01$, ***$p<0.001$). For total-Hb, (a, b) there is a significant difference in coherence between intra- and inter- hemisphere of mTBI patients during the resting state and task performance. During task performance, mTBI patients exhibit significantly lower coherence in both intra- and inter-hemispheres compared with controls.

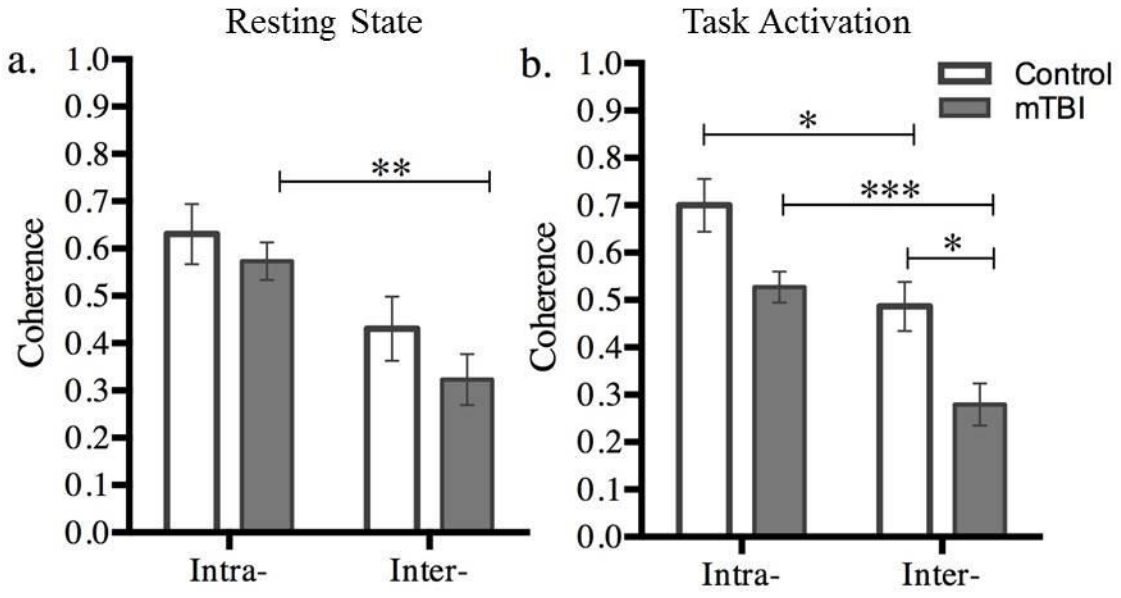

Figure 5-5. Coherence in the motor cortex in controls and mTBI patients for oxy-Hb

Intra- refers connectivity within hemisphere of region of interest or seed that was selected for comparison; in this case the task is right hand tapping, therefore left hemisphere activation. Inter- refers to connectivity in the contralateral hemisphere to reference seed chosen. a. shows data from the resting state, and b. shows data from the motor task (task activation). The bars indicate standard deviation of the mean (*$p<0.05$, **$p<0.01$, ***$p<0.001$). For total-Hb, (a, b) there is a significant difference in coherence between intra- and inter- hemisphere of mTBI patients during the resting state and task performance. During task performance, mTBI patients exhibit significantly lower coherence in both intra- and inter-hemispheres compared with controls.

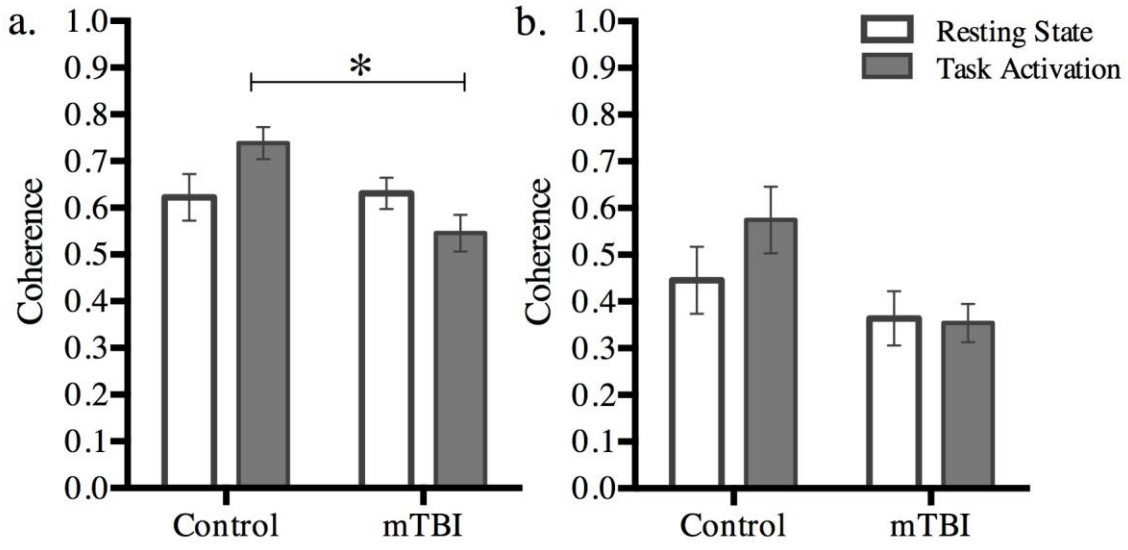

Figure 5-6. Effect of task activation on coherence within each hemisphere for total-Hb
Coherence for resting state and task activation are illustrated for a. intra-hemisphere and b. inter-hemisphere. The bars indicate standard deviation of the mean (*$p<0.05$). a.Within hemisphere, represents the effect of task activation on coherence on the surrounding motor cortex to seed selected. b. Inter-hemisphere, shows the effect of task activation on coherence in the contralateral hemisphere (inter-hemispheric coherence). There is a significant difference between a. intra-hemispheric coherence in control and mTBI during task activation. In a. intra-hemispheric coherence there is a significant interaction between the effect of group and task.

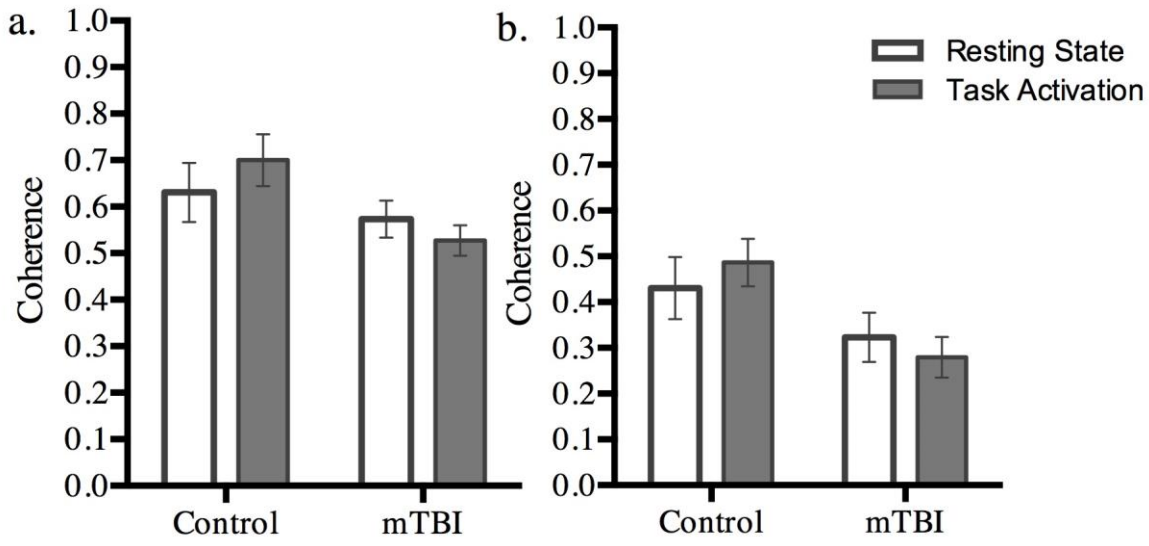

Figure 5-7. Effect of task activation on coherence within each hemisphere for oxy-Hb
Coherence for resting state and task activation are illustrated for a. intra-hemisphere and b. inter-hemisphere. The bars indicate standard deviation of the mean (*$p<0.05$). a. Within hemisphere, represents the effect of task activation on coherence on the surrounding motor cortex to seed selected. b. Inter-hemisphere, shows the effect of task activation on coherence in the contralateral hemisphere (inter-hemispheric coherence). There is a significant difference between a. intra-hemispheric coherence in control and mTBI during task activation. In a. intra-hemispheric coherence there is a significant interaction between the effect of group and task.

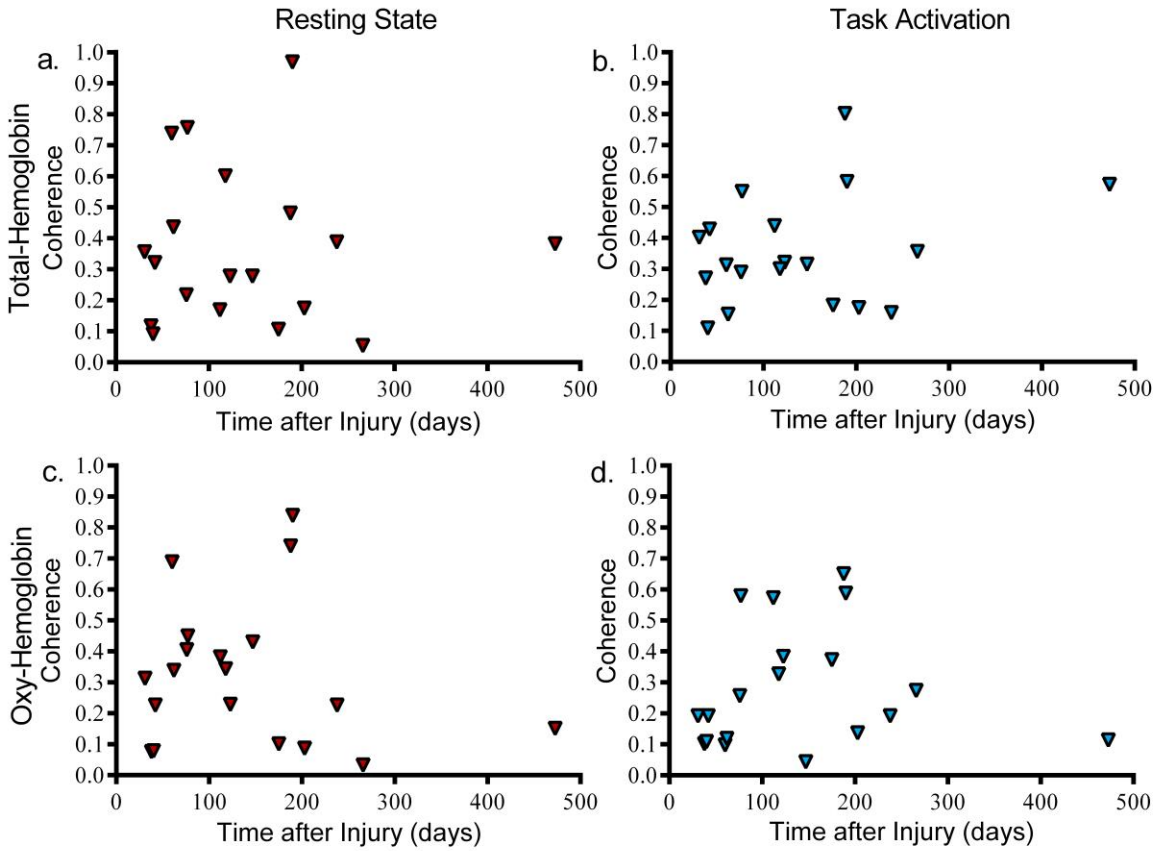

Figure 5-8. Relationship of inter-hemispheric coherence to time after injury in mTBI subjects

Graphs are illustrate the relationship of time after injury (days) to coherence values in a, c resting state and b, d during task activation in the contralateral hemisphere to seed. a, b are values derived from total-Hb, while c,d are values derived from oxy-Hb. a, c are resting state coherence values, and b, d are coherence during task activation. There was no significant relationship between time after injury (days) and inter-hemispheric coherence in resting state and task activation in total-Hb and oxy-Hb.

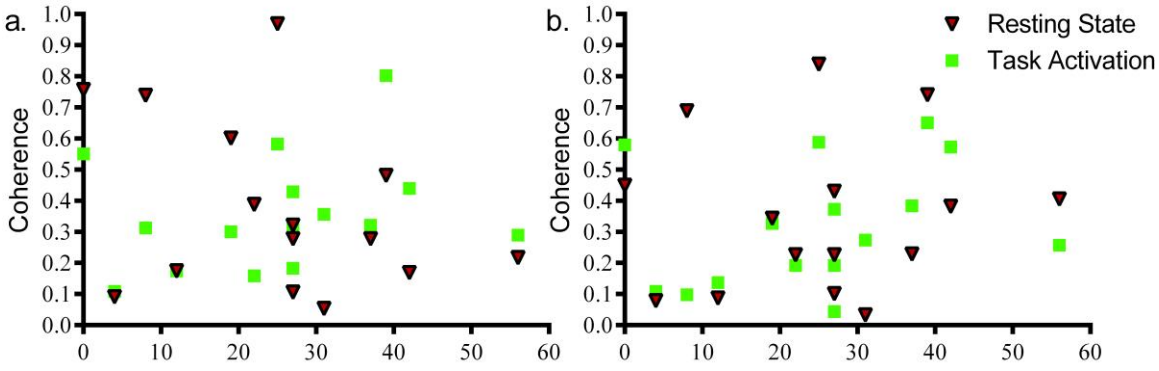

Figure 5-9. Rivermead post concussion questionnaire scores in comparison to individual inter-hemispheric coherence

Total-Hb (a) and oxy-Hb (b) inter-hemispheric coherence from contralateral side to seed as compared to Rivermead scores reported by each mTBI participant. Red triangles are individual coherence values in resting state; green triangles are individual coherence during task activation. The y-axis is total Rivermead Score for each individual.

* Rivermead scores were collected for 15 of 19 participants.

Patient	*Gender*	*Age*	*Days after Injury ~*	*# of previous mTBI's*	*Rivermead score*	*Mechanism of Injury*
1	M	18	473	1	*	MVA
2	M	15	38	0	*	MVA
3	F	18	31	0	*	Fall
4	F	13	42	0	27	Sport
5	F	16	203	2	12	Sport
6	M	15	238	0	22	Sport
7	M	16	147	2	27	Sport
8	F	13	175	0	27	Sport
9	F	15	188	0	39	Sport
10	F	13	40	1	4	MVA
11	M	15	60	1	8	Sport
12	M	17	266	2	31	Sport
13	F	13	62	1	*	Sport
14	F	16	112	1	42	Sport
15	F	16	190	2	25	Fall
16	M	15	123	0	37	Sport
17	M	15	77	2	0	Sport
18	M	14	102	2	19	Sport
19	F	14	76	2	56	Sport

Table 5-1. Demographic information for mTBI participants enrolled in the study

Table includes each subject's age, gender, days after injury upon completing study, number of previous mTBI's (none within the last year), Rivermeed score, and mechanism of injury. '*' indicates participants that did not complete questionnaire.

Physical	*%*	*Cognitive*	*%*	*Sleep*	*%*
Headache	63	Feeling Mentally Foggy	47	Drowsiness	47
Nausea	21	Slowed Down	47	Sleep Less than Usual	32
Vomiting	6	Difficulty Concentrating	68	Sleep More than Usual	26
Balance Problems	47	Difficulty Remembering	53	Trouble Falling Asleep	47
Dizziness	58				
Visual Problems	37	*Emotional*	*%*		
Fatigue	63	Irritable	37		
Sensitivity to Light	47	Sadness	42		
Sensitivity to Noise	42	More Emotional	37		
Numbness/Tingling	5	Nervousness	32		

Table 5-2. Reported persistent symptoms in mTBI participants

Types of persistent symptoms as described by mTBI patients within the past few days prior to NIRS testing. Each estimate is based on whether the individual has the symptom, therefore answered either yes or no.

	Hemisphere	*Task*	*Control (n=10)* *(mean ± S.E.M)*	*mTBI (n=19)*
a.	Left	*Resting state*	0.62 ± 0.05	0.63 ±0.03
Total-Hb		*Task Activation*	0.74 ± 0.03	0.55 ± 0.04
	Right	*Resting state*	0.45 ± 0.07	0.36 ± 0.06
		Task Activation	0.57 ± 0.07	0.35 ± 0.04
b.	Left	*Resting state*	0.63 ± 0.06	0.57 ± 0.04
Oxy-Hb		*Task Activation*	0.70 ± 0.06	0.53 ± 0.03
	Right	*Resting state*	0.43 ± 0.07	0.32 ± 0.05
		Task Activation	0.48 ± 0.05	0.28 ± 0.04

Table 5-3. Coherence values of total-Hb and Oxy-Hb averages for control and mTBI subjects

Average coherence values for resting state and during task activation. The tapping task was completed with the right hand, therefore activating the left hemisphere. The left hemisphere coherence is representative of intra-hemispheric values, whereas the right hemisphere coherence is representative of inter-hemispheric values.

Chapter Six: **Technical Considerations**

6.1 Overview

fNIRS successfully detected functional activation during tapping paradigm. There are several considerations that should be made prior to creating a research paradigm involving fNIRS in order to optimize the data. This chapter includes discussion on fNIRS data collection and technical considerations.

6.2 Technical Considerations

6.2.1 Data Filtering and Analysis

Data collection is takes up to 15-20 minutes including head cap installation. However, raw data filtering and analysis takes a considerable amount of time. In order to decrease processing time it would be beneficial to optimize our software by creating MATLAB scripts to automate processing time. This could be achieved with scripts for file saving for coherence analysis, and increasing the number of frequencies analyzed. This would also allow us to look at a larger amount of variables as fNIRS data collects up to 100Hz at two different wavelengths and many frequencies.

6.2.2 Probe Placement

The head cap used for this study was designed to eliminate crosstalk between wavelengths [153]. The headcap covers 10cm medial to lateral and 5cm anterior to posterior. The headcap is placed using an International EEG Placement Guide. Additionally, confirmation of motor cortex region is verified through activation with tapping. However we cannot delineate whether some of the signal is from the somatosensory cortex. The somatosensory cortex is

located posterior to the central gyrus [187]. Therefore it would be beneficial to introduce a sensory stimulus to separate motor cortex activation from somatosensory activation.

6.2.3 Magnitude of Concentration

The measurement we use for magnitude of activation is relative to each individual's resting state. This is important as there are several scattering mediums which the near infrared light must pass before coming into contact with cortex. The tissues include skin, muscle, bone, meninges and cerebrospinal fluid [146,157]. The scattering and absorption properties for these tissues are different amongst each other. They are highly variable among individuals and may affect the data collection. It is not possible to measure the path-length in our subjects using the CW system [170]. Therefore, the path-length that near-infrared light takes is assumed in the modified beer lambert law equation. The assumptions are based on Monte Carlo simulations, which have shown that the path length is dependent on the chosen source-detector pair distance [156]. With optimal source-detector distance and wavelength selection, the near-infrared light can penetrate up to 1cm in the cerebral cortex [145,156].

Another concern with collection of microvascular saturation is the relative input of pial arteries and veins to the NIRS signal. NIRS is sensitive enough to measures the small change in concentration of microvascular saturation of oxy-Hb and deoxy-Hb in the capillaries or venules [174]. In the pial arteries and veins there are large changes in oxy-Hb and deoxy-Hb concentrations, which would cause near infrared light to be greatly absorbed affecting the detection of near infrared light. It has been shown that arterial flow affects oxy-Hb concentration, whereas venous flow influences deoxy-Hb changes [174].

6.2.4 Source-Detector Selection for Magnitude of Activation Calculations

In response to tapping there is an evident hemodynamic response in the contralateral hemisphere with an increase in oxy-Hb and total-Hb. Tapping causes a hemodynamic response that peaks at 3-4 seconds after tapping begins and plateaus at 5-15s. Once tapping ceases there is a decrease to resting state levels. The response in deoxy-Hb is usually characterized by a rapid decrease with task activation and then stabilization [15,156,185]. We did not evaluate this in our study as several fNIRS studies have found that total-Hb and oxy-Hb signals to be superior to that of deoxy-Hb as compared to fMRI [80,188,189]. We found that activation is not isolated to a single source-detector pair but is also evident two or three source-detector pairs in close anatomical proximity. The hemodynamic response to task activation in our study is consistent with several studies investigating the motor cortex using fNIRS [142,157,178,185].

6.2.5 Subject Variability

In total- and oxy-Hb, there was a large variability in the both the control and mTBI for magnitude of activation. Each individual's magnitude of activation was calculated by subtraction of the tapping concentration (10s from plateau) from resting state concentration. This was completed to lower the effect of individual factors on magnitude of activation, thus regardless of each person's resting state, the magnitude of activation was recorded. This measurement is based on concentration changes in micromolar (mm) units, therefore even small differences are detected [185].

There could be reasons for the variability as head-cap positioning, contact of probes to head, subject's movement noise in the data, or even color of hair. Head-cap positioning could vary among individuals due to their head size. We measured the length from the bridge of the

nose to the occipital bone and based midline positioning of the headcap 40% of the distance measured. However, in future studies it would be helpful to measure length from the top of mandibular condyle, which is anterior to the ear, from left to right over the superior aspect of the skull. This is particularly important when considering the differences in gender and age on head cap positioning. The positioning of the hand on the motor homunculus is located anterior-laterally in the pre-central gyrus between the leg and face. The hand area occupies the most space proportionally, and there is specific activation of motor cortex corresponding to thumbs and fingers [187,190]. Our head cap is large enough to cover this area, however it would help eliminate any possible human error in head-cap placement and reduced variability in measurements.

It is possible to ensure proper head contact to probe through the CW5 data collection system by investigating the detector signal. However, there can still be variability in the transmission of near-infrared light if the probe is not tightly strapped. There is an automatic calibration process that takes into account the propagation of light and scattering effect, however we cannot adjust the power manually without altering the hardware itself. The new CW6 systems allow to adjust for power manually, that would even allow us to account for darker hair color which has been shown to absorb near-infrared light greater than light hair color [154,191].

6.2.6 Coherence Analysis Considerations

In order to complete the coherence analysis, several parameters needed to be established to optimize our results. This included seed selection, and the number of seeds used in the analysis. The source-detector with greatest magnitude of activation is chosen as the seed, or region of interest to use for the coherence analysis. This is chosen through initial recognition of

an increase in activation based on tomographs and then quantitatively analyzed for concentration changes for each source-detector pair. Similarly to the magnitude of activation, for analysis of coherence the source-detector pairs in close anatomical proximity are chosen for intra-hemispheric coherence. Inter-hemispheric coherence is then measured in similar anatomical position in the right hemisphere or ipsilateral to the finger tapping hand.

Previous published and unpublished work in our laboratory found that using the anatomical seeds in the ipsilateral hemisphere based on the inference from contralateral hemisphere was successful [178,185]. When comparing to left hand tapping, the activation of the motor cortex in the right hemisphere was similar to the identified source-detector pairs by anatomical position. In our study we used the anatomically matched position to identify motor cortex in the ipsilateral hemisphere to tapping. Interestingly, in some subjects we saw a small increase in concentration corresponding to the hemodynamic response in ipsilateral hemisphere. This was evident in these source-detector pairs selected by anatomical positions.

Since all the coherence data is compared to our selected seed, we needed to decide how many source-detector pairs we would use for our final coherence value. For the intra-hemispheric coherence we chose to average the coherence values for 3 source-detector pairs in close anatomical proximity to seed. We could not choose the seed for our coherence value as it is assigned a value of 1. Our choice of source-detector pairs was consistent to source-detector pairs chosen for the magnitude of activation analysis. In the ipsilateral hemisphere, 4 source-detector pairs in anatomically similar positions were averaged. In some situations, we chose to only use 3 source-detector pairs as the coherence value was close to 0. This could be due to noise in our data collection in that particular source-detector pair. By averaging several source-detector coherence values we are also eliminating the effect of noise directly on the result, as if we were

to use 1 source-detector pair to compare. This method was also used in other studies in our laboratory with comparable coherence values in healthy controls [178,185].

6.2.7 Frequency Band Selection

It was important to select an appropriate frequency band for our coherence analysis as our data collection included frequency ranges up to 50 Hz. For our main analysis we chose to use a frequency band of 0.04 to 0.1 Hz. This was based on previous studies of functional connectivity in fNIRS and fMRI studies [163,168,192]. Furthermore, our coherence analysis of fNIRS data collection is based on hemodynamic activity of the brain, which undergoes slow temporal changes in response to task activation. Therefore, selection of this frequency band was appropriate to study these slower frequencies at resting state and during task activation.

Prior to completing our coherence analysis it was important to discuss the presence of spontaneous high amplitude low frequency oscillations during resting state. It was critical to remove systematic oscillations in order to optimize our investigation of neuronal activity. We removed the respiratory signals from our data by applying a bandpass filter below 0-0.08 Hz to reduce the high frequency physiological components. The low frequency oscillations are due to systematic fluctuations such as respiration, blood pressure, heart rate variation and cardiac pulsation [168,193–195]. These oscillations have been observed in resting state functional connectivity studies in fNIRS and fMRI [168]. Low frequency oscillations are consistently seen in fNIRS frequency analysis at 0.01Hz, 0.04 Hz, 0.08Hz and 0.1 Hz [168,193,196,197]. Similarly, oscillations at a frequency of 0.02 Hz, 0.04 Hz and 0.1 Hz have been seen in fMRI [159,198–200]. The contribution of 0.02- 0.03 Hz, and 0.1 Hz low frequency oscillations has been attributed to respiratory and cardiac pulsation, respectively [194,197].

6.2.8 Chromophore Selection for Coherence Analysis

One advantage of using fNIRS for functional connectivity analysis is the ability to derive several hemodynamic parameters including total-Hb, oxy-Hb and deoxy-Hb values. Functional connectivity measured in fMRI is based on deoxy-Hb, however fNIRS is more sensitive to changes in oxy-Hb, and total-Hb measurements [197,201]. In our analysis we found that using total-Hb and oxy-Hb showed greater coherence with less variability between and within control and mTBI subjects (results are in appendix a). Therefore, for our main analysis we chose total-Hb and oxy-Hb for coherence analysis. This is consistent with other fNIRS connectivity analysis studies which used total-Hb or oxy-Hb to optimize the data [192,193,202].

6.2.9 Section Summary

This section discussed the technological aspects of using fNIRS to study brain communication and the hemodynamic response during motor cortex activation. There are many opportunities to utilize fNIRS in studying brain function in clinical studies. In devising future studies using the fNIRS system the user should take into consideration the suggestions made above to optimize data collection and analysis.

Chapter Seven: **Discussion and Future Considerations**

7.1 Overview

This thesis demonstrates the feasibility and utility of using fNIRS in a pediatric population with mTBI to evaluate brain function. fNIRS can calculate microvascular hemoglobin saturation during resting state and task activation. It can also measure the low frequency oscillations using a coherence analysis to detect functional connectivity. This study found that there are differences in brain function between controls and participants with PCS.

7.1.1 Aims and Objectives

The first objective of this study was to establish whether fNIRS is capable of detecting functional alterations in the response to task activation in children with PCS. We hypothesized that PCS children will have altered hemodynamic responses with task activation in the motor cortex. Contrary to our hypothesis, we found that PCS children did not have an altered hemodynamic response to tapping. Children with PCS did not differ from controls in their magnitude of activation.

The second objective of this study was to assess alterations in brain communication between controls and PCS patients using a coherence analysis. We hypothesized that there is reduced inter-hemispheric coherence in patients with PCS as compared to controls. In acceptance of our second hypothesis, we found that PCS children had alterations in inter-hemispheric coherence during resting state and task activation.

7.2 Hemodynamic Response in Motor Cortex

Previous studies have proposed that brain activation is altered following mTBI [97,99,104,203–205]. Studies of adults have shown reduced task-related activation in the normal brain network, and hyper-activation of areas outside of this network [203]. A fMRI study of symptomatic pediatric patients performing a working memory task demonstrated hypo-activation of the normal networks involved and a hyper-activation of a larger, more dispersed group of networks [103]. It has been proposed that the amount of recruitment to achieve the same task requires greater functional activation and such activation can be dispersed over a larger area [103]. Our study did not support this during a motor task for total-Hb and oxy-Hb concentrations. The magnitude of response to tapping task was not significantly different between mTBI and control patients.

In our study we did not see significant difference in the magnitude of activation of the primary cortex. There could have been altered activation in other brain regions during tapping that we did not investigate. In children, a large neural circuitry is activated during finger tapping [206,207]. The brain regions responsible for tapping are the primary motor cortex, cerebellum vermis and supplementary motor area [207]. Thus it may be possible that brain regions like the cerebellum, which is activated during rhythmic tapping in children, could be differentially activated in mTBI patients but are not measured in our study [206,207]. In adults during finger tapping there is activation of contralateral sensorimotor cortex, ipsilateral cerebellum, basal ganglia, thalamus and sensory cortex [208–210]. There is some evidence that some of these areas can be disrupted in mTBI and evidence of hypo-activation in the sub-cortical structures, such as the basal ganglia, thalamus and cerebellum during attentional tasks [92,93]. Other tasks, such as response inhibition, are associated with increased cerebellar activation in mTBI subjects [211]. Although we did not see

a significant difference in the primary motor cortex, there could be alterations in brain regions that are responsible for finger tapping that are outside our data collection fields.

Brain activation is also dependent on whether the tapping is internally or externally initiated such as through auditory or visual pathways [212]. In our study we used a metronome to deliver an auditory cue to finger tapping. During auditory cues there is activation in bilateral supplementary motor cortex, caudal dorsal and ventral premotor cortex, ipsilateral DLPFC and M1, whereas visual cues tend to involve parietal brain regions [212]. This synchronization to auditory cues require a greater mental work load in children [206,213]. Although, there is a possibility that our data collection could be contaminated by somatosensory activation, as we study older children this is less likely to have a significant effect, and further, any effect would be present in both groups.

As children with PCS are relatively well and have very good motor function, the simple finger-tapping task like this may not be sensitive enough to evaluate changes in magnitude of activation in M1 of our PCS subjects. In adults, it has been previously suggested that there are differential responses based on level of difficulty non-motor tasks within one month of mTBI [94,95]. In a working memory task, there was a difference in the response to increasing working load in comparison to control subjects without any changes in task performance. The mTBI subjects had less activation in low working load, and significantly greater activation than control patients in the high processing loads in right DLPFC and right parietal brain regions [94]. Another study showed that mTBI patients had a disproportionate increase in working memory brain regions in moderate task, with very little increase to high working load [95]. Both studies confirmed that in mTBI subjects there are changes in recruitment and allocation of resources to complete the task. There are alterations in PCS patients with working memory and attention

deficits symptoms [90]. There was a larger increase in brain regions, and there was also an increases in brain regions normally not recruited to achieve the task. The extent of activation was related to severity of PCS symptoms, although we did not find this in our study. There is evidence of different patterns of BOLD activation to finger tapping frequency, suggesting that altering the frequency may involve different brain regions and working loads [214]. In order to determine whether the magnitude of response in M1 or other cortical regions is altered there could be a more difficult task used to increase sensitivity.

In our study we used a unilateral finger tapping paradigm to investigate brain activity. TMS and fMRI have studied the role of the corpus callosum in uni-lateral finger movements. Rhythmic unilateral finger tapping has shown an increase in activation in contralateral sensorimotor cortex, subthalamic regions and the ipsilateral cerebellum, with a decrease in ipsilateral sensorimotor cortex, subthalamic regions and contralateral cerebellum [215]. This study suggests that brain regions activation due to response unilateral finger tapping is important because inter-hemispheric communication between the motor cortices helps facilitate coordinated and efficient movement. The inter-hemispheric inhibition occurs through the white matter tracts located in the corpus callosum, called the trans-callosal fibers [215,216]. Any disruption to these communication pathways may impair this inhibitory (decrease in activation) response. Therefore further exploration needs to be completed using a unilateral finger tapping task with both hands in order to determine whether the sensorimotor cortex is disrupted. One way to explore white matter tract damage or disruption of the corpus callosum is to evaluate the functional connectivity or white matter tract. These findings will be discussed below with discussion of our results.

7.3 Functional Connectivity

7.3.1 Inter-hemispheric Connectivity

The most significant finding in our study is the reduction of total- and oxy-Hb coherence during motor task activation in the contralateral hemisphere in PCS patients. This suggests impairment in inter-hemispheric functional connectivity. Specifically, the total- and oxy-Hb coherence is reduced relative to controls during task activation. There has been a study performed comparing functional connectivity during task activation using a coherence analysis with EEG for functional connectivity in mTBI. This study explored different brain regions involved in working memory, while we explored the motor cortex. Similar to our study, inter-hemispheric connectivity was reduced during working memory tasks in mTBI patients [217]. There was a significant reduction in inter-hemispheric coherence in frontal brain regions during verbal working memory and visual-spatial tasks. This suggests that inter-hemispheric connectivity disruption may be apparent in various brain networks following mTBI. Although limited research has been conducted in mTBI, there is evidence of decreased inter-hemispheric functional connectivity during task activation in severe TBI and neuro-degenerative diseases, such as multiple sclerosis, vascular dementia, and Alzheimer's [178,218–221]. These diseases are characterized by loss of brain communication or disruption in brain network function. Currently the mechanism for a decrease in functional connectivity in mTBI is not fully understood.

Our study also demonstrated a significant reduction between inter-hemispheric and intra-hemispheric coherence values of total and oxy-Hb for mTBI participants, and in oxy-Hb for controls. This is similar to changes seen in adult patients with multiple sclerosis during task activation [178].

During resting state, inter-hemispheric coherence was lower in both controls and mTBI and was seen in total- and oxy-Hb values. This finding is supported by a previous finding in adult mTBI patients where inter-hemispheric connectivity was lower but comparable to controls in frontal and temporal brain regions [217]. This suggests that there is disruption in resting state communication in several brain networks in PCS subjects. When comparing intra-hemispheric to inter-hemispheric coherence, there was a significant magnitude of decrease in mTBI patients in total-Hb and oxy-Hb. Although there is a small reduction in inter-hemispheric connectivity (as compared to intra-hemispheric connectivity) in healthy populations [178,193]. This significant reduction is seen in the mTBI group during resting state and is similar to the disruption in functional connectivity of the default mode network in fMRI studies of mTBI [110,111,114,222,223].

7.3.2 Comparison between resting state and task activation of Intra-hemispheric connectivity

In our study, task activation led to an increase in coherence in controls in both intra-hemispheric (left) and inter-hemispheric connectivity in total-Hb and oxy-Hb. Although this increase was not significant, it is similar to previous studies of task activation in which, there is an increase in functional connectivity (or coherence) with task activation [178,217,224]. Investigations of the motor cortex have also shown that functional connectivity increases during task activation as compared to the resting state [206,224–226]. However, in mTBI subjects there was a non-significant decrease in intra-hemispheric and inter-hemispheric coherence in oxy-Hb and total-Hb. This interaction between task and group was significant in total-Hb.

In healthy patients there is an inhibitory deactivation in the ipsilateral M1 to tapping, with a corresponding large increase in activation in the contralateral hemisphere. The increase in

functional connectivity in M1 during tapping has been suggested to relate to this increased activity of the inter-hemispheric inhibitory pathways associated with motor control[206,224].

A reduction in task specific coherence is consistent with the altered connectivity/cortical activation during task activation in fMRI, transcranial magnetic stimulation (TMS) and electroencephalogram (EEG) of mTBI patients [116,117,119,227,228]. This study is the first to show reduced coherence with fNIRS in pediatric mTBI patients within the motor cortex during resting state and task activation.

7.3.3 Subject Demographics Versus Coherence Values

Our study did not find any correlation between subject time after injury and with individual coherence values. There are many variables that need to be considered as gender and age effects, mechanism of injury and pre-injury coherence. Without acquiring a baseline coherence prior to injury it is difficult to find similarities in coherence between individuals in correlation to time after injury. It would also be beneficial to increase subjects numbers in both control and mTBI groups.

Unlike our study, there have been a few studies that have found correlations between severity of symptoms and functional connectivity. Functional connectivity decreases in the default mode network were correlated to the prediction of cognitive symptoms such as distractibility and cognitive fatigue [113]. More so, evaluation of thalamo-cortical connectivity found that a re-distribution to brain regions outside the resting state network were related to diminished neuro-cognition [118]. PCS patients who reported a decrease in cognitive and emotional symptoms on a follow up test at 6 months still presented with decreased functional connectivity in comparison to controls [229]. This study suggested that brain recovery did not necessary

correlate with symptom recovery. In order to understand the underlying brain function in relation to functional connectivity further studies need to be completed. Particularly with larger patient numbers, controlling for any confounders such as age, gender, and symptomatology. In our study we evaluated coherence in the motor cortex, which is not involved in cognition, or behaviour. A comparable measure could be measuring the performance during a motor task in comparison to primary motor cortex coherence.

7.4 General Discussion

Without further study, it is not clear whether these changes reflect dysfunction in the white matter tracts or a metabolic dysfunction. Reduction of coherence could be a result of white matter volume loss [230], focal axonal injury [131], metabolic dysfunction in the corpus callosum [231], or the primary motor cortex [76]. The decrease in coherence could also be due to cellular damage following an mTBI [96].

Inter-hemispheric functional connectivity is dependent on the function of the corpus callosum. The degree of synchrony in functional connectivity is positively correlated with the structural integrity of white matter [232]. White matter track damage or dysfunction has been reported based on DTI studies, which is consistent with our finding of disruption in functional connectivity between left and right motor cortices in mTBI patients [124,126,233–235]. A correlation has been reported between fractional anisotropy (FA) and task reaction times in several areas of the brain including the genu of the corpus callosum and the thalamus [123,233,235]. In particular, a decrease in FA values in the ascending fiber tracts from the corpus callosum to the primary motor cortex following mTBI [76]. A previous fNIRS study on patients with multiple sclerosis, a disorder associated with white matter damage, also reported reduced coherence during task

activation compared with controls [178]. This result was similar to a study of coherence in multiple sclerosis, which there was a slight decrease in coherence with tapping task [178]. Interestingly, studies of multiple sclerosis have found that there is a decrease of inhibitory outputs that may be caused by corpus callosum atrophy [236–238].

Reduced inter-hemispheric connectivity has been suggested to be correlated to a decrease in communication between hemispheres [239]. Even during resting state, inter-hemispheric connectivity was lower in mTBI patients suggesting disruption or alteration in communication pathways between the hemispheres. In the healthy brain, the communication between cortices can occur as a result of excitatory or inhibitory inputs to transcallosal fibers in the corpus callosum [240,241]. This consistent communication occurring during resting state that has been suggested to be dependent on the readiness of the motor cortex [240]. TMS studies have shown in adult mTBI studies that there is an alteration in the balance of excitatory and inhibitory inputs between motor cortices [242–244]. The reduction in communication could be a result of the decreased functional connectivity in mTBI patients.

Another possibility for the reduction in inter-hemispheric connectivity in our mTBI patients could be due to changes at the electrophysiological level. Our mTBI subjects elicited a reduction from rest to task activation in intra-hemispheric and inter-hemispheric connectivity, whereas control subjects increased connectivity. Increases in connectivity due to task activation have been correlated with corresponding increases in neuronal activation in EEG, and hemodynamic response in fNIRS, fMRI studies [159,178,193,199]. There is evidence of a disruption in the balance of inter-hemispheric excitatory and inhibitory pathways in mTBI subjects as measured by TMS [242,244,245]. Furthermore, motor threshold, a way to measure cortical excitability and the conduction of inhibitory and excitatory pathways, is elevated in mTBI subjects [242,245].

This means that neuronal activation of the fibers between hemispheres could be less sensitive to activation, which could be reflected in our results of the reduction in functional connectivity in mTBI patients.

There is evidence of metabolic disruption in M1 and the corpus callous of chronic mTBI subjects [55,76,78,246]. Another marker of dysfunction in metabolism are decreases in glutamine/glutatmate in the grey matter of patients with symptoms present at 1 month [73].These disruptions could affect the increase in cerebral blood flow which normally occurs as a result of healthy neurovascular coupling [247,248]. This relationship between neuronal activation and the corresponding increase in microvascular oxygen is related to corresponding increases in functional connectivity during task activation [159,168,199]. In our control subjects we saw an increase in intra-hemispheric and inter-hemispheric functional connectivity during task activation, however in our mTBI subjects functional connectivity slightly decreased or did not change. This suggests that there are differential responses to finger tapping in the mTBI subjects involved in the communication between motor cortices.

7.5 Benefits

Children with mTBI and PCS often have headaches, fatigue easily and are intolerant of noise or bright lights. fNIRS is quiet, and the participant can sit comfortably in a chair and complete tasks. Further, in our study fNIRS was well tolerated and completed with a 94% success rate. fNIRS could be a useful tool for studies of cortical function, especially in children with PCS.

Another consideration is the ease and speed of completing the fNIRS method. The research assistant simply needs to be able to comfortably fit the cap over the head while gently moving

the hair out of the way. In some cases, there may hair that is difficult to remove, to which the research assistant simply presses the calibration button on the CW data collection system. It is important to consider that the children may be hesitant to allow anything on their head if it is put on forcefully.

Unlike BOLD fMRI, where the patients are required to lay still in a supine position, fNIRS probes are malleable allowing for studies including movement, sitting or standing. The portability and the ability to measure while subjects are completing other tasks like neuropsychological testing could allow us to measure brain function in a variety of situations. Furthermore, we can apply fNIRS to measure brain development, different disease states and or to have a better understanding of brain function in general.

7.6 Limitations

A limitation of the study is the sample size, although this group number was sufficient to show significant changes between groups. We only recruited ten controls subjects to this study, however we need to expand this to have normalized values for the pediatric population. Most of the studies conducted are in the adult population and it is known that there are differences in brain development between the pediatric and adult population [213,249]. Furthermore, it would have been beneficial to retest the subjects over time as to see whether coherence scores improved over time and whether control coherence values remained stable over time.

Also, it remains possible that the motor cortex may not be the location with the largest differences in inter-hemispheric communication. Further analysis should incorporate other brain regions such as the dorsal lateral prefrontal cortex (DLPFC) which shows functional impairment after mTBI.[250,251] A larger mapping study should be done to examine other regions. This would

also allow us to investigate the correlation between symptom presence and fNIRS measurements such as cognitive deficits in PCS.

There was also a large variability in time after injury and symptom presence. If symptoms changed with time, this could account for part of the variance. Although we found a group difference compared to controls, the sample size is too small to determine if there is a relationship between time after injury and the magnitude of the change in coherence.

One of the most significant limitations is the lack of established baseline on a normal population and from each individual to be able to differentiate between. For example the hemodynamic response and brain connectivity may simply be different in patients who are seeing PCS symptoms rather than a causation of the mTBI. Furthermore, there may be a difference between populations, age and gender. Future studies need to combine fNIRS with fMRI and or DTI studies in order to explore if there are cross correlations between the results we discover.

7.7 Conclusion and Significance

This is the first fNIRS study of which we are aware to use coherence analysis in an mTBI population to explore cortical communication. This study provides evidence of underlying disruption in inter-cortical functional connectivity based on a reduction in inter-hemispheric coherence in pediatric mTBI PCS patients compared with controls. fNIRS combined with coherence analysis provides an objective protocol which may be used to assess mTBI. fNIRS may also provide a portable, quantitative tool which one can used to monitor functional impairment following mTBI as well as to monitor treatment response and recovery.

7.8 Future Directions and Possibilities

7.8.1 fNIRS head cap and technology development

In order to better study the functional changes in mTBI and PCS it would be beneficial to investigate other brain regions that have been found in fMRI, DTI or EEG studies to be disrupted. There are few studies being conducted on the motor cortices in mTBI, therefore by examining similar areas we could cross-validate the results we are seeing with other studies.

Other considerations need to take place in terms of technology development. First, with the increase in data collection and analysis program there is possibility to increase the amount of source-detector pairs and expand our headcap. By doing this we could evaluate larger areas of the brain, which would allow us to investigate the evidence from fMRI that has shown increases in activation outside of normally activated brain regions with tasks. To facilitate for larger data sets it would be important to further develop processing of data. Obtaining concentrations and completing coherence analysis is time consuming, by creating a more automated program we could analysis a larger amount of the data including different frequency bands and regions of interest simultaneously (see Table 7-1). This type of analysis is common in fMRI studies and allows for variability among individuals. It could also provide us on more information about resting state and task activation coherence.

It would be interesting to look at frequencies used by EEG including theta (4-8Hz), alpha-1 (8-11Hz), and alpha-2 (11-14Hz) [227,252,253]. Figure 7-1 is an example of high frequency analysis coherence maps at a variety of bands. We analyzed frequency bands between 0.04-0.1Hz, 0.1-1Hz, 1-2Hz, 2-3Hz, 3-4Hz, 4-8Hz, 8-10Hz and 10-50Hz. There were higher coherence from 0.04-2Hz followed by a drop between 3-8Hz. We found an increase in coherence

during task activation above 8 Hz. Further investigations are currently ongoing to understand these findings.

7.8.2 fNIRS and Neuropsychological Testing

There are several ways that fNIRS could be used to evaluate children following mTBI. Head cap design should be altered to look at the frontal cortex, as growing evidence shows disruption in DLPFC regions. Once head cap can look at DLPFC there is possibility to explore cognitive dysfunction. These studies could include monitoring brain oxygenation and coherence during neuropsychological testing, tasks involving dual-cost paradigms, and or neurocognitive testing.

7.8.3 Multi-modal Protocols

The recent advances in fNIRS data collection and analysis allows us to gather information about oxy-Hb and deoxy-Hb microvascular saturation at a high spatial resolution, furthermore integration of several technologies could help us answer many questions about the healthy and damaged brain. fNIRS could further our knowledge of mTBI in combination with TMS, EEG, or MEG. Each technique has particular spatial and temporal resolution and investigates different aspects of brain activation [15]. EEG, MEG and TMS investigate the electrophysiological responses to neuronal activation, whereas fNIRS studies the hemodynamic response. The electrophysiological response occurs immediately following neuronal activation and is followed by the slower hemodynamic response. The hemodynamic response may be more disperse and lasts longer. Multimodal approaches could provide us with more information on the coupling

between neuronal activation and the hemodynamic response and increase our knowledge of brain disorders that may have alterations in electrophysiology or neurovascular coupling.

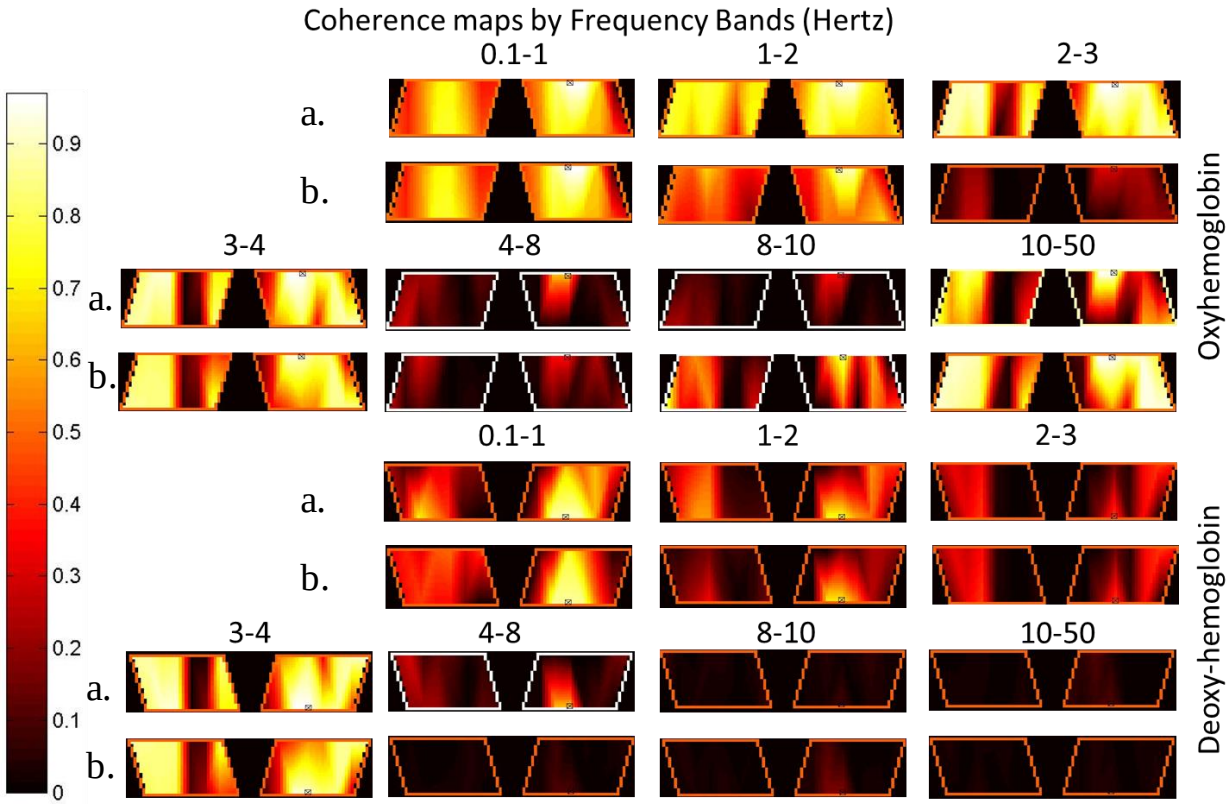

Figure 7-1. Example of multiple frequency coherence analysis of subject

Resting state (a) and task activation (b) coherence maps at various frequency bands including 0.1-1 Hz, 1-2 Hz, 2-3 Hz, 3-4 Hz, 4-8 Hz, 8-10 Hz, and 10-50 Hz. Coherence maps were obtained for oxy-Hb and deoxy-Hb for healthy subject. Oxy-Hb high frequency analysis shows high coherence during lower frequency bands, with a drop between 4-8 Hz and an increase above 8Hz particularly during task activation. High frequency analysis is usually used in EEG functional connectivity studies. Further studies need to be conducted to understand these results.

Technology Development	Description
Eliminate User-Dependent File Saving.	To derive concentration and frequency data, each source-detector pair must be saved independently in delta-optical-density and concentration. By automating this process it would save between 10-25 minutes.
Eliminate File Conversion Time	File conversion takes majority of the processing time. In order to make this automated it would increase time efficiency and eliminate possible human errors.
Develop Region Specific Selection	Currently in coherence analysis each source-detector pair (region of interest) needs to be individually pre-selected and entered through the MATLAB program. This program would allow generation of coherence data as compared to each region of interest (R.O.I.) selection. Furthermore, it would allow for more specific, efficient and provide more R.O.I. analysis.

Table 7-1. Possible technology development opportunities to optimize processing times

Suggested technology development opportunities to decrease processing time. Another possible advantage would be processing of each source detector pair and more frequency bands. This would allow us to look at several regions of interest and utilize the high data collection of fNIRS.

Appendix 1: Rivermead Post Concussion Questionnaire

The Rivermead Post-Concussion Symptoms Questionnaire*

After a head injury or accident some people experience symptoms which can cause worry or nuisance. We would like to know if you now suffer from any of the symptoms given below. As many of these symptoms occur normally, we would like you to compare yourself now with before the accident. For each one, please circle the number closest to your answer.

0 = Not experienced at all
1 = No more of a problem
2 = A mild problem
3 = A moderate problem
4 = A severe problem

Compared with before the accident, do you now (i.e., over the last 24 hours) suffer from:

Headaches	0	1	2	3	4
Feelings of Dizziness	0	1	2	3	4
Nausea and/or Vomiting	0	1	2	3	4
Noise Sensitivity, easily upset by loud noise	0	1	2	3	4
Sleep Disturbance	0	1	2	3	4
Fatigue, tiring more easily	0	1	2	3	4
Being Irritable, easily angered	0	1	2	3	4
Feeling Depressed or Tearful	0	1	2	3	4
Feeling Frustrated or Impatient	0	1	2	3	4
Forgetfulness, poor memory	0	1	2	3	4
Poor Concentration	0	1	2	3	4
Taking Longer to Think	0	1	2	3	4
Blurred Vision	0	1	2	3	4
Light Sensitivity, Easily upset by bright light	0	1	2	3	4
Double Vision	0	1	2	3	4
Restlessness	0	1	2	3	4

Are you experiencing any other difficulties?

1. _____	0	1	2	3	4
2. _____	0	1	2	3	4

*King, N., Crawford, S., Wenden, F., Moss, N., and Wade, D. (1995) J. Neurology 242: 587-592

06/23/08

Appendix 2: Chromophore Selection for Coherence Analysis

Intra-hemispheric Coherence during Resting State				
	dOD	**Total-Hb**	**Oxy-Hb**	**Deoxy-Hb**
Control 1	0.726	0.625	0.811	0.675
Control 2	0.815	0.842	0.558	0.867
Control 3	0.62	0.416	0.527	0.395
Control 4	0.58	0.415	0.826	0.737
Control 5	0.59	0.416	0.527	0.328
Control 6	0.599	0.599	0.679	0.565
Mean±S.T.D	0.655±0.09	0.543±0.19	0.65±0.16	0.595±0.21

Inter-Hemispheric during Resting State				
	dOD	**Total-Hb**	**Oxy-Hb**	**Deoxy-Hb**
Control 1	0.877	0.294	0.339	0.375
Control 2	0.445	0.699	0.663	0.654
Control 3	0.503	0.377	0.169	0.225
Control 4	0.905	0.485	0.314	0.366
Control 5	0.594	0.377	0.169	0.059
Control 6	0.349	0.480	0.510	0.281
Mean±S.T.D	0.612±0.23	0.446±0.16	0.331±0.2	0.327±0.2

Intra-hemispheric during Task Activation				
	dOD	**Total-Hb**	**Oxy-Hb**	**Deoxy-Hb**
Control 1	0.49	0.869	0.798	0.593
Control 2	0.796	0.743	0.907	0.945
Control 3	0.578	0.617	0.522	0.891
Control 4	0.581	0.895	0.870	0.281
Control 5	0.617	0.617	0.522	0.303
Control 6	0.715	0.745	0.664	0.426
Mean±S.T.D	0.63±0.11	0.748±0.13	0.724±0.19	0.573±0.29

Inter-hemispheric during Task Activation				
	dOD	**Total-Hb**	**Oxy-Hb**	**Deoxy-Hb**
Control 1	0.883	0.438	0.251	0.007
Control 2	0.707	0.704	0.529	0.616
Control 3	0.427	0.649	0.545	0.814
Control 4	0.848	0.815	0.795	0.533
Control 5	0.146	0.649	0.545	0.314
Control 6	0.285	0.157	0.320	0.226
Mean±S.T.D.	0.549±0.31	0.651±0.14	0.533±0.19	0.418±0.29

Intra-hemispheric Coherence during Resting State				
	dOD	Total-Hb	Oxy-Hb	Deoxy-Hb
mTBI 1	0.63	0.657	0.380	0.591
mTBI 2	0.522	0.528	0.470	0.219
mTBI 3	0.5	0.532	0.380	0.544
mTBI 4	0.783	0.828	0.525	0.577
mTBI 5	0.508	0.375	0.743	0.48
Mean±S.T.D.	0.589±0.12	0.584±0.17	0.5±0.15	0.482±0.15

Inter-Hemispheric during Resting State				
	dOD	Total-Hb	Oxy-Hb	Deoxy-Hb
mTBI 1	0.563	0.321	0.226	0.238
mTBI 2	0.2	0.175	0.087	0.082
mTBI 3	0.322	0.388	0.226	0.411
mTBI 4	0.054	0.054	0.033	0.296
mTBI 5	0.254	0.278	0.229	0.053
Mean±S.T.D.	0.279±0.19	0.243±0.13	0.16±0.09	0.216±0.15

Intra-hemispheric during Task Activation				
	dOD	Total-Hb	Oxy-Hb	Deoxy-Hb
mTBI 1	0.42	0.391	0.409	0.097
mTBI 2	0.518	0.528	0.424	0.594
mTBI 3	0.387	0.424	0.409	0.577
mTBI 4	0.622	0.583	0.646	0.436
mTBI 5	0.555	0.485	0.520	0.273
Mean±S.T.D.	0.5±0.10	0.482±0.08	0.482±0.1	0.395±0.21

Inter-hemispheric during Task Activation				
	dOD	Total-Hb	Oxy-Hb	Deoxy-Hb
mTBI 1	0.417	0.429	0.192	0.064
mTBI 2	0.202	0.175	0.137	0.139
mTBI 3	0.157	0.159	0.192	0.353
mTBI 4	0.352	0.356	0.274	0.174
mTBI 5	0.312	0.321	0.384	0.485
Mean±S.T.D.	0.288±0.11	0.288±0.12	0.236±0.1	0.243±0.17

References

1. McKinlay, A., Grace, R.C., Horwood, L.J., Fergusson, D.M., Ridder, E.M., and MacFarlane, M.R. (2008). Prevalence of traumatic brain injury among children, adolescents and young adults: prospective evidence from a birth cohort. Brain Inj 22, 175–181.

2. Menon, D.K., Schwab, K., Wright, D.W., Maas, A.I., and Health, D. and C.A.W.G. of the I. and I.I. toward C.D.E. for R. on T.B.I. and P. (2010). Position statement: definition of traumatic brain injury. Arch Phys Med Rehabil 91, 1637–1640.

3. Center for Disease Control and prevention (CDC). (2014). Heads Up: Facts for Physicians about Mild Traumatic Brain Injury.Available from: http://www.cdc.gov/concussion/headsup/pdf/Facts_for_Physicians_booklet-a.pdf.

4. Corrigan, J.D., Selassie, A.W., and Orman, J.A.L. ([date unknown]). The epidemiology of traumatic brain injury. J. Head Trauma Rehabil. 25, 72–80.

5. Barlow, K.M., Crawford, S., Stevenson, A., Sandhu, S.S., Belanger, F., and Dewey, D. (2010). Epidemiology of postconcussion syndrome in pediatric mild traumatic brain injury. Pediatrics 126, e374–81.

6. Emanuelson, I., Wendt, L. V, Hagberg, I., Marchioni-Johansson, M., Ekberg, G., Olsson, U., Larsson, J., Egerlund, H., Lindgren, K., and Pestat, C. (2003). Early community outreach intervention in children with acquired brain injury. Int J Rehabil Res 26, 257–264.

7. Gagnon, I., Swaine, B., Friedman, D., and Forget, R. (2005). Exploring children's self-efficacy related to physical activity performance after a mild traumatic brain injury. J Head Trauma Rehabil 20, 436–449.

8. Guskiewicz, K.M., and Valovich McLeod, T.C. (2011). Pediatric sports-related concussion. Physcial Med. Rehabil. 3, 353–64.

9. Shrey, D.W., Griesbach, G.S., and Giza, C.C. (2011). The pathophysiology of concussions in youth. Phys Med Rehabil Clin N Am 22, 577–602, vii.

10. McCrory, P., Meeuwisse, W.H., Aubry, M., Cantu, B., Dvorak, J., Echemendia, R.J., Engebretsen, L., Johnston, K., Kutcher, J.S., Raftery, M., Sills, A., Benson, B.W., Davis, G.A., Ellenbogan, R., Guskiewicz, K., Herring, S.A., Iverson, G.L., Jordan, B.D., Kissick, J., McCrea, M., McIntosh, A.S., Maddocks, D., Makdissi, M., Purcell, L., Putukian, M., Schneider, K., Tator, C.H., and Turner, M. (2013). Consensus Statement on Concussion in Sport: The 4(th) International Conference on Concussion in Sport Held in Zurich, November 2012. J Am Coll Surg 216, e55–71.

11. Barkhoudarian, G., Hovda, D.A., and Giza, C.C. (2011). The molecular pathophysiology of concussive brain injury. Clin Sport. Med 30, 33–48, vii–iii.

12. Giza, C.C., and Hovda, D.A. (2014). The New Neurometabolic Cascade of Concussion. Neurosurgery 75 (4), 24–33.

13. Uludağ, K., Dubowitz, D.J., Yoder, E.J., Restom, K., Liu, T.T., and Buxton, R.B. (2004). Coupling of cerebral blood flow and oxygen consumption during physiological activation and deactivation measured with fMRI. Neuroimage 23, 148–55.

14. Figley, C.R., and Stroman, P.W. (2011). The role(s) of astrocytes and astrocyte activity in neurometabolism, neurovascular coupling, and the production of functional neuroimaging signals. Eur. J. Neurosci. 33, 577–88.

15. Shibasaki, H. (2008). Human brain mapping: hemodynamic response and electrophysiology. Clin. Neurophysiol. 119, 731–43.

16. Pieper, P., and Garvan, C. (2013). Health-related quality-of-life in the first year following a childhood concussion. Brain Inj 1, 105–113.

17. Bigler, E.D., Deibert, E., and Filley, C.M. (2013). When is a concussion no longer a concussion? Neurology Available from: (http://www.cdc.gov/ncipc/tbi/Physician_Tool_Kit.

18. Ryali, S., Glover, G.H., Chang, C., and Menon, V. (2009). Development, validation, and comparison of ICA-based gradient artifact reduction algorithms for simultaneous EEG-spiral in/out and echo-planar fMRI recordings. Neuroimage 48, 348–361.

19. Congeni, J. (2009). Management of the adolescent concussion victim. Adolesc Med State Art Rev 20, 41–56.

20. Faul M, Xu L, Wald MM, C.V. (2010). Traumatic Brain Injury in the United States: Emergency Department Visits, Hospitalizations and Deaths 2002–2006. Centers Dis. Control Prev. Natl. Cent. Inj. Prev. Control , 891–904.

21. Sosin, D.M., Sniezek, J.E., and Thurman, D.J. (1996). Incidence of mild and moderate brain injury in the United States, 1991. Brain Inj. 10, 47–54.

22. Choe, M.C., Babikian, T., DiFiori, J., Hovda, D.A., and Giza, C.C. (2012). A pediatric perspective on concussion pathophysiology. Curr Opin Pediatr 24, 689–695.

23. Stewart, T.C., Gilliland, J., and Fraser, D.D. (2014). An epidemiologic profile of pediatric concussions: identifying urban and rural differences. J. Trauma Acute Care Surg. 76, 736–42.

24. Selassie, A.W., Wilson, D.A., Pickelsimer, E.E., Voronca, D.C., Williams, N.R., and Edwards, J.C. (2013). Incidence of sport-related traumatic brain injury and risk factors of severity: a population-based epidemiologic study. Ann Epidemiol 23, 750–756.

25. Seiger, A., Goldwater, E., and Deibert, E. (2014). Does Mechanism of Injury Play a Role in Recovery from Concussion? J. Head Trauma Rehabil. .

26. Boyce, S.H., and Quigley, M.A. (2003). An audit of sports injuries in children attending an Accident & Emergency department. Scott. Med. J. 48, 88–90.

27. Kelly, K.D., Lissel, H.L., Rowe, B.H., Vincenten, J.A., and Voaklander, D.C. (2001). Sport and recreation-related head injuries treated in the emergency department. Clin. J. Sport Med. 11, 77–81.

28. Andersson, E.E., Sejdhage, R., and Wage, V. (2012). Mild traumatic brain injuries in children between 0-16 years of age: a survey of activities and places when an accident occurs. Dev. Neurorehabil. 15, 26–30.

29. Gessel, L.M., Fields, S.K., Collins, C.L., Dick, R.W., and Comstock, R.D. (2007). Concussions among United States high school and collegiate athletes. J. Athl. Train. 42, 495–503.

30. Guskiewicz, K.M., and Mihalik, J.P. (2011). Biomechanics of sport concussion: quest for the elusive injury threshold. Exerc Sport Sci Rev 39, 4–11.

31. Ommaya, A.K., and Gennarelli, T.A. (1974). Cerebral concussion and traumatic unconsciousness. Correlation of experimental and clinical observations of blunt head injuries. Brain 97, 633–654.

32. Ommaya, A.K., Goldsmith, W., and Thibault, L. (2002). Biomechanics and neuropathology of adult and paediatric head injury. Br. J. Neurosurg. 16, 220–242.

33. Cassidy, J.D., Carroll, L.J., Peloso, P.M., Borg, J., von Holst, H., Holm, L., Kraus, J., and Coronado, V.G. (2004). Incidence, risk factors and prevention of mild traumatic brain injury: results of the WHO Collaborating Centre Task Force on Mild Traumatic Brain Injury. J. Rehabil. Med. , 28–60.

34. Ponsford, J., Cameron, P., Fitzgerald, M., Grant, M., and Mikocka-Walus, A. (2011). Long-term outcomes after uncomplicated mild traumatic brain injury: a comparison with trauma controls. J. Neurotrauma 28, 937–946.

35. Ayr, L.K., Yeates, K.O., Taylor, H.G., and Browne, M. (2009). Dimensions of postconcussive symptoms in children with mild traumatic brain injuries. J Int Neuropsychol Soc 15, 19–30.

36. McCrory, P., Collie, A., Anderson, V., and Davis, G. (2004). Can we manage sport related concussion in children the same as in adults? Br J Sport. Med 38, 516–519.

37. Barlow, K.M. (2014). Postconcussion Syndrome: A Review. J. Child Neurol. , e–pub.

38. McCauley, S.R., Boake, C., Pedroza, C., Brown, S.A., Levin, H.S., Goodman, H.S., and Merritt, S.G. (2008). Correlates of persistent postconcussional disorder: DSM-IV criteria versus ICD-10. J. Clin. Exp. Neuropsychol. 30, 360–79.

39. McCauley, S.R., Boake, C., Pedroza, C., Brown, S.A., Levin, H.S., Goodman, H.S., and Merritt, S.G. (2005). Postconcussional disorder: Are the DSM-IV criteria an improvement over the ICD-10? J. Nerv. Ment. Dis. 193, 540–50.

40. Brown, N.J., Mannix, R.C., O'Brien, M.J., Gostine, D., Collins, M.W., and Meehan, W.P. (2014). Effect of cognitive activity level on duration of post-concussion symptoms. Pediatrics 133, e299–304.

41. Babcock, L., Byczkowski, T., Wade, S.L., Ho, M., Mookerjee, S., and Bazarian, J.J. (2013). Predicting postconcussion syndrome after mild traumatic brain injury in children and adolescents who present to the emergency department. JAMA Pediatr. 167, 156–61.

42. Zemek, R., Clarkin, C., Farion, K.J., Vassilyadi, M., Anderson, P., Irish, B., Goulet, K., Barrowman, N., and Osmond, M.H. (2013). Parental anxiety at initial acute presentation is not associated with prolonged symptoms following pediatric concussion. Acad Emerg Med 20, 1041–1049.

43. Smyth, K., Sandhu, S.S., Crawford, S., Dewey, D., Parboosingh, J., and Barlow, K.M. (2014). The role of serotonin receptor alleles and environmental stressors in the development of post-concussive symptoms after pediatric mild traumatic brain injury. Dev. Med. Child Neurol. 56, 73–7.

44. McNally, K.A., Bangert, B., Dietrich, A., Nuss, K., Rusin, J., Wright, M., Taylor, H.G., and Yeates, K.O. (2013). Injury versus noninjury factors as predictors of postconcussive symptoms following mild traumatic brain injury in children. Neuropsychology 27, 1–12.

45. Kaufman, Y., Tzischinsky, O., Epstein, R., Etzioni, A., Lavie, P., and Pillar, G. (2001). Long-term sleep disturbances in adolescents after minor head injury. Pediatr. Neurol. 24, 129–34.

46. Meehan, W.P., d'Hemecourt, P., and Comstock, R.D. (2010). High school concussions in the 2008-2009 academic year: mechanism, symptoms, and management. Am. J. Sports Med. 38, 2405–9.

47. Guskiewicz, K.M., Perrin, D.H., and Gansneder, B.M. (1996). Effect of mild head injury on postural stability in athletes. J. Athl. Train. 31, 300–6.

48. Slobounov, S., Slobounov, E., Sebastianelli, W., Cao, C., and Newell, K. (2007). Differential rate of recovery in athletes after first and second concussion episodes. Neurosurgery 61, 338–44; discussion 344.

49. Gagnon, I., Swaine, B., Friedman, D., and Forget, R. (2004). Children show decreased dynamic balance after mild traumatic brain injury. Arch Phys Med Rehabil 85, 444–452.

50. Yeates, K.O., Taylor, H.G., Rusin, J., Bangert, B., Dietrich, A., Nuss, K., Wright, M., Nagin, D.S., and Jones, B.L. (2009). Longitudinal trajectories of postconcussive symptoms in children with mild traumatic brain injuries and their relationship to acute clinical status. Pediatrics 123, 735–743.

51. Taylor, H.G., Dietrich, A., Nuss, K., Wright, M., Rusin, J., Bangert, B., Minich, N., and Yeates, K.O. (2010). Post-concussive symptoms in children with mild traumatic brain injury. Neuropsychology 24, 148–59.

52. Prins, M., Greco, T., Alexander, D., and Giza, C.C. (2013). The pathophysiology of traumatic brain injury at a glance. Dis. Model. Mech. 6, 1307–15.

53. Giza, C.C., and Hovda, D.A. (2001). The Neurometabolic Cascade of Concussion. J Athl Train 36, 228–235.

54. Henry, L.C., Tremblay, S., Boulanger, Y., Ellemberg, D., and Lassonde, M. (2010). Neurometabolic changes in the acute phase after sports concussions correlate with symptom severity. J Neurotrauma 27, 65–76.

55. Henry, L.C., Tremblay, S., Leclerc, S., Khiat, A., Boulanger, Y., Ellemberg, D., and Lassonde, M. (2011). Metabolic changes in concussed American football players during the acute and chronic post-injury phases. BMC Neurol 11, 105.

56. Kirov, I.I., Tal, A., Babb, J.S., Reaume, J., Bushnik, T., Ashman, T.A., Flanagan, S., Grossman, R.I., and Gonen, O. (2013). Proton MR Spectroscopy Correlates Diffuse Axonal Abnormalities with Post-Concussive Symptoms in Mild Traumatic Brain Injury. J Neurotrauma 30, 1200–1204.

57. Bonne, O., Gilboa, A., Louzoun, Y., Kempf-Sherf, O., Katz, M., Fishman, Y., Ben-Nahum, Z., Krausz, Y., Bocher, M., Lester, H., Chisin, R., and Lerer, B. (2003). Cerebral blood flow in chronic symptomatic mild traumatic brain injury. Psychiatry Res 124, 141–152.

58. Ge, Y., Patel, M.B., Chen, Q., Grossman, E.J., Zhang, K., Miles, L., Babb, J.S., Reaume, J., and Grossman, R.I. (2009). Assessment of thalamic perfusion in patients with mild traumatic brain injury by true FISP arterial spin labelling MR imaging at 3T. Brain Inj 23, 666–674.

59. Lee, C.H., Yoo, K.-Y., Choi, J.H., Park, O.K., Hwang, I.K., Kwon, Y.-G., Kim, Y.-M., and Won, M.-H. (2010). Melatonin's protective action against ischemic neuronal damage is associated with up-regulation of the MT2 melatonin receptor. J. Neurosci. Res. 88, 2630–40.

60. Golding, E.M., Robertson, C.S., and Bryan Jr., R.M. (1999). The consequences of traumatic brain injury on cerebral blood flow and autoregulation: a review. Clin Exp Hypertens 21, 299–332.

61. Katayama, Y., Becker, D.P., Tamura, T., and Hovda, D. a. (1990). Massive increases in extracellular potassium and the indiscriminate release of glutamate following concussive brain injury. J. Neurosurg. 73, 889–900.

62. Wu, P., Zhao, Y., Haidacher, S.J., Wang, E., Parsley, M.O., Gao, J., Sadygov, R.G., Starkey, J.M., Luxon, B. a, Spratt, H., Dewitt, D.S., Prough, D.S., and Denner, L. (2013). Detection of structural and metabolic changes in traumatically injured hippocampus by quantitative differential proteomics. J. Neurotrauma 30, 775–88.

63. Lemka, M., Brockhuis, B., Lass, P., and Pilarska, E. (2005). [Headache occurrence and assessment of regional blood flow after brain concussion in children]. Neurol Neurochir Pol 39, S42–8.

64. Gowda, N.K., Agrawal, D., Bal, C., Chandrashekar, N., Tripati, M., Bandopadhyaya, G.P., Malhotra, A., and Mahapatra, A.K. (2006). Technetium Tc-99m ethyl cysteinate dimer brain single-photon emission CT in mild traumatic brain injury: a prospective study. AJNR Am J Neuroradiol 27, 447–451.

65. Mandera, M., Larysz, D., and Wojtacha, M. (2002). Changes in cerebral hemodynamics assessed by transcranial Doppler ultrasonography in children after head injury. Childs Nerv Syst 18, 124–128.

66. Garnett, M.R., Blamire, A.M., Corkill, R.G., Cadoux-Hudson, T.A., Rajagopalan, B., and Styles, P. (2000). Early proton magnetic resonance spectroscopy in normal-appearing brain correlates with outcome in patients following traumatic brain injury. Brain 123 (Pt 1, 2046–54.

67. Vagnozzi, R., Signoretti, S., Cristofori, L., Alessandrini, F., Floris, R., Isgrò, E., Ria, A., Marziale, S., Zoccatelli, G., Tavazzi, B., Del Bolgia, F., Sorge, R., Broglio, S.P., McIntosh, T.K., Lazzarino, G., and Isgro, E. (2010). Assessment of metabolic brain damage and recovery following mild traumatic brain injury: a multicentre, proton magnetic resonance spectroscopic study in concussed patients. Brain 133, 3232–3242.

68. Vagnozzi, R., Signoretti, S., Floris, R., Marziali, S., Manara, M., Amorini, A.M., Belli, A., Di Pietro, V., D'urso, S., Pastore, F.S., Lazzarino, G., and Tavazzi, B. (2013). Decrease in

N-Acetylaspartate Following Concussion May Be Coupled to Decrease in Creatine. J Head Trauma Rehabil 28, 284–292.

69. Vagnozzi, R., Signoretti, S., Tavazzi, B., Floris, R., Ludovici, A., Marziali, S., Tarascio, G., Amorini, A.M., Di Pietro, V., Delfini, R., and Lazzarino, G. (2008). Temporal window of metabolic brain vulnerability to concussion: a pilot 1H-magnetic resonance spectroscopic study in concussed athletes--part III. Neurosurgery 62, 1286.

70. Govind, V., Gold, S., Kaliannan, K., Saigal, G., Falcone, S., Arheart, K.L., Harris, L., Jagid, J., and Maudsley, A.A. (2010). Whole-brain proton MR spectroscopic imaging of mild-to-moderate traumatic brain injury and correlation with neuropsychological deficits. J. Neurotrauma 27, 483–96.

71. Govindaraju, V., Gauger, G.E., Manley, G.T., Ebel, A., Meeker, M., and Maudsley, A.A. (2004). Volumetric proton spectroscopic imaging of mild traumatic brain injury. AJNR Am J Neuroradiol 25, 730–737.

72. Johnson, B., Gay, M., Zhang, K., Neuberger, T., Horovitz, S.G., Hallett, M., Sebastianelli, W., and Slobounov, S. (2012). The use of magnetic resonance spectroscopy in the subacute evaluation of athletes recovering from single and multiple mild traumatic brain injury. J Neurotrauma 29, 2297–2304.

73. Gasparovic, C., Yeo, R., Mannell, M., Ling, J., Elgie, R., Phillips, J., Doezema, D., and Mayer, A.R. (2009). Neurometabolite concentrations in gray and white matter in mild traumatic brain injury: an 1H-magnetic resonance spectroscopy study. J. Neurotrauma 26, 1635–43.

74. Yeo, R.A., Gasparovic, C., Merideth, F., Ruhl, D., Doezema, D., and Mayer, A.R. (2011). A longitudinal proton magnetic resonance spectroscopy study of mild traumatic brain injury. J Neurotrauma 28, 1–11.

75. Chamard, E., Henry, L., Boulanger, Y., Lassonde, M., and Theoret, H. (2013). A Follow-Up Study of Neurometabolic Alterations in Female Concussed Athletes. J Neurotrauma 31, 339–345.

76. Chamard, E., Lassonde, M., Henry, L., Tremblay, J., Boulanger, Y., De Beaumont, L., Théoret, H., and Theoret, H. (2013). Neurometabolic and microstructural alterations following a sports-related concussion in female athletes. Brain Inj 27, 1038–1046.

77. Dean, P.J., Otaduy, M.C., Harris, L.M., McNamara, A., Seiss, E., and Sterr, A. (2013). Monitoring long-term effects of mild traumatic brain injury with magnetic resonance spectroscopy: a pilot study. Neuroreport 24, 677–681.

78. Bartnik-Olson, B.L., Holshouser, B., Wang, H., Grube, M., Tong, K., Wong, V., and Ashwal, S. (2014). Impaired Neurovascular Unit Function Contributes to Persistent Symptoms after Concussion: a Pilot Study. J. Neurotrauma , 1497–1506.

79. Buxton, R.B., and Frank, L.R. (1997). A model for the coupling between cerebral blood flow and oxygen metabolism during neural stimulation. J Cereb Blood Flow Metab 17, 64–72.

80. Strangman, G., Culver, J.P., Thompson, J.H., and Boas, D.A. (2002). A quantitative comparison of simultaneous BOLD fMRI and NIRS recordings during functional brain activation. Neuroimage 17, 719–731.

81. Len, T.K., and Neary, J.P. (2011). Cerebrovascular pathophysiology following mild traumatic brain injury. Clin Physiol Funct Imaging 31, 85–93.

82. Stepien, A., Maksymiuk, G., Skrzynski, S., Chmielowski, K., Podgorski, J.K., Kwasucki, J., and Pietrzykowski, J. (1999). [Assessment of regional blood flow in patients after mild head trauma]. Neurol Neurochir Pol 33, 119–129.

83. Becelewski, J., and Pierzchala, K. (2002). [Dynamic assessment of blood flow in pre-cranial and intracranial arteries in patients with mild head injuries]. Neurol Neurochir Pol 36, 1135–1138.

84. McQuire, J.C., Sutcliffe, J.C., and Coats, T.J. (1998). Early changes in middle cerebral artery blood flow velocity after head injury. J Neurosurg 89, 526–532.

85. Raichle, M.E. (1997). Food for thought. The metabolic and circulatory requirements of cognition. Ann. N. Y. Acad. Sci. 835, 373–85.

86. Ogawa, S., Menon, R.S., Tank, D.W., Kim, S.G., Merkle, H., Ellermann, J.M., and Ugurbil, K. (1993). Functional brain mapping by blood oxygenation level-dependent contrast magnetic resonance imaging. A comparison of signal characteristics with a biophysical model. Biophys J 64, 803–812.

87. Jantzen, K.J., Anderson, B., Steinberg, F.L., and Kelso, J.A. (2004). A prospective functional MR imaging study of mild traumatic brain injury in college football players. AJNR Am J Neuroradiol 25, 738–745.

88. Lovell, M.R., Pardini, J.E., Welling, J., Collins, M.W., Bakal, J., Lazar, N., Roush, R., Eddy, W.F., and Becker, J.T. (2007). Functional brain abnormalities are related to clinical recovery and time to return-to-play in athletes. Neurosurgery 61, 352–360.

89. Schatz, P., and Maerlender, A. (2013). A Two-Factor Theory for Concussion Assessment Using ImPACT: Memory and Speed. Arch Clin Neuropsychol 28, 791–797.

90. Smits, M., Dippel, D.W.J., Houston, G.C., Wielopolski, P.A., Koudstaal, P.J., Hunink, M.G.M., and van der Lugt, A. (2009). Postconcussion syndrome after minor head injury: brain activation of working memory and attention. Hum. Brain Mapp. 30, 2789–803.

91. Pardini, J.E., Pardini, D.A., Becker, J.T., Dunfee, K.L., Eddy, W.F., Lovell, M.R., and Welling, J.S. (2010). Postconcussive symptoms are associated with compensatory cortical recruitment during a working memory task. Neurosurgery 67, 1020–1028.

92. Mayer, A.R., Mannell, M. V, Ling, J., Elgie, R., Gasparovic, C., Phillips, J.P., Doezema, D., and Yeo, R.A. (2009). Auditory orienting and inhibition of return in mild traumatic brain injury: a FMRI study. Hum Brain Mapp 30, 4152–4166.

93. Yang, Z., Yeo, R.A., Pena, A., Ling, J.M., Klimaj, S., Campbell, R., Doezema, D., and Mayer, A.R. (2012). An FMRI study of auditory orienting and inhibition of return in pediatric mild traumatic brain injury. J Neurotrauma 29, 2124–2136.

94. McAllister, T.W., Saykin, A.J., Flashman, L.A., Sparling, M.B., Johnson, S.C., Guerin, S.J., Mamourian, A.C., Weaver, J.B., and Yanofsky, N. (1999). Brain activation during working memory 1 month after mild traumatic brain injury: a functional MRI study. Neurology 53, 1300–1308.

95. McAllister, T.W., Sparling, M.B., Flashman, L.A., Guerin, S.J., Mamourian, A.C., and Saykin, A.J. (2001). Differential working memory load effects after mild traumatic brain injury. Neuroimage 14, 1004–1012.

96. Keightley, M.L., Chen, J.K., and Ptito, A. (2012). Examining the neural impact of pediatric concussion: a scoping review of multimodal and integrative approaches using functional and structural MRI techniques. Curr Opin Pediatr 24, 709–716.

97. Slobounov, S.M., Zhang, K., Pennell, D., Ray, W., Johnson, B., and Sebastianelli, W. (2010). Functional abnormalities in normally appearing athletes following mild traumatic brain injury: a functional MRI study. Exp Brain Res 202, 341–354.

98. Krivitzky, L.S., Roebuck-Spencer, T.M., Roth, R.M., Blackstone, K., Johnson, C.P., and Gioia, G. (2011). Functional magnetic resonance imaging of working memory and response inhibition in children with mild traumatic brain injury. J Int Neuropsychol Soc 17, 1143–1152.

99. Chen, J.K., Johnston, K.M., Frey, S., Petrides, M., Worsley, K., and Ptito, A. (2004). Functional abnormalities in symptomatic concussed athletes: an fMRI study. Neuroimage 22, 68–82.

100. Chen, J.-K.K., Johnston, K.M., Collie, A., McCrory, P., and Ptito, A. (2007). A validation of the post concussion symptom scale in the assessment of complex concussion using cognitive testing and functional MRI. J Neurol Neurosurg Psychiatry 78, 1231–1238.

101. Chen, J.K., Johnston, K.M., Petrides, M., and Ptito, A. (2008). Recovery from mild head injury in sports: evidence from serial functional magnetic resonance imaging studies in male athletes. Clin J Sport Med 18, 241–247.

102. Gosselin, N., Bottari, C., Chen, J.-K., Petrides, M., Tinawi, S., de Guise, E., and Ptito, A. (2011). Electrophysiology and functional MRI in post-acute mild traumatic brain injury. J. Neurotrauma 28, 329–41.

103. Keightley, M.L., Saluja, R.S., Chen, J.K., Gagnon, I., Leonard, G., Petrides, M., and Ptito, A. (2013). An fMRI Study of Working Memory in Youth Following Sports-related Concussion: Is it Still Working? J Neurotrauma 5, 437–451.

104. Hammeke, T.A., McCrea, M., Coats, S.M., Verber, M.D., Durgerian, S., Flora, K., Olsen, G.S., Leo, P.D., Gennarelli, T.A., and Rao, S.M. (2013). Acute and Subacute Changes in Neural Activation during the Recovery from Sport-Related Concussion. J Int Neuropsychol Soc , 1–10.

105. Terry, D.P., Faraco, C.C., Smith, D., Diddams, M.J., Puente, A.N., and Miller, L.S. (2012). Lack of long-term fMRI differences after multiple sports-related concussions. Brain Inj 26, 1684–1696.

106. Ciuciu, P., Abry, P., and He, B.J. (2014). Interplay between functional connectivity and scale-free dynamics in intrinsic fMRI networks. Neuroimage , 248–263.

107. Damoiseaux, J.S., Rombouts, S.A., Barkhof, F., Scheltens, P., Stam, C.J., Smith, S.M., and Beckmann, C.F. (2006). Consistent resting-state networks across healthy subjects. Proc Natl Acad Sci U S A 103, 13848–13853.

108. Johnson, B., Zhang, K., Gay, M., Horovitz, S., Hallett, M., Sebastianelli, W., and Slobounov, S. (2012). Alteration of brain default network in subacute phase of injury in concussed individuals: resting-state fMRI study. Neuroimage 59, 511–518.

109. Li, R., Chen, K., Fleisher, A.S., Reiman, E.M., Yao, L., and Wu, X. (2011). Large-scale directional connections among multi resting-state neural networks in human brain: a functional MRI and Bayesian network modeling study. Neuroimage 56, 1035–1042.

110. Zhou, Y., Milham, M.P., Lui, Y.W., Miles, L., Reaume, J., Sodickson, D.K., Grossman, R.I., and Ge, Y. (2012). Default-mode network disruption in mild traumatic brain injury. Radiology 265, 882–892.

111. Mayer, A.R., Yang, Z., Yeo, R.A., Pena, A., Ling, J.M., Mannell, M. V, Stippler, M., and Mojtahed, K. (2012). A functional MRI study of multimodal selective attention following mild traumatic brain injury. Brain Imaging Behav 6, 343–354.

112. Zhang, K., Johnson, B., Gay, M., Horovitz, S.G., Hallett, M., Sebastianelli, W., and Slobounov, S. (2012). Default mode network in concussed individuals in response to the YMCA physical stress test. J Neurotrauma 29, 756–765.

113. Mayer, A.R., Mannell, M. V, Ling, J., Gasparovic, C., and Yeo, R.A. (2011). Functional connectivity in mild traumatic brain injury. Hum Brain Mapp 32, 1825–1835.

114. Zhu, D.C., Covassin, T., Nogle, S., Doyle, S., Russell, D., Pearson, R.L., Monroe, J., Liszewski, C.M., DeMarco, J.K., and Kaufman, D.I. (2014). A Potential Biomarker in Sports-Related Concussion: Brain Functional Connectivity Alteration of the Default-Mode Network Measured with Longitudinal Resting-State fMRI over 30 Days. J. Neurotrauma .

115. Sours, C., Rosenberg, J., Kane, R., Roys, S., Zhuo, J., Shanmuganathan, K., and Gullapalli, R.P. (2014). Associations between interhemispheric functional connectivity and the Automated Neuropsychological Assessment Metrics (ANAM) in civilian mild TBI. Brain Imaging Behav. .

116. Slobounov, S.M., Gay, M., Zhang, K., Johnson, B., Pennell, D., Sebastianelli, W., Horovitz, S., and Hallett, M. (2011). Alteration of brain functional network at rest and in response to YMCA physical stress test in concussed athletes: RsFMRI study. Neuroimage 55, 1716–27.

117. Shumskaya, E., Andriessen, T.M., Norris, D.G., and Vos, P.E. (2012). Abnormal whole-brain functional networks in homogeneous acute mild traumatic brain injury. Neurology 79, 175–182.

118. Tang, L., Ge, Y., Sodickson, D.K., Miles, L., Zhou, Y., Reaume, J., and Grossman, R.I. (2011). Thalamic resting-state functional networks: disruption in patients with mild traumatic brain injury. Radiology 260, 831–40.

119. Zhou, Y., Lui, Y.W., Zuo, X.-N., Milham, M.P., Reaume, J., Grossman, R.I., and Ge, Y. (2014). Characterization of thalamo-cortical association using amplitude and connectivity of functional MRI in mild traumatic brain injury. J. Magn. Reson. Imaging 39, 1558–68.

120. Messe, A., Caplain, S., Pelegrini-Issac, M., Blancho, S., Levy, R., Aghakhani, N., Montreuil, M., Benali, H., and Lehericy, S. (2013). Specific and evolving resting-state network alterations in post-concussion syndrome following mild traumatic brain injury. PLoS One 8, e65470.

121. Gardner, A., Kay-Lambkin, F., Stanwell, P., Donnelly, J., Williams, W.H., Hiles, A., Schofield, P., Levi, C., and Jones, D.K. (2012). A systematic review of diffusion tensor imaging findings in sports-related concussion. J Neurotrauma 29, 2521–2538.

122. Bazarian, J.J., Zhong, J., Blyth, B., Zhu, T., Kavcic, V., and Peterson, D. (2007). Diffusion tensor imaging detects clinically important axonal damage after mild traumatic brain injury: a pilot study. J Neurotrauma 24, 1447–1459.

123. Miles, L., Grossman, R.I., Johnson, G., Babb, J.S., Diller, L., and Inglese, M. (2008). Short-term DTI predictors of cognitive dysfunction in mild traumatic brain injury. Brain Inj 22, 115–122.

124. Rutgers, D.R., Fillard, P., Paradot, G., Tadie, M., Lasjaunias, P., and Ducreux, D. (2008). Diffusion tensor imaging characteristics of the corpus callosum in mild, moderate, and severe traumatic brain injury. AJNR Am J Neuroradiol 29, 1730–1735.

125. Wilde, E.A., McCauley, S.R., Hunter, J. V, Bigler, E.D., Chu, Z., Wang, Z.J., Hanten, G.R., Troyanskaya, M., Yallampalli, R., Li, X., Chia, J., and Levin, H.S. (2008). Diffusion tensor imaging of acute mild traumatic brain injury in adolescents. Neurology 70, 948–955.

126. Mayer, A.R., Ling, J., Mannell, M. V, Gasparovic, C., Phillips, J.P., Doezema, D., Reichard, R., and Yeo, R.A. (2010). A prospective diffusion tensor imaging study in mild traumatic brain injury. Neurology 74, 643–650.

127. Cubon, V.A., Putukian, M., Boyer, C., and Dettwiler, A. (2011). A diffusion tensor imaging study on the white matter skeleton in individuals with sports-related concussion. J Neurotrauma 28, 189–201.

128. Henry, L.C., Tremblay, J., Tremblay, S., Lee, A., Brun, C., Lepore, N., Theoret, H., Ellemberg, D., and Lassonde, M. (2011). Acute and chronic changes in diffusivity measures after sports concussion. J Neurotrauma 28, 2049–2059.

129. Smits, M., Houston, G.C., Dippel, D.W., Wielopolski, P.A., Vernooij, M.W., Koudstaal, P.J., Hunink, M.G., and van der Lugt, A. (2011). Microstructural brain injury in post-concussion syndrome after minor head injury. Neuroradiology 53, 553–563.

130. Bazarian, J.J., Zhu, T., Blyth, B., Borrino, A., and Zhong, J. (2012). Subject-specific changes in brain white matter on diffusion tensor imaging after sports-related concussion. Magn Reson Imaging 30, 171–180.

131. Kasahara, K., Hashimoto, K., Abo, M., and Senoo, A. (2012). Voxel- and atlas-based analysis of diffusion tensor imaging may reveal focal axonal injuries in mild traumatic brain injury -- comparison with diffuse axonal injury. Magn Reson Imaging 30, 496–505.

132. Lange, R.T., Iverson, G.L., Brubacher, J.R., Madler, B., and Heran, M.K. (2012). Diffusion tensor imaging findings are not strongly associated with postconcussional disorder 2 months following mild traumatic brain injury. J Head Trauma Rehabil 27, 188–198.

133. Lipton, M.L., Kim, N., Park, Y.K., Hulkower, M.B., Gardin, T.M., Shifteh, K., Kim, M., Zimmerman, M.E., Lipton, R.B., and Branch, C.A. (2012). Robust detection of traumatic axonal injury in individual mild traumatic brain injury patients: intersubject variation, change over time and bidirectional changes in anisotropy. Brain Imaging Behav 6, 329–342.

134. Zhang, K., Johnson, B., Gay, M., Horovitz, S.G., Hallett, M., Sebastianelli, W., and Slobounov, S. (2012). Default mode network in concussed individuals in response to the YMCA physical stress test. J Neurotrauma 29, 756–765.

135. Bouix, S., Pasternak, O., Rathi, Y., Pelavin, P.E., Zafonte, R., and Shenton, M.E. (2013). Increased gray matter diffusion anisotropy in patients with persistent post-concussive symptoms following mild traumatic brain injury. PLoS One 8, e66205.

136. Grossman, E.J., Ge, Y., Jensen, J.H., Babb, J.S., Miles, L., Reaume, J., Silver, J.M., Grossman, R.I., and Inglese, M. (2012). Thalamus and cognitive impairment in mild traumatic brain injury: a diffusional kurtosis imaging study. J Neurotrauma 29, 2318–2327.

137. Kou, Z., Gattu, R., Kobeissy, F., Welch, R.D., O'Neil, B.J., Woodard, J.L., Ayaz, S.I., Kulek, A., Kas-Shamoun, R., Mika, V., Zuk, C., Tomasello, F., and Mondello, S. (2013). Combining biochemical and imaging markers to improve diagnosis and characterization of mild traumatic brain injury in the acute setting: results from a pilot study. PLoS One 8, e80296.

138. Shenton, M.E., Hamoda, H.M., Schneiderman, J.S., Bouix, S., Pasternak, O., Rathi, Y., Vu, M.A., Purohit, M.P., Helmer, K., Koerte, I., Lin, A.P., Westin, C.F., Kikinis, R., Kubicki, M., Stern, R.A., and Zafonte, R. (2012). A review of magnetic resonance imaging and diffusion tensor imaging findings in mild traumatic brain injury. Brain Imaging Behav 6, 137–192.

139. Wozniak, J.R., Krach, L., Ward, E., Mueller, B.A., Muetzel, R., Schnoebelen, S., Kiragu, A., and Lim, K.O. (2007). Neurocognitive and neuroimaging correlates of pediatric traumatic brain injury: a diffusion tensor imaging (DTI) study. Arch Clin Neuropsychol 22, 555–568.

140. Raichle, M.E., Grubb, R.L., Gado, M.H., Eichling, J.O., and Ter-Pogossian, M.M. (1976). Correlation between regional cerebral blood flow and oxidative metabolism. In vivo studies in man. Arch Neurol 33, 523–526.

141. Roy, C.S., and Sherrington, C.S. (1890). On the Regulation of the Blood-supply of the Brain. J. Physiol. 11, 85–158.17.

142. Franceschini, M.A., Fantini, S., Thompson, J.H., Culver, J.P., and Boas, D.A. (2003). Hemodynamic evoked response of the sensorimotor cortex measured noninvasively with near-infrared optical imaging. Psychophysiology 40, 548–560.

143. Leenders, K.L., Perani, D., Lammertsma, A.A., Heather, J.D., Buckingham, P., Healy, M.J., Gibbs, J.M., Wise, R.J., Hatazawa, J., and Herold, S. (1990). Cerebral blood flow, blood volume and oxygen utilization. Normal values and effect of age. Brain 113 (Pt 1, 27–47.

144. Kim, S.G., and Ogawa, S. (2012). Biophysical and physiological origins of blood oxygenation level-dependent fMRI signals. J Cereb Blood Flow Metab 32, 1188–1206.

145. Gagnon, L., Yucel, M.A., Dehaes, M., Cooper, R.J., Perdue, K.L., Selb, J., Huppert, T.J., Hoge, R.D., and Boas, D.A. (2012). Quantification of the cortical contribution to the NIRS signal over the motor cortex using concurrent NIRS-fMRI measurements. Neuroimage 59, 3933–3940.

146. Strangman, G., Franceschini, M.A., and Boas, D.A. (2003). Factors affecting the accuracy of near-infrared spectroscopy concentration calculations for focal changes in oxygenation parameters. Neuroimage 18, 865–79.

147. Center for Disease Control and prevention (CDC). (2010). Facts about Concussion and Brain injury., 1–16 [cited 2014 Oct 14] Available from: http://www.cdc.gov/concussion/pdf/Fact_Sheet_ConcussTBI-a.pdf.

148. Jöbsis, F.F. (1977). Noninvasive, infrared monitoring of cerebral and myocardial oxygen sufficiency and circulatory parameters. Science 198, 1264–1267.

149. Obrig, H., and Villringer, A. (2003). Beyond the visible--imaging the human brain with light. J. Cereb. Blood Flow Metab. 23, 1–18.

150. Delpy, D.T., Cope, M., van der Zee, P., Arridge, S., Wray, S., and Wyatt, J. (1988). Estimation of optical pathlength through tissue from direct time of flight measurement. Phys. Med. Biol. 33, 1433–42.

151. Wray, S., Cope, M., Delpy, D.T., Wyatt, J.S., and Reynolds, E.O. (1988). Characterization of the near infrared absorption spectra of cytochrome aa3 and haemoglobin for the non-invasive monitoring of cerebral oxygenation. Biochim. Biophys. Acta 933, 184–92.

152. Sato, H., Kiguchi, M., Kawaguchi, F., and Maki, A. (2004). Practicality of wavelength selection to improve signal-to-noise ratio in near-infrared spectroscopy. Neuroimage 21, 1554–62.

153. Okui, N., and Okada, E. (2005). Wavelength dependence of crosstalk in dual-wavelength measurement of oxy- and deoxy-hemoglobin. J. Biomed. Opt. 10, 11015.

154. Joseph, D.K., Huppert, T.J., Franceschini, M.A., and Boas, D.A. (2006). Diffuse optical tomography system to image brain activation with improved spatial resolution and validation with functional magnetic resonance imaging. Appl. Opt. 45, 8142–51.

155. Ferrari, M., and Quaresima, V. (2012). A brief review on the history of human functional near-infrared spectroscopy (fNIRS) development and fields of application. Neuroimage 63, 921–35.

156. Huppert, T.J., Diamond, S.G., Franceschini, M.A., and Boas, D.A. (2009). HomER: a review of time-series analysis methods for near-infrared spectroscopy of the brain. Appl Opt 48, D280–98.

157. Boas, D.A., Gaudette, T., Strangman, G., Cheng, X., Marota, J.J., and Mandeville, J.B. (2001). The accuracy of near infrared spectroscopy and imaging during focal changes in cerebral hemodynamics. Neuroimage 13, 76–90.

158. Arfanakis, K., Cordes, D., Haughton, V.M., Moritz, C.H., Quigley, M.A., and Meyerand, M.E. (2000). Combining independent component analysis and correlation analysis to probe interregional connectivity in fMRI task activation datasets. Magn. Reson. Imaging 18, 921–30.

159. Biswal, B., Yetkin, F.Z., Haughton, V.M., and Hyde, J.S. (1995). Functional connectivity in the motor cortex of resting human brain using echo-planar MRI. Magn. Reson. Med. 34, 537–41.

160. Seeley, W.W., Crawford, R.K., Zhou, J., Miller, B.L., and Greicius, M.D. (2009). Neurodegenerative diseases target large-scale human brain networks. Neuron 62, 42–52.

161. Buxton, R.B., Griffeth, V.E.M., Simon, A.B., and Moradi, F. (2014). Variability of the coupling of blood flow and oxygen metabolism responses in the brain: a problem for interpreting BOLD studies but potentially a new window on the underlying neural activity. Front. Neurosci. 8, 139.

162. Biswal, B.B., Van Kylen, J., and Hyde, J.S. (1997). Simultaneous assessment of flow and BOLD signals in resting-state functional connectivity maps. NMR Biomed. 10, 165–70.

163. Sun, F.T., Miller, L.M., and D'Esposito, M. (2004). Measuring interregional functional connectivity using coherence and partial coherence analyses of fMRI data. Neuroimage 21, 647–58.

164. Lindquist, M.A. (2008). The Statistical Analysis of fMRI Data. Stat. Sci. 23, 439–464.

165. Fries, P. (2005). A mechanism for cognitive dynamics: neuronal communication through neuronal coherence. Trends Cogn. Sci. 9, 474–80.

166. Maurits, N.M., Scheeringa, R., van der Hoeven, J.H., and de Jong, R. (2006). EEG coherence obtained from an auditory oddball task increases with age. J. Clin. Neurophysiol. 23, 395–403.

167. Marchini, J.L., and Ripley, B.D. (2000). A new statistical approach to detecting significant activation in functional MRI. Neuroimage 12, 366–80.

168. Obrig, H., Neufang, M., Wenzel, R., Kohl, M., Steinbrink, J., Einhäupl, K., and Villringer, A. (2000). Spontaneous low frequency oscillations of cerebral hemodynamics and metabolism in human adults. Neuroimage 12, 623–39.

169. Okada, E., and Delpy, D.T. (2003). Near-infrared light propagation in an adult head model. II. Effect of superficial tissue thickness on the sensitivity of the near-infrared spectroscopy signal. Appl Opt 42, 2915–2922.

170. Scholkmann, F., Kleiser, S., Metz, A.J., Zimmermann, R., Mata Pavia, J., Wolf, U., and Wolf, M. (2014). A review on continuous wave functional near-infrared spectroscopy and imaging instrumentation and methodology. Neuroimage 85 Pt 1, 6–27.

171. Boas, D.A., Elwell, C.E., Ferrari, M., and Taga, G. (2014). Twenty years of functional near-infrared spectroscopy: introduction for the special issue. Neuroimage 85 Pt 1, 1–5.

172. Chiarelli, A.M., Romani, G.L., and Merla, A. (2014). Fast optical signals in the sensorimotor cortex: General Linear Convolution Model applied to multiple source-detector distance-based data. Neuroimage 85 Pt 1, 245–54.

173. Alderliesten, T., De Vis, J.B., Lemmers, P.M.A., van Bel, F., Benders, M.J.N.L., Hendrikse, J., and Petersen, E.T. (2014). Simultaneous quantitative assessment of cerebral physiology using respiratory-calibrated MRI and near-infrared spectroscopy in healthy adults. Neuroimage 85 Pt 1, 255–63.

174. Huppert, T.J., Hoge, R.D., Diamond, S.G., Franceschini, M.A., and Boas, D.A. (2006). A temporal comparison of BOLD, ASL, and NIRS hemodynamic responses to motor stimuli in adult humans. Neuroimage 29, 368–82.

175. Obrig, H. (2013). NIRS in clinical neurology - a "promising" tool? Neuroimage 85 Pt 1, 535–546.

176. Homae, F. (2014). A brain of two halves: insights into interhemispheric organization provided by near-infrared spectroscopy. Neuroimage 85 Pt 1, 354–62.

177. Imai, M., Watanabe, H., Yasui, K., Kimura, Y., Shitara, Y., Tsuchida, S., Takahashi, N., and Taga, G. (2014). Functional connectivity of the cortex of term and preterm infants and infants with Down's syndrome. Neuroimage 85 Pt 1, 272–8.

178. Jimenez, J.J., Yang, R., Nathoo, N., Varshney, V.P., Golestani, A.-M., Goodyear, B.G., Metz, L.M., and Dunn, J.F. (2014). Detection of reduced interhemispheric cortical communication during task execution in multiple sclerosis patients using functional near-infrared spectroscopy. J. Biomed. Opt. 19, 076008.

179. Piper, S.K., Krueger, A., Koch, S.P., Mehnert, J., Habermehl, C., Steinbrink, J., Obrig, H., and Schmitz, C.H. (2014). A wearable multi-channel fNIRS system for brain imaging in freely moving subjects. Neuroimage 85 Pt 1, 64–71.

180. Jasper, H.H. (1958). The ten-twenty electrode system of the International Federation. Electroencephalogr. Clin. Neurophysiol. 10, 371–375.

181. Weatherall, A., Skowno, J., Lansdown, A., Lupton, T., and Garner, A. (2012). Feasibility of cerebral near-infrared spectroscopy monitoring in the pre-hospital environment. Acta Anaesthesiol Scand 56, 172–177.

182. Strangman, G., Boas, D.A., and Sutton, J.P. (2002). Non-invasive neuroimaging using near-infrared light. Biol Psychiatry 52, 679–693.

183. Barlow, K.M., Brooks, B.L., MacMaster, F.P., Kirton, A., Seeger, T., Esser, M., Crawford, S., Nettel-Aguirre, A., Zemek, R., Angelo, M., Kirk, V., Emery, C.A., Johnson, D., Hill, M.D., Buchhalter, J., Turley, B., Richer, L., Platt, R., Hutchison, J., and Dewey, D. (2014). A double-blind, placebo-controlled intervention trial of 3 and 10 mg sublingual melatonin for post-concussion syndrome in youths (PLAYGAME): study protocol for a randomized controlled trial. Trials 15, 271.

184. King, N.S., Crawford, S., Wenden, F.J., Moss, N.E., and Wade, D.T. (1995). The Rivermead Post Concussion Symptoms Questionnaire: a measure of symptoms commonly experienced after head injury and its reliability. J Neurol 242, 587–592.

185. Varshney, V., Liapounova, A., Golestani, A.M., Goodyear, B., and Dunn, J.F. (2013). Detection of inter-hemispheric functional connectivity in motor cortex with coherence analysis. J Eur. Opt Soc Rap Public 7 .

186. Wright, S.P. (University of T. (1992). Adjusted P-Values for Simultaneous Inferences. Biometrics 48, 1005–1013.

187. Indovina, I., and Sanes, J.N. (2001). On somatotopic representation centers for finger movements in human primary motor cortex and supplementary motor area. Neuroimage 13, 1027–34.

188. Culver, J.P., Siegel, A.M., Franceschini, M.A., Mandeville, J.B., and Boas, D.A. (2005). Evidence that cerebral blood volume can provide brain activation maps with better spatial resolution than deoxygenated hemoglobin. Neuroimage 27, 947–59.

189. Sheth, S.A., Nemoto, M., Guiou, M., Walker, M., Pouratian, N., Hageman, N., and Toga, A.W. (2004). Columnar specificity of microvascular oxygenation and volume responses: implications for functional brain mapping. J. Neurosci. 24, 634–41.

190. Penfield, W., and Boldrey, E. (1937). Somatic motor and sensory representation in the cerebral cortex of man as studied by electrical stimulation. J. Neurol. Brain 60, 389–443.

191. Boas, D.A., Dale, A.M., and Franceschini, M.A. (2004). Diffuse optical imaging of brain activation: approaches to optimizing image sensitivity, resolution, and accuracy. Neuroimage 23, S275–88.

192. Sasai, S., Homae, F., Watanabe, H., and Taga, G. (2011). Frequency-specific functional connectivity in the brain during resting state revealed by NIRS. Neuroimage 56, 252–257.

193. Mesquita, R.C., Franceschini, M.A., and Boas, D.A. (2010). Resting state functional connectivity of the whole head with near-infrared spectroscopy. Biomed Opt Express 1, 324–336.

194. Birn, R.M., Diamond, J.B., Smith, M.A., and Bandettini, P.A. (2006). Separating respiratory-variation-related fluctuations from neuronal-activity-related fluctuations in fMRI. Neuroimage 31, 1536–48.

195. Pierro, M.L., Sassaroli, A., Bergethon, P.R., Ehrenberg, B.L., and Fantini, S. (2012). Phase-amplitude investigation of spontaneous low-frequency oscillations of cerebral hemodynamics with near-infrared spectroscopy: a sleep study in human subjects. Neuroimage 63, 1571–84.

196. Hoshi, Y., Kosaka, S., Xie, Y., Kohri, S., and Tamura, M. (1998). Relationship between fluctuations in the cerebral hemoglobin oxygenation state and neuronal activity under resting conditions in man. Neurosci. Lett. 245, 147–50.

197. Tong, Y., Lindsey, K.P., and deB Frederick, B. (2011). Partitioning of physiological noise signals in the brain with concurrent near-infrared spectroscopy and fMRI. J. Cereb. Blood Flow Metab. 31, 2352–62.

198. Biswal, B., Hudetz, A.G., Yetkin, F.Z., Haughton, V.M., and Hyde, J.S. (1997). Hypercapnia reversibly suppresses low-frequency fluctuations in the human motor cortex during rest using echo-planar MRI. J. Cereb. Blood Flow Metab. 17, 301–8.

199. Li, S.J., Biswal, B., Li, Z., Risinger, R., Rainey, C., Cho, J.K., Salmeron, B.J., and Stein, E.A. (2000). Cocaine administration decreases functional connectivity in human primary visual and motor cortex as detected by functional MRI. Magn. Reson. Med. 43, 45–51.

200. Mitra, P.P., Ogawa, S., Hu, X., and Uğurbil, K. (1997). The nature of spatiotemporal changes in cerebral hemodynamics as manifested in functional magnetic resonance imaging. Magn. Reson. Med. 37, 511–8.

201. Strangman, G., Culver, J.P., Thompson, J.H., and Boas, D.A. (2002). A Quantitative Comparison of Simultaneous BOLD fMRI and NIRS Recordings during Functional Brain Activation. Neuroimage 17, 719–731.

202. Sassaroli, A., Zheng, F., Pierro, M., Bergethon, P.R., and Fantini, S. (2011). Phase Difference between low-frequency oscillations of cerebral deoxy- and oxy- hemoglobin concentrations during a mental task. J. Innov. Opt. Health Sci. 4, 151–158.

203. Chen, J.K., Johnston, K.M., Collie, A., McCrory, P., and Ptito, A. (2007). A validation of the post concussion symptom scale in the assessment of complex concussion using cognitive testing and functional MRI. J Neurol Neurosurg Psychiatry 78, 1231–1238.

204. Zhang, K., Johnson, B., Pennell, D., Ray, W., Sebastianelli, W., and Slobounov, S. (2010). Are functional deficits in concussed individuals consistent with white matter structural alterations: combined FMRI & DTI study. Exp Brain Res 204, 57–70.

205. Bryer, E.J., Medaglia, J.D., Rostami, S., and Hillary, F.G. (2013). Neural Recruitment after Mild Traumatic Brain Injury Is Task Dependent: A Meta-analysis. J Int Neuropsychol Soc , 1–12.

206. De Guio, F., Jacobson, S.W., Molteno, C.D., Jacobson, J.L., and Meintjes, E.M. (2012). Functional magnetic resonance imaging study comparing rhythmic finger tapping in children and adults. Pediatr. Neurol. 46, 94–100.

207. Rivkin, M.J., Vajapeyam, S., Hutton, C., Weiler, M.L., Hall, E.K., Wolraich, D.A., Yoo, S.S., Mulkern, R. V, Forbes, P.W., Wolff, P.H., and Waber, D.P. (2003). A functional magnetic resonance imaging study of paced finger tapping in children. Pediatr. Neurol. 28, 89–95.

208. Dhamala, M., Pagnoni, G., Wiesenfeld, K., Zink, C.F., Martin, M., and Berns, G.S. (2003). Neural correlates of the complexity of rhythmic finger tapping. Neuroimage 20, 918–26.

209. Witt, S.T., Lovejoy, D.W., Pearlson, G.D., and Stevens, M.C. (2010). Decreased prefrontal cortex activity in mild traumatic brain injury during performance of an auditory oddball task. Brain Imaging Behav 4, 232–247.

210. Jäncke, L., Loose, R., Lutz, K., Specht, K., and Shah, N.J. (2000). Cortical activations during paced finger-tapping applying visual and auditory pacing stimuli. Brain Res. Cogn. Brain Res. 10, 51–66.

211. Krivitzky, L.S., Roebuck-Spencer, T.M., Roth, R.M., Blackstone, K., Johnson, C.P., and Gioia, G. (2011). Functional magnetic resonance imaging of working memory and response inhibition in children with mild traumatic brain injury. J Int Neuropsychol Soc 17, 1143–1152.

212. Lewis, P.A., Wing, A.M., Pope, P.A., Praamstra, P., and Miall, R.C. (2004). Brain activity correlates differentially with increasing temporal complexity of rhythms during initialisation, synchronisation, and continuation phases of paced finger tapping. Neuropsychologia 42, 1301–12.

213. Schapiro, M.B., Schmithorst, V.J., Wilke, M., Byars, A.W., Strawsburg, R.H., and Holland, S.K. (2004). BOLD fMRI signal increases with age in selected brain regions in children. Neuroreport 15, 2575–8.

214. Riecker, A., Wildgruber, D., Mathiak, K., Grodd, W., and Ackermann, H. (2003). Parametric analysis of rate-dependent hemodynamic response functions of cortical and subcortical brain structures during auditorily cued finger tapping: a fMRI study. Neuroimage 18, 731–9.

215. Allison, J.D., Meador, K.J., Loring, D.W., Figueroa, R.E., and Wright, J.C. (2000). Functional MRI cerebral activation and deactivation during finger movement. Neurology 54, 135–42.

216. Takeuchi, N., Ikoma, K., Chuma, T., and Matsuo, Y. (2006). Measurement of transcallosal inhibition in traumatic brain injury by transcranial magnetic stimulation. Brain Inj. 20, 991–6.

217. Kumar, S., Rao, S.L., Chandramouli, B.A., and Pillai, S. V. (2009). Reduction of functional brain connectivity in mild traumatic brain injury during working memory. J Neurotrauma 26, 665–675.

218. Bleich-Cohen, M., Sharon, H., Weizman, R., Poyurovsky, M., Faragian, S., and Hendler, T. (2012). Diminished language lateralization in schizophrenia corresponds to impaired inter-hemispheric functional connectivity. Schizophr. Res. 134, 131–6.

219. Xu, J., Lou, W., Zhao, S., and Wang, C. (2014). Altered Directed Connectivity in Patients with Early Vascular Dementia During a Visual Oddball Task. Brain Topogr. , E–Pub.

220. Rytsar, R., Fornari, E., Frackowiak, R.S., Ghika, J.A., and Knyazeva, M.G. (2011). Inhibition in early Alzheimer's disease: an fMRI-based study of effective connectivity. Neuroimage 57, 1131–9.

221. Bianchi, A.M. (2010). Measures of connectivity among the different brain areas during an attention task. Conf. Proc. ... Annu. Int. Conf. IEEE Eng. Med. Biol. Soc. IEEE Eng. Med. Biol. Soc. Annu. Conf. 2010, 1710–3.

222. Johnson, B., Zhang, K., Gay, M., Horovitz, S., Hallett, M., Sebastianelli, W., and Slobounov, S. (2012). Alteration of brain default network in subacute phase of injury in concussed individuals: resting-state fMRI study. Neuroimage 59, 511–518.

223. Zhang, K., Johnson, B., Gay, M., Horovitz, S.G., Hallett, M., Sebastianelli, W., and Slobounov, S. (2012). Default mode network in concussed individuals in response to the YMCA physical stress test. J Neurotrauma 29, 756–765.

224. Newton, A.T., Morgan, V.L., and Gore, J.C. (2007). Task demand modulation of steady-state functional connectivity to primary motor cortex. Hum. Brain Mapp. 28, 663–72.

225. Rissman, J., Gazzaley, A., and D'Esposito, M. (2004). Measuring functional connectivity during distinct stages of a cognitive task. Neuroimage 23, 752–63.

226. Jiang, T., He, Y., Zang, Y., and Weng, X. (2004). Modulation of functional connectivity during the resting state and the motor task. Hum. Brain Mapp. 22, 63–71.

227. Kumar, S., Rao, S.L., Chandramouli, B.A., and Pillai, S. V. (2009). Reduction of functional brain connectivity in mild traumatic brain injury during working memory. J Neurotrauma 26, 665–675.

228. Tallus, J., Lioumis, P., Hamalainen, H., Kahkonen, S., and Tenovuo, O. (2013). Transcranial magnetic stimulation-electroencephalography responses in recovered and symptomatic mild traumatic brain injury. J Neurotrauma 30, 1270–1277.

229. McAllister, T.W., Flashman, L.A., McDonald, B.C., and Saykin, A.J. (2006). Mechanisms of working memory dysfunction after mild and moderate TBI: evidence from functional MRI and neurogenetics. J Neurotrauma 23, 1450–1467.

230. Zhou, Y., Kierans, A., Kenul, D., Ge, Y., Rath, J., Reaume, J., Grossman, R.I., and Lui, Y.W. (2013). Mild Traumatic Brain Injury: Longitudinal Regional Brain Volume Changes. Radiology 267, 880–890.

231. Johnson, B., Zhang, K., Gay, M., Neuberger, T., Horovitz, S., Hallett, M., Sebastianelli, W., and Slobounov, S. (2012). Metabolic alterations in corpus callosum may compromise brain functional connectivity in MTBI patients: an 1H-MRS study. Neurosci. Lett. 509, 5–8.

232. Sponheim, S.R., McGuire, K.A., Kang, S.S., Davenport, N.D., Aviyente, S., Bernat, E.M., and Lim, K.O. (2011). Evidence of disrupted functional connectivity in the brain after combat-related blast injury. Neuroimage 54 Suppl 1, S21–9.

233. Grossman, E.J., Jensen, J.H., Babb, J.S., Chen, Q., Tabesh, A., Fieremans, E., Xia, D., Inglese, M., and Grossman, R.I. (2013). Cognitive impairment in mild traumatic brain

injury: a longitudinal diffusional kurtosis and perfusion imaging study. AJNR Am J Neuroradiol 34, 951–7, S1–3.

234. Miles, L., Grossman, R.I., Johnson, G., Babb, J.S., Diller, L., and Inglese, M. (2008). Short-term DTI predictors of cognitive dysfunction in mild traumatic brain injury. Brain Inj 22, 115–122.

235. Niogi, S.N., Mukherjee, P., Ghajar, J., Johnson, C., Kolster, R.A., Sarkar, R., Lee, H., Meeker, M., Zimmerman, R.D., Manley, G.T., and McCandliss, B.D. (2008). Extent of microstructural white matter injury in postconcussive syndrome correlates with impaired cognitive reaction time: a 3T diffusion tensor imaging study of mild traumatic brain injury. AJNR Am J Neuroradiol 29, 967–973.

236. Manson, S.C., Palace, J., Frank, J.A., and Matthews, P.M. (2006). Loss of interhemispheric inhibition in patients with multiple sclerosis is related to corpus callosum atrophy. Exp. brain Res. 174, 728–33.

237. Chistyakov, a V, Soustiel, J.F., Hafner, H., Trubnik, M., Levy, G., and Feinsod, M. (2001). Excitatory and inhibitory corticospinal responses to transcranial magnetic stimulation in patients with minor to moderate head injury. J. Neurol. Neurosurg. Psychiatry 70, 580–7.

238. Tremblay, S., de Beaumont, L., Lassonde, M., and Théoret, H. (2011). Evidence for the specificity of intracortical inhibitory dysfunction in asymptomatic concussed athletes. J. Neurotrauma 28, 493–502.

239. Doron, K.W., and Gazzaniga, M.S. (2008). Neuroimaging techniques offer new perspectives on callosal transfer and interhemispheric communication. Cortex. 44, 1023–9.

240. Fling, B.W., Benson, B.L., and Seidler, R.D. (2013). Transcallosal sensorimotor fiber tract structure-function relationships. Hum. Brain Mapp. 34, 384–95.

241. Meyer, B.U., Röricht, S., and Woiciechowsky, C. (1998). Topography of fibers in the human corpus callosum mediating interhemispheric inhibition between the motor cortices. Ann. Neurol. 43, 360–9.

242. Tallus, J., Lioumis, P., Hamalainen, H., Kahkonen, S., Tenovuo, O., Hämäläinen, H., and Kähkönen, S. (2013). Transcranial magnetic stimulation-electroencephalography responses in recovered and symptomatic mild traumatic brain injury. J Neurotrauma 30, 1270–1277.

243. Chistyakov, a V, Soustiel, J.F., Hafner, H., Elron, M., and Feinsod, M. (1998). Altered excitability of the motor cortex after minor head injury revealed by transcranial magnetic stimulation. Acta Neurochir. (Wien). 140, 467–72.

244. De Beaumont, L., Mongeon, D., Tremblay, S., Messier, J., Prince, F., Leclerc, S., Lassonde, M., and Théoret, H. (2011). Persistent motor system abnormalities in formerly concussed athletes. J. Athl. Train. 46, 234–40.

245. Tallus, J., Lioumis, P., Hamalainen, H., Kahkonen, S., and Tenovuo, O. (2012). Long-lasting TMS motor threshold elevation in mild traumatic brain injury. Acta Neurol Scand 126, 178–182.

246. Babikian, T., Deboard Marion, S., Copeland, S., Alger, J.R., Neill, J.O., Cazalis, F., Mink, R., Giza, C.C., Vu, J.A., Hilleary, S.M., Kernan, C.L., Newman, N., and Asarnow, R.F. (2010). Metabolic Levels in the Corpus Callosum and Their Structural and Behavioral Correlates after Moderate to Severe TBI. J. Neurotrauma 27, 473–481.

247. Azevedo, E., Rosengarten, B., Santos, R., Freitas, J., and Kaps, M. (2007). Interplay of cerebral autoregulation and neurovascular coupling evaluated by functional TCD in different orthostatic conditions. J Neurol 254, 236–241.

248. Perthen, J.E., Lansing, A.E., Liau, J., Liu, T.T., and Buxton, R.B. (2008). Caffeine-induced uncoupling of cerebral blood flow and oxygen metabolism: a calibrated BOLD fMRI study. Neuroimage 40, 237–47.

249. Thomason, M.E., Burrows, B.E., Gabrieli, J.D., and Glover, G.H. (2005). Breath holding reveals differences in fMRI BOLD signal in children and adults. Neuroimage 25, 824–837.

250. Talavage, T.M., Nauman, E.A., Breedlove, E.L., Yoruk, U., Dye, A.E., Morigaki, K.E., Feuer, H., and Leverenz, L.J. (2013). Functionally-Detected Cognitive Impairment in High School Football Players Without Clinically-Diagnosed Concussion. J Neurotrauma 31, 327–338.

251. Lipton, M.L., Gulko, E., Zimmerman, M.E., Friedman, B.W., Kim, M., Gellella, E., Gold, T., Shifteh, K., Ardekani, B.A., and Branch, C.A. (2009). Diffusion-tensor imaging implicates prefrontal axonal injury in executive function impairment following very mild traumatic brain injury. Radiology 252, 816–824.

252. Pfurtscheller, G., Daly, I., Bauernfeind, G., and Müller-Putz, G.R. (2012). Coupling between intrinsic prefrontal HbO2 and central EEG beta power oscillations in the resting brain. PLoS One 7, e43640.

253. Babiloni, C., Vecchio, F., Altavilla, R., Tibuzzi, F., Lizio, R., Altamura, C., Palazzo, P., Maggio, P., Ursini, F., Ercolani, M., Soricelli, A., Noce, G., Rossini, P.M., and Vernieri, F. (2014). Hypercapnia affects the functional coupling of resting state electroencephalographic rhythms and cerebral haemodynamics in healthy elderly subjects and in patients with amnestic mild cognitive impairment. Clin. Neurophysiol. 125, 685–93.